

**DISSECTION OF NOVEL PATHWAYS LEADING TO PODOCYTE DYSFUNCTION  
AND PROTEINURIA**

by

**Dan Wang**

B.S. in Biological Technology, Zhejiang University, 2003

Submitted to the Graduate Faculty of  
School of Medicine in partial fulfillment  
of the requirements for the degree of  
Doctor of Philosophy in Cellular and Molecular Pathology

University of Pittsburgh

2010

UNIVERSITY OF PITTSBURGH

SCHOOL OF MEDICINE

This dissertation was presented

by

Dan Wang

It was defended on

November 22, 2010

and approved by

Satdarshan P.S. Monga, MD, Associate Professor, Department of Pathology

Donna B. Stolz, PhD, Associate Professor, Department of Cell Biology & Physiology

Ora A. Weisz, PhD, Professor, Department of Medicine, Department of Cell Biology &  
Physiology

Cary Wu, PhD, Professor, Department of Pathology

Committee Chair: Reza Zarnegar, PhD, Professor, Department of Pathology

Dissertation Advisor: Youhua Liu, PhD, Professor, Department of Pathology

Copyright © by Dan Wang

2010

# **DISSECTION OF NOVEL PATHWAYS LEADING TO PODOCYTE DYSFUNCTION AND PROTEINURIA**

Dan Wang

University of Pittsburgh, 2010

Podocytes are highly differentiated glomerular epithelial cells that play an essential role in the establishment of the glomerular filtration barrier, a structural apparatus that selectively restricts the filtration of different macromolecules in the blood stream on the basis of their sizes, shape and charge. Podocyte dysfunction, one of the major causes of proteinuria, is of pathogenetic and prognostic significance in human glomerular disease. My study is focused on the investigation of novel pathways leading to podocyte dysfunction and proteinuria.

In the first part, immunoblotting and quantitative reverse transcriptase PCR (RT-PCR) were used to demonstrate that LIM and senescent cell antigen-like domains 1 (PINCH1) is induced and undergoes nuclear translocation in podocytes after transforming growth factor, beta 1 (TGF- $\beta$ 1) treatment. Bioinformatics analysis revealed the putative nuclear export signal/nuclear localization signal (NES/NLS) at the PINCH1 C-terminus which is required for its nuclear translocation. Immunoprecipitation and GST pull-down assay identified the interaction between PINCH1 and Wilms tumor 1 (WT1) which led to suppression of the WT1-mediated podocalyxin gene expression. *In vivo*, PINCH1 also underwent nuclear translocation and interacted with WT1 after TGF- $\beta$ 1 stimulation. Our data identifies nuclear transcription factor WT1 as a novel binding partner for PINCH1, and provides novel insight into the mechanism of podocyte dysfunction under pathological conditions.

In the second part, RT-PCR results revealed that treatment with TGF- $\beta$ 1 induced gene expression of several wingless-type MMTV integration site family members (Wnts), predominantly Wnt1, and activated  $\beta$ -catenin in mouse podocytes. Wnt antagonist Dickkopf-1 (DKK1) blocked TGF- $\beta$ 1-induced  $\beta$ -catenin activation and preserved nephrin expression. *In vivo*, ectopic expression of constitutively active TGF- $\beta$ 1 induced Wnt1 expression, activated glomerular  $\beta$ -catenin, upregulated its downstream target genes, and led to podocyte injury and proteinuria. Consistently, concomitant expression of DKK1 gene abolished  $\beta$ -catenin activation in mouse glomeruli, inhibited TGF- $\beta$ 1-triggered Wnt/ $\beta$ -catenin target genes, and ameliorated proteinuria. These results establish a role for Wnt/ $\beta$ -catenin signaling in the pathogenesis of podocyte injury and also suggest that this signaling pathway could be exploited as a therapeutic target for the treatment of proteinuric kidney diseases.

## TABLE OF CONTENTS

<b>PREFACE.....</b>	<b>XIV</b>
<b>1.0 INTRODUCTION.....</b>	<b>1</b>
<b>1.1 GLOMERULAR FILTRATION BARRIER AND PROTEINURIA.....</b>	<b>1</b>
<b>1.1.1 Glomerulus overview and function.....</b>	<b>1</b>
<b>1.1.2 Filtration barrier structure and function.....</b>	<b>3</b>
<b>1.1.2.1 Glomerular endothelial cells (GECs) .....</b>	<b>3</b>
<b>1.1.2.2 Glomerular basement membrane.....</b>	<b>6</b>
<b>1.1.2.3 Podocyte foot process.....</b>	<b>7</b>
<b>1.1.3 Defective filtration and proteinuria .....</b>	<b>8</b>
<b>1.2 PODOCYTES .....</b>	<b>9</b>
<b>1.2.1 Podocyte structure.....</b>	<b>9</b>
<b>1.2.2 Signaling in podocytes.....</b>	<b>11</b>
<b>1.2.2.1 Signaling at the slit diaphragm.....</b>	<b>11</b>
<b>1.2.2.2 Signaling between GBM and foot processes .....</b>	<b>12</b>
<b>1.2.2.3 Signaling at the apical surface .....</b>	<b>13</b>
<b>1.2.3 Transcription regulator WT1.....</b>	<b>14</b>
<b>1.2.4 Podocyte dysfunction and proteinuria.....</b>	<b>16</b>
<b>1.3 TRANSFORMING GROWTH FACTOR-<math>\beta</math> AND PODOCYTE INJURY .</b>	<b>19</b>

1.3.1	TGF- $\beta$ structure and activation .....	19
1.3.2	TGF- $\beta$ signaling pathway .....	21
1.3.3	TGF- $\beta$ signaling in kidney diseases.....	23
1.4	PINCH .....	26
1.4.1	IPP complex and integrin signaling pathway.....	26
1.4.2	PINCH structure and function .....	29
1.4.3	PINCH in diseases .....	31
1.5	WNT/ $\beta$ -CATENIN SIGNALING PATYWAY .....	32
1.5.1	Components of Wnt signaling .....	32
1.5.2	$\beta$ -catenin in the canonical Wnt pathway .....	33
1.5.3	Regulation of Wnt/ $\beta$ -catenin signaling .....	35
1.5.4	Wnt/ $\beta$ -catenin signaling in kidney diseases and podocyte injury .....	36
2.0	PINCH1 IS TRANSCRIPTIONAL REGULATOR THAT INTERACTS WITH WT1 AND REPRESSES PODOCALYXIN EXPRESSION.....	39
2.1	ABSTRACT.....	39
2.2	MATERIALS AND METHODS.....	40
2.2.1	Cell culture and treatment.....	40
2.2.2	Animal models.....	41
2.2.3	Isolation of glomeruli.....	41
2.2.4	Construction of various expression vectors.....	42
2.2.5	RT-PCR and real-time PCR.....	42
2.2.6	Western blot analysis.....	44
2.2.7	Immunoprecipitation.....	44

2.2.8	Nuclear and cytoplasmic fractionation.....	45
2.2.9	Purification of GST fusion protein and pull down assay .....	45
2.2.10	Luciferase reporter assay .....	46
2.2.11	Urinary albumin and creatinine assay .....	46
2.2.12	Statistical analysis.....	47
2.3	RESULTS .....	47
2.3.1	Induction of PINCH1 expression by TGF- $\beta$ 1 in glomerular podocyte.....	47
2.3.2	Nuclear translocation of PINCH1 in podocytes after TGF- $\beta$ 1 stimulation 48	
2.3.3	Nuclear translocation of PINCH1 requires its putative NES/NLS motif.	51
2.3.4	PINCH1 interacts with nuclear transcription factor WT1.....	54
2.3.5	Delineation of the structural domains mediating PINCH1/WT1 interaction .....	55
2.3.6	PINCH1 represses WT1-mediated podocalyxin expression .....	58
2.3.7	PINCH1/WT1 interaction occurs <i>in vivo</i> and is associated with proteinuria .....	60
2.4	DISCUSSION.....	61
3.0	WNT/ $\beta$ -CATENIN SIGNALING MEDIATES TGF- $\beta$ 1-DRIVEN PODOCYTE INJURY AND PROTEINURIA .....	66
3.1	ABSTRACT.....	66
3.2	MATERIALS AND METHODS .....	67
3.2.1	Cell culture and treatment.....	67
3.2.2	Animal models.....	68



3.2.3	Isolation of glomeruli.....	68
3.2.4	Urinary albumin and creatinine assay.....	69
3.2.5	Construction of pCA-TGF- $\beta$ 1 vector.....	69
3.2.6	RT-PCR and real-time PCR.....	69
3.2.7	Western blot analysis.....	72
3.2.8	Nuclear and cytoplasmic fractionation.....	72
3.2.9	Immunofluorescent and Immunohistochemical staining.....	73
3.2.10	Statistical analysis.....	73
3.3	RESULTS .....	74
3.3.1	Induction of Wnt expression by TGF- $\beta$ 1 in podocytes .....	74
3.3.2	Activation of $\beta$ -catenin in podocytes by TGF- $\beta$ 1 .....	75
3.3.3	DKK1 blocks Wnt/ $\beta$ -catenin signaling in podocytes .....	76
3.3.4	Ectopic TGF- $\beta$ 1 expression targets podocyte <i>in vivo</i> and induces proteinuria .....	80
3.3.5	Activation of Wnt/ $\beta$ -catenin signaling <i>in vivo</i> by TGF- $\beta$ 1 .....	81
3.3.6	Ectopic expression of DKK1 gene blocks Wnt/ $\beta$ -catenin signaling and reduces proteinuria .....	85
3.4	DISCUSSION.....	87
4.0	GENERAL DISCUSSION AND FUTURE DIRECTIONS .....	92
4.1	GENERAL DISCUSSION .....	93
4.1.1	Conditionally immortalized podocyte cell lines .....	93
4.1.2	TGF- $\beta$ 1 mouse model .....	95
4.1.3	Potential drawbacks .....	96

4.1.4	Therapeutic implication and future directions .....	98
BIBLIOGRAPHY .....		101

## **LIST OF TABLES**

<b>Table 1. Genes involved in podocyte associated genetic glomerular diseases. ....</b>	<b>18</b>
<b>Table 2. Nucleotide sequences of the primers used for RT-PCR .....</b>	<b>43</b>
<b>Table 3. Nucleotide sequences of the primers used for RT-PCR .....</b>	<b>70</b>

## LIST OF FIGURES

<b>Figure 1. Structure of nephron and glomerulus .....</b>	<b>2</b>
<b>Figure 2. Glomerular filtration barrier .....</b>	<b>5</b>
<b>Figure 3. Podocyte foot process. ....</b>	<b>10</b>
<b>Figure 4. The overview of Wnt/<math>\beta</math>-catenin signaling pathway. ....</b>	<b>35</b>
<b>Figure 5. TGF-<math>\beta</math>1 induces PINCH1 mRNA and protein expression in human podocytes..</b>	<b>48</b>
<b>Figure 6. TGF-<math>\beta</math>1 induces nuclear translocation of PINCH1 in human podocytes.....</b>	<b>50</b>
<b>Figure 7. PINCH1 nuclear translocation induced by TGF-<math>\beta</math>1 is regulated by a mechanism independent of its abundance. ....</b>	<b>51</b>
<b>Figure 8. Subcellular localization of PINCH1 is dictated by a putative motif in its C-terminus. ....</b>	<b>53</b>
<b>Figure 9. PINCH1 physically interacts with nuclear transcription factor WT1 in human podocytes.....</b>	<b>56</b>
<b>Figure 10. Delineation of the structural domains that mediate PINCH1/WT1 interaction</b>	<b>57</b>
<b>Figure 11. PINCH1 blocks WT1-mediated podocalyxin expression in human podocytes .</b>	<b>59</b>
<b>Figure 12. PINCH1 undergoes nuclear translocation and forms interaction with WT1 <i>in vivo</i> .....</b>	<b>61</b>
<b>Figure 13. Expression of Wnt genes is induced by TGF-<math>\beta</math>1 in podocytes.....</b>	<b>75</b>

<b>Figure 14. <math>\beta</math>-catenin is activated by TGF-<math>\beta</math>1 in podocytes.....</b>	<b>78</b>
<b>Figure 15. Exogenous Wnt antagonist DKK1 blocks Wnt signaling induced by TGF-<math>\beta</math>1 in podocytes.....</b>	<b>79</b>
<b>Figure 16. Ectopic expression of TGF-<math>\beta</math>1 targets glomerular podocytes <i>in vivo</i> .....</b>	<b>82</b>
<b>Figure 17. Ectopic expression of TGF-<math>\beta</math>1 causes proteinuria and podocyte dysfunction...</b>	<b>83</b>
<b>Figure 18. Ectopic expression TGF-<math>\beta</math>1 activates Wnt/<math>\beta</math>-catenin signaling and induces its downstream target gene expression <i>in vivo</i> .....</b>	<b>84</b>
<b>Figure 19. Ectopic expression of DKK1 blocks <math>\beta</math>-catenin activation and reduces albuminuria induced by TGF-<math>\beta</math>1 <i>in vivo</i>.....</b>	<b>86</b>
<b>Figure 20. Exogenous DKK1 blocks Wnt/<math>\beta</math>-catenin target gene expression induced by TGF-<math>\beta</math>1 <i>in vivo</i>.....</b>	<b>87</b>
<b>Figure 21. Diagram of two signaling pathways under TGF-<math>\beta</math>1 stimulation leading to podocyte dysfunction and proteinuria .....</b>	<b>94</b>

## **PREFACE**

At the beginning of my dissertation, I would like to take this opportunity to express my sincere gratitude to the following people.

My greatest appreciation goes to my thesis advisor Dr. Youhua Liu, who is an outstanding mentor not only in my academic study, but also in my life. Joining the laboratory of Dr. Youhua Liu provided me a great opportunity to conduct fundamental biomedical studies and develop my scientific career. More importantly, he taught me the attitude toward science. His enthusiasm to research and spirit of hardworking make me realize how to become a successful scientist. I would have never fulfilled my graduate training without all his invaluable mentoring and kindly help.

My committee members, Dr. Reza Zarnegar, Dr. Cary Wu, Dr. Donna Stolz, Dr. Satdarshan Monga and Dr. Ora Weisz, were another critical component of my Ph.D training. Their guidance, support and helpful involvement in helping me with every aspect of my study were beyond what I could have asked for.

I would like to thank my colleagues in Dr. Liu's laboratory, particularly Dr. Chunsun Dai, Dr. Yingjian Li, Lin Lin, Weichun He, Sha Hao, and Xiaoyue Tan. They have become friends instead of just colleagues. They helped me with many aspects of my study and made coming to work everyday an enjoyable experience.

I would also like to thank all members in Department of Pathology, and Interdisciplinary Program. Wendy Mars, our program director was a helpful counselor and instructor. The administrative staff of the CMP and INTBP program was also of great assistance to me including Shari Tipton, Cindy Duffy, Veronica Cardamone, Carol Williams, and Nicole Paterline.

At last but most certainly not least, I would like to thank the people who I love most, my family. My parents and my husband, You Li, have always been there for me, to support and encourage me, their unconditional love means the most to me. Without each and every one of you, I would not have made it to this far in my career and life. And with all your support, I would continue to overcome all the new challenges in the future.

## **1.0 INTRODUCTION**

### **1.1 GLOMERULAR FILTRATION BARRIER AND PROTEINURIA**

As the vital component of urinary system, the kidneys regulate the balance of essential chemicals in the blood, and removes waste products and excess water from the body in the form of urine. The nephron is the basic functional unit of the kidney and plays an essential role in receiving and filtering all of the body's blood. The human kidney is made up of millions of nephrons. Nephrons are composed of 3 parts: the glomerulus, the Bowman's capsule, and the tubule, which are all essential in the filtration, re-absorption, and excretion processes.

#### **1.1.1 Glomerulus overview and function**

The glomerulus resembles a tiny ball-shaped structure made up of a twisted mass of capillaries and is surrounded by the Bowman's capsule (Figure 1A). The glomerulus is semi-permeable, sieving the blood plasma and yielding a filtrate as urine through ultrafiltration, excluding albumin (68,000 mol wt) and larger serum proteins [1]. A large volume of ultrafiltrate is produced by the glomerulus into the capsule. As this liquid traverses the proximal convoluted tubule, most of its water and salt are reabsorbed. Glomerular filtration rate, defined by the flow rate of filtered fluid through the kidney, is usually used to evaluate overall renal function.



The glomerulus comprises four resident cell types. Mesangial cells, endothelial cells and podocytes are within the glomerular tuft (Figure 1B), whereas parietal epithelial cells (PECs) comprise the extra-glomerular tuft [2-3]. They are supported by the glomerular basement membrane (GBM). Although those cells have different functions under physiological conditions, they are dependent on each other during glomerular development and for carrying out normal kidney function, as demonstrated in human genetic glomerular disease and experimental studies with cell-specific gene manipulations [4]. Cytokine cross-talk between cells is essential to maintain the anatomic structure and function of the glomerulus under both physiological and pathological conditions.

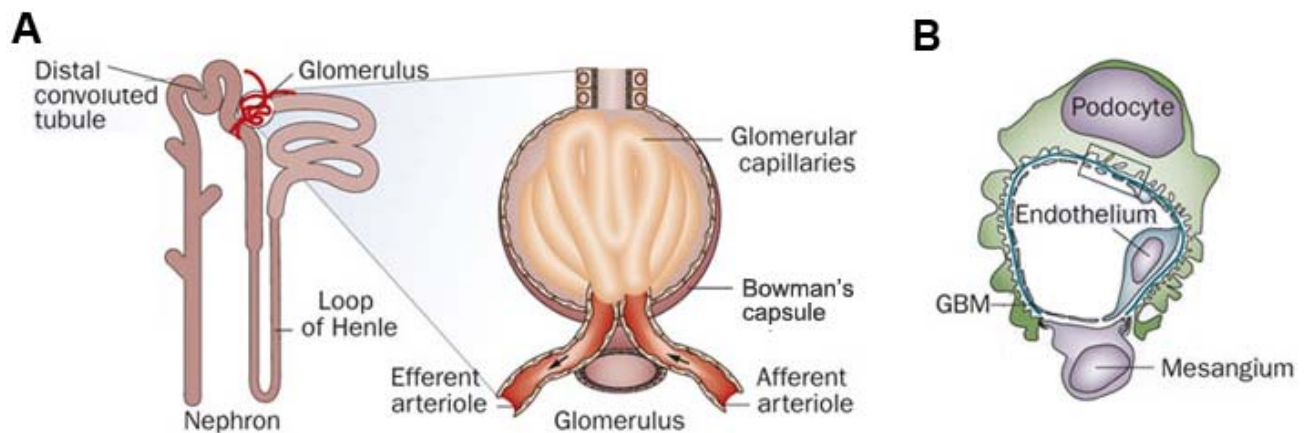


**Figure 1. Structure of nephron and glomerulus.** A, Each human kidney contains about 1 million nephrons, which are each composed of a glomerulus, a distal and proximal convoluted tubule and a microvascular system. B, The glomerulus contains a fenestrated endothelium, the GBM, and podocytes. Figure modified from reference [5].

### **1.1.2 Filtration barrier structure and function**

The glomerular filtration barrier, as a delicate structure apparatus, is composed of three different layers: the fenestrated endothelium, GBM, and the epithelial podocyte layer (Figure 2A, B) [1, 5-8]. It prevents the movement of large plasma-borne molecules from the capillary lumen to the space encompassed by the Bowman capsule; however, transglomerular pressure enables water and small molecular solutes to be filtered through this structure [5]. For the past three decades, with the advancement of tracer experiments, electron microscopes and various animal models, great progress has been made in the recognition of the structure, function and mechanism of the filtration barrier. However, the location and nature of the filtering layers and the exact mechanisms of filtration have been a matter of debate [9-10].

#### **1.1.2.1 Glomerular endothelial cells (GECs)**

Glomerular endothelial cells (GECs) are highly specialized fenestrated cells, which constitute 20-50% of the glomerular capillary surface area [2, 10], allowing a higher rate of water and small solute exchange, restricting the permeability of macromolecules [11]. In the 1970s, tracer experiments revealed the characterization of the fenestration structure of endothelial cells as numerous, circular, 50-100 nm diameter units (Figure 2C) [12-14]. These features allows the GEC barrier to be freely permeable to substances of small molecular dimensions, such as albumin (~7 nm) [11] and ferritin (~11 nm) [14]; as a result, GECs were not originally considered as a formal part of the glomerular filtration barrier [9].

Although Ichimura *et al.* have demonstrated that only about 2% of endothelial cells form diaphragmed fenestrae [15], the endothelial cell fenestrae in the glomerular barrier are not just empty holes. The GECs are covered by a negatively charged hydrated structure known as the

endothelial cell surface layer (ESL), which is composed of glycocalyx that may prevent the passage of albumin and other plasma proteins [7, 10-11, 16]. Electron microscopy and confocal microscopy of conditionally immortalized glomerular endothelial cells revealed a 200-nm thick glycocalyx over the plasma membrane [17], while another study showed the thickness of this surface layer as thick as 500 nm in animal models [18]. Previous studies have shown that the endothelial cell layer is important for glomerular size and charge selectivity. In a murine study, treatment with glycocalyx-degrading enzymes such as hyaluronidase, heparinase, or chondroitinase, resulted in significantly increased urinary albumin excretion [19]. Furthermore, a recent study has shown that oxidative stress causes glomerular ESL deterioration by increasing heparanase levels, resulting in exacerbation of glomerular permselectivity and development of albuminuria [20].

The essential role of vascular endothelial growth factor (VEGF) in maintaining the GECs filtration function has been demonstrated by several studies. A brief report from The New England Journal of Medicine has illustrated that anti-VEGF antibody treatment in patients can induce GEC defects associated with proteinuria, which is supported by podocyte specific inactivation of VEGF in mouse model [21-22]. Additionally, podocyte-specific overexpression of the VEGF-164 isoform led to collapsing glomerulopathy in HIV-associated nephropathy and diabetic nephropathy [22-23]. These results suggest that GECs are critical in maintaining the integrity and function of glomerular filtration barrier.

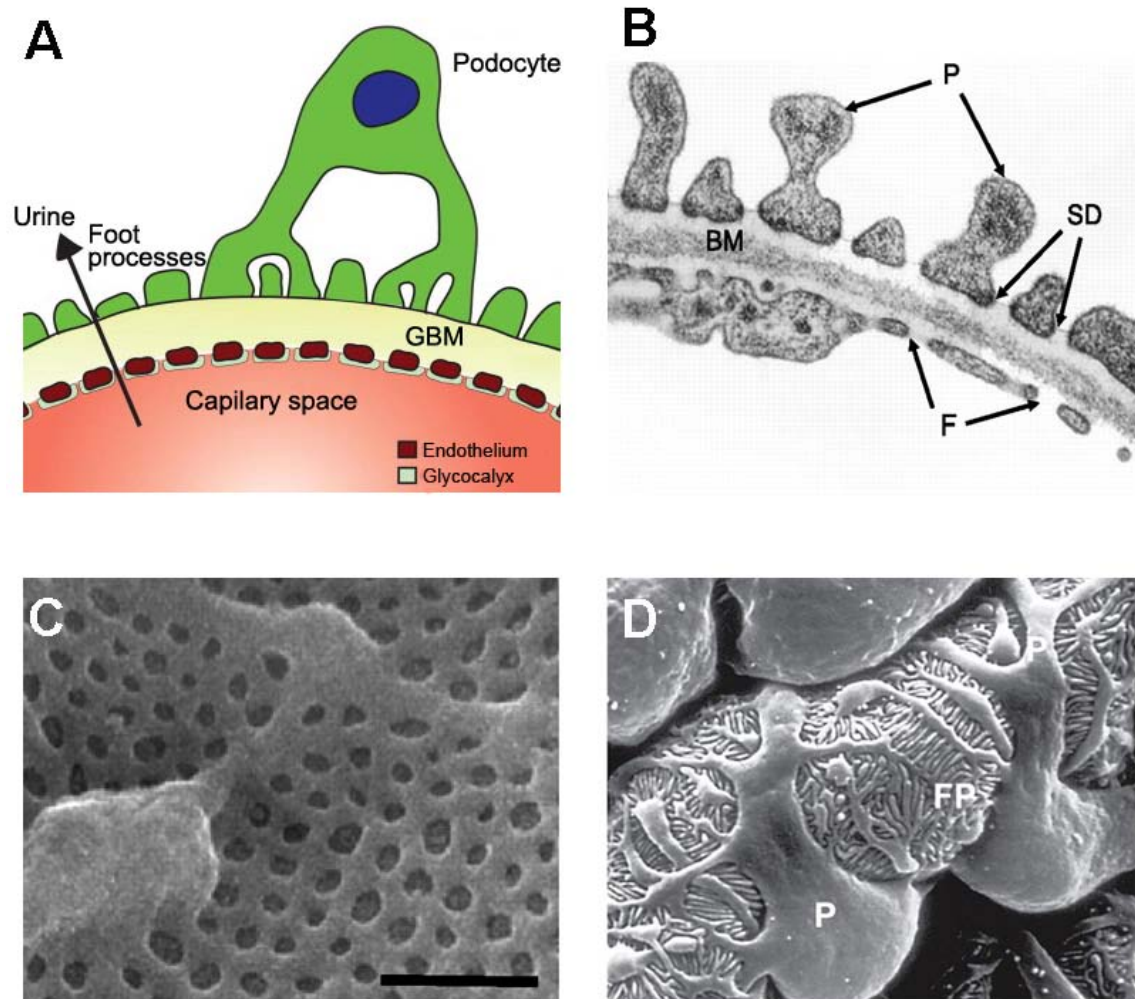


**Figure 2. Glomerular filtration barrier.** A, Glomerular filtration barrier is composed of three layers: an inner fenestrated endothelium with glycocalyx, the glomerular basement membrane (GBM), and podocytes with foot processes. B, Transmission electron micrograph of a transverse section through the wall of a normal rat glomerular capillary. C, Scanning electron micrograph of glomerular endothelial cell fenestration in a mouse glomerular capillary. D, Scanning electron micrograph of the interdigitating foot processes encompassing capillary loops. P, podocyte cell body; FP, foot process; SD, slit diaphragm; GBM, glomerular basement membrane; F, endothelial fenestration. Figure modified from reference [10-11, 24].

### **1.1.2.2 Glomerular basement membrane**

The glomerular basement membrane (GBM) is an acellular matrix and fundamental structure of the glomerular capillary. Glomerular endothelial cells and podocytes anchor to each side of GBM. The GBM is a 300-350 nm thick gel-like structure that arises from the fusion of two basement membranes during the development: one is synthesized by the glomerular endothelium, and the other is from the glomerular epithelium during the early stages' development [1]. It is mainly composed of the type IV collagen, laminin, entactin/nidogen and the heparin sulfate proteoglycans (HSPGs) [25].

The GBM had been considered to play a central role as a size- and charge-selective filtration barrier. However, recent studies have presented challenges to this concept. HSPGs are believed to provide anionic charge to the GBM and contribute to the charge selectivity. Decreased expression of HSPGs has been shown in the patients with diabetic kidney disease by immunostaining [26-28] and in an animal model of active Heymann nephritis [29]. Intravenous injection of monoclonal antibody against GBM heparin sulfate has been reported to induce a dose-dependent, transient and selective proteinuria that was maximal immediately after the injection [30]. Also, knock-in mice lacking the HS chains at the N-terminal domain I of perlecan (a major component of HSPG in the glomerular basement membrane) were highly susceptible to protein overload [31]. To question this concept, Dr. Miner's group revealed that agrin- or perlecan-heparan sulfate- deficient and conditional knockout mice do not alter glomerular permselectivity, even though agrin contributes significantly to the anionic charge to the GBM [32-33]. Furthermore, other studies questioned the significance of the charge selectivity of glomerular barrier using charged and uncharged macromolecules [34-35].

Type IV collagen is across-linked network of three sets of triple-helical molecules that self associate with their C-terminal domains and middle triple-helical regions [36]. The network of type IV collagen mainly functions as a basic basement membrane scaffold with laminin to the glomerular capillary wall, although it makes little contribution to filtration selectivity [9, 36]. The mutations in type IV collagen genes, such as *COL4A3*, *COL4A4* or *COL4A5*, lead to the autosomal recessive Alport syndrome characterized by hematuria, proteinuria (less than 1 to 2 g of protein excreted per day), progressive renal failure, and sensorineural deafness [37].

Laminins are heterotrimeric proteins, which form a network with type IV collagen in the GBM. The main laminin in the mature GBM is laminin-521, which is composed by  $\alpha 5$ ,  $\beta 2$  and  $\gamma 1$  chains [10]. Laminin-521 has been demonstrated to play as essential role in maintaining the glomerular ultrafiltration function by laminin- $\beta 2$  deficient mice which develop massive proteinuria [38]. In human patients with Pierson syndrome (a rare congenital nephrotic syndrome), mutations in gene *LAMB2* have been identified [39]. Jarad G. *et al* have shown that GBM permeability to ferritin was dramatically elevated in *Lamb2*<sup>-/-</sup> mice by electron-dense tracer experiments, even before the appearance of foot process effacement, which demonstrates the significance of GBM in the glomerular barrier being a different perspective [40].

### **1.1.2.3 Podocyte foot process**

Podocytes are highly differentiated glomerular visceral epithelial cells, which are characterized by their sophisticated foot processes described as the interdigitation structure between the neighboring cells (Figure 2D). The foot processes are anchored firmly to the underlying GBM by transmembrane cell receptors and proteins, such as integrins and tetraspanins [9]. The podocyte foot processes form 30-45 nm-wide filtration slits that are connected through

specialized adhesion complexes known as the slit diaphragm [14]. This porous substructure of the glomerular slit diaphragm was revealed by Rodewald *et al.* with transmission electron microscopy in 1974, which suggested the principal role of the slit diaphragm in the glomerular filtration selection [14]. In the past decade, the role of the podocyte in the filtration process has become the focus of nephrology research, and increasingly convincing findings have expanded the understanding of biology and pathology of the glomerular filtration barrier. The structure features of podocyte will be addressed in detail in Chapter 1.2.

### **1.1.3 Defective filtration and proteinuria**

From the clinical standpoint, glomerular diseases are generally classified into two categories based on the magnitude of proteinuria and the presence of red blood cells: nephritic syndrome and nephrotic syndrome [2]. Nephritic syndrome is characterized by diffuse inflammatory changes in the glomeruli; however, nephrotic syndrome is characterized by the defects in glomerular capillary wall permeability, with heavy proteinuria [41]. Proteinuria, the clinical manifestation of structural and functional defects in glomerular filtration barrier, often occurs in the early stages of many forms of primary glomerular disease [42]. In the most common proteinuric kidney diseases, including focal segmental glomerulosclerosis, minimal change disease, membranous nephropathy (including lupus), diabetic nephropathy, and IgA nephropathy, proteinuria is closely related to a defective filtration process.

The maintenance of normal filtration function is based on the integrity of all three layers of the glomerular capillary wall, even though studies from the last decade demonstrate the pivotal role of podocyte foot processes in the filtering process. Advances in understanding the molecular structure of the filtration barrier will allow for the identification of genetic defects as

the cause of numerous glomerular diseases. Molecular profiling, transgenic mice and gene therapy will reveal novel therapeutic strategies for the treatment of proteinuric glomerular diseases in the future.

## **1.2    PODOCYTES**

### **1.2.1   Podocyte structure**

Podocytes are highly differentiated epithelial cells which are developmentally derived from the metanephric mesenchyme through mesenchymal to epithelial transdifferentiation (MET) [43]. The interdigitating foot processes of podocytes are the unique aspect of glomerular development, and are the fundamental structure that maintains filtration function and prevents glomerular disease. On the basal side, the foot processes are anchored firmly to the GBM through transmembrane proteins and receptors and are arranged in a highly organized way to envelope the capillary wall. On the lateral side, foot processes of two adjacent podocytes are connected through specialized adhesion complexes termed the glomerular slit diaphragm. Podocalyxin, the main molecular component on the apical side, is responsible for the negative charge to maintain the normal podocyte architecture [44] .

Although the three domains are functionally independent with specialized protein expression, the cytoskeleton is connected to all three plasma membrane domains and brings signals together from the extracellular matrix, as shown in Figure 3. In foot processes, the cytoskeleton is highly organized in actin-based bundles that run parallel to the longitudinal axis of foot processes [10]. Foot processes are thought to modulate the permeability of the filtration



barrier through changes in foot process morphology. Interference with any of the three foot process domains changes the actin cytoskeleton from parallel contractile bundles into a dense network, which leads to foot process effacement [45].

### Podocyte foot process

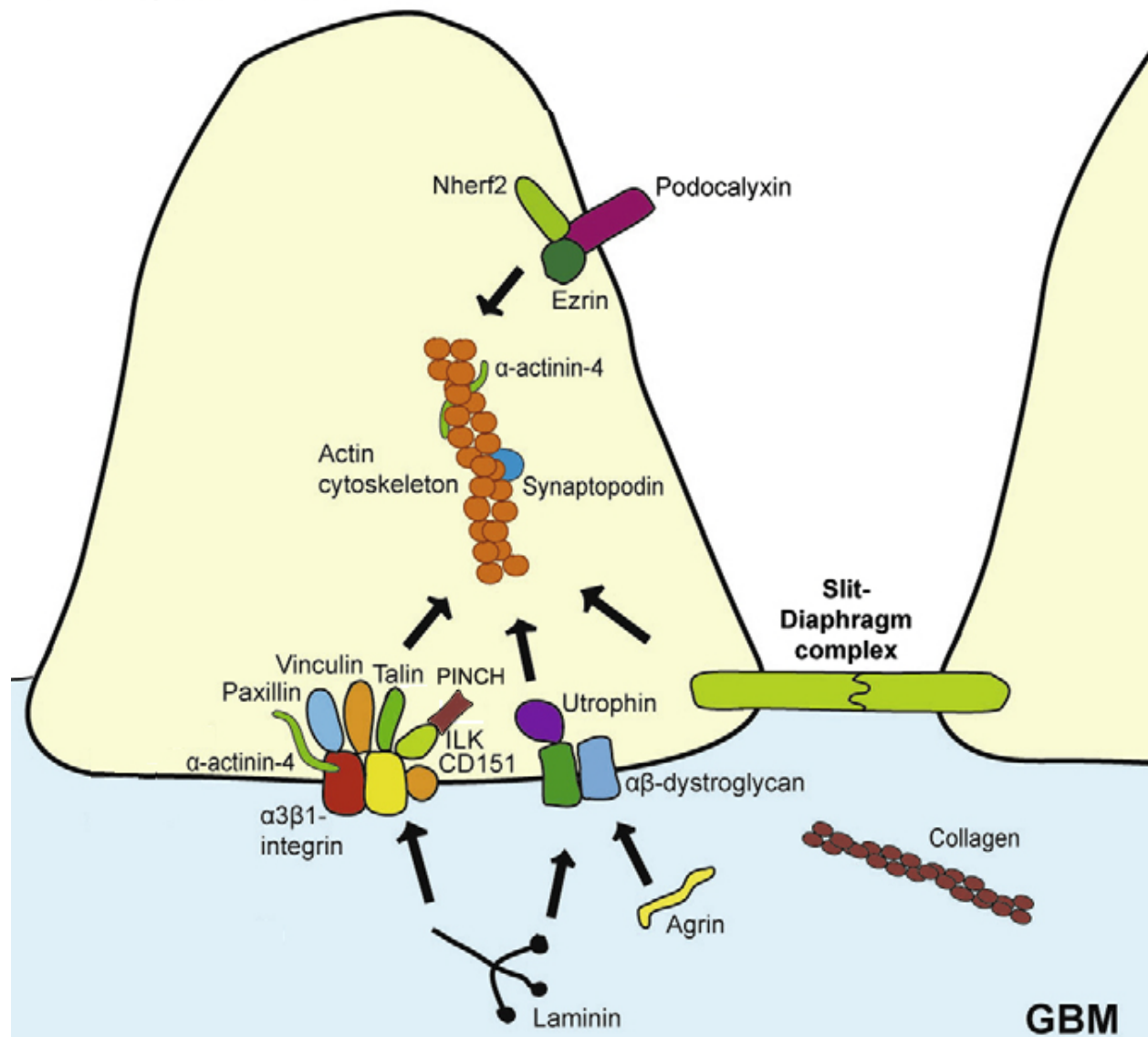


**Figure 3. Podocyte foot process.** At basal domain, podocyte foot processes are attached to the GBM through integrins and dystroglycans; at lateral domain, slit diaphragm complex cover the space between adjacent foot processes and connects them together; at apical domain, negatively charged podocalyxin is the main component. The actin cytoskeleton interconnects three plasma membrane domains together through adaptor proteins. Figure modified from reference [10].

## 1.2.2 Signaling in podocytes

### 1.2.2.1 Signaling at the slit diaphragm

The slit diaphragm complex is composed of several plasma-membrane proteins including nephrin, podocin, NEPH1-3, Fat1, VE-cadherin and P-cadherin [9]. Nephrin, podocin, NEPH1, and Fat1 are essential for the normal glomerular filtration function. Nephrin was the first slit diaphragm protein cloned by the Tryggvason group in 1998 [46]. Their report was the first to reveal that nephrin-coding gene (*NPHS1*) is mutated in congenital nephritic syndrome of the Finnish type, and also provided fundamental insight into the molecular mechanisms of glomerular filtration. Nephrin is a transmembrane protein that belongs to the immunoglobulin superfamily. It contains eight extracellular immunoglobulin domains which interact with the other immunoglobulin domains from adjacent foot process to form a zipper-like structure. The cytoplasmic region of nephrin has a series of conserved tyrosine-based motifs which upon phosphorylation can serve as binding sites for SH2 domain containing proteins, such as the adaptor protein Nck [47-49]. Like other transmembrane receptors, nephrin can signal via second messengers to the cytoskeleton through the binding of intracellular adaptor proteins. Nephrin knockout mice are born without typical slit diaphragms and have severe proteinuria [50]. Furthermore, the reduction and pattern change of nephrin expression has been observed in several human nephropathies and animal disease models, which suggests that nephrin is essential for normal glomerular function.

Several other components of the slit diaphragm have been recently identified, allowing us to better understand this delicate complex. In 2000, Boute, N. *et al* identified the causative gene for the congenital nephritic syndrome type 2, *NPHS2*, using positional cloning [51]. The *NPHS2* gene encodes a membrane protein named podocin, which is localized at the slit diaphragm region

and mediates nephron signaling through interaction with the cytoplasmic tail of nephrin [52]. *Nphs2*<sup>-/-</sup> mice displayed rearrangement of foot processes and lack of the slit diaphragm, associated with proteinuria during the antenatal period, and died a few days after birth from renal failure caused by massive mesangial sclerosis [53].

CD2AP, an adaptor protein, binds directly with nephrin and podocin, and serves as an anchor between the slit diaphragm and actin cytoskeleton [54-55]. CD2AP knockout mice exhibited defects in foot processes and died at 6 to 7 weeks of age due to massive proteinuria and renal failure [56]. Similarly, the adaptor protein Nck has also been shown to interact with the intracellular tail of nephrin upon its phosphorylation and link it to the actin cytoskeleton in the podocytes [47, 49]. Mice missing Nck proteins in podocytes develop massive proteinuria and foot process effacement [47]. Taken together, adaptor proteins linking the slit diaphragm to the cytoskeleton are crucial to mediate actin polymerization and the cytoskeleton reorganization in maintaining foot process structure and function.

#### **1.2.2.2 Signaling between GBM and foot processes**

Podocytes attach to the underlying GBM through two major cell adhesion complexes: integrins and dystroglycans [57]. Integrins are  $\alpha\beta$  heterodimeric proteins that are indirectly linked to the actin cytoskeleton through integrin associated proteins. In podocytes,  $\alpha3\beta1$  integrin is the most abundant isoform. Mice with a homozygous mutation of  $\alpha3$  integrin exhibited defects in kidney development, including decreased extent of branching of glomerular capillary loops, disorganized glomerular basement membrane and failure to form mature foot processes [58]. Podocyte specific deletion of  $\beta1$  integrin in mice leads to massive proteinuria, foot process effacement and podocyte detachment from GBM [59-60]. Beta1 integrin binds to

laminins, an important component of GBM. The lack of  $\beta 1$  integrin results in the failure to form heterotrimeric laminins due to the absence of  $\alpha 1$  and  $\alpha 5$  laminin chain recruitment into the assembled basement membrane [59]. The disruption of the interaction between integrins and laminins may weaken the interaction between GBM and podocytes and induce foot process loss and podocyte detachment. The role of dystroglycans in foot process is still poorly understood. A recent paper has shown that the antibody against  $\alpha$ -dystroglycan on podocytes induces intracellular calcium signaling, which leads to altered cytoskeleton architecture and foot process effacement [61].

Integrin linked kinase (ILK) has also been demonstrated to play an important role in the glomerular filtration barrier. Two independent studies reported progressive proteinuric renal disease in mice with podocyte-specific deletion of ILK. Although one study focused on the thickening of the GBM followed by the abnormal distribution of  $\alpha 3$  integrin, the other emphasized the interaction between ILK, nephrin and  $\alpha$ -actinin-4, and the redistribution of nephrin caused by the disruption of this complex [62-63].

### **1.2.2.3 Signaling at the apical surface**

Podocalyxin is the main component coating the apical membrane of foot processes and the major sialoprotein in the glycocalyx of glomerular podocytes [44]. This membrane protein is responsible for the negative charge of the foot process apical domain and maintaining open urinary space. Podocalyxin knockout mice fail to form foot processes and slit diaphragms and instead exhibit cell-cell junctional complexes (tight and adherens junctions) and died of the renal failure. In addition, the corresponding reduction in permeable, glomerular filtration surface area presumably leads to the observed block in urine production [64]. This suggests that podocalyxin

is crucial for the development of the normal podocyte foot process structure and filtration function. It has also been shown that podocalyxin is linked to actin cytoskeleton through ezrin, Na<sup>+</sup>/H<sup>+</sup>-exchanger and NHERF1 in podocytes, and induce actin reorganization [65-67]. The disruption of this complex has been reported in some animal models with foot process effacement and proteinuria.

### **1.2.3 Transcription regulator WT1**

The delicate morphology and function of podocytes are ultimately controlled by their unique nuclear transcriptional program. In this regard, WT1, the product of Wilms tumor suppressor gene, is the key transcription factor that plays a fundamental role in controlling the expression of major podocyte-specific genes in the adult kidney [68-73]. During kidney development, WT1 expression is first detected in the uncondensed metanephric blastema, and dramatically increases in condensed mesenchyme during the mesenchymal to epithelial transdifferentiation [74]. It has been shown that WT1 expression is strongly associated with differentiation of metanephric blastemal cells into epithelial cells [75]. In adult kidney, WT1 expression is exclusively restricted to glomerular podocytes, and is not present in other terminally differentiated cells, including epithelial cells. Based on these findings, WT1 is often utilized as a molecular marker for evaluating podocyte number and density under different circumstances [76]. In humans, *WT1* mutations are associated with several glomerulopathies, including Wilms tumor, Deny-Drash syndrome, Frasier syndrome and diffuse mesangial sclerosis.

As a transcription factor, WT1 contains four zinc-finger DNA-binding motifs at the carboxyl-terminus and a proline/glutamine-rich domain at the amino-terminus. WT1 has 24 transcript variants due to the different start sites, alternative RNA splicing at two coding exons

and RNA editing, and it has been shown that this process is tissue-specific and developmentally regulated [77]. Three alternative translation start sites have been identified: major ATG site, CTG site at 204 bp upstream of the major site; and the second in-frame ATG at 381 bp [74]. additionally, two alternatively spliced exons are also known: one effects exon 5, which encodes 17 amino acids that are included or omitted between the Pro/Glu-rich N-terminus and the Zn finger domain; the other effects exon 9 by insertion or exclusion of three amino acids KTS (lysine-threonine-serine) between the third and fourth zinc fingers [69, 74]. Also, an RNA editing site has been shown to lead to the replacement of an amino acid in exon 6 in the transcription of human and rat *WT1* gene [77].

Among the 24 isoforms, we know very little about isoforms produced from alternative translation start sites. WT1 isoforms with exon 5 slow cell growth to a lesser extent than the isoform without exon 5, and result in altered cellular morphology and initiate the mesenchyme-to-epithelial transition during metanephric development [78]. The mouse model carrying the deletion of exon 5 showed that exon 5 is not a major modifier of WT1 function [79]. The ratio of exon 5 spliced isoforms differs among cell types, species and developmental stages, whereas the ratio between WT1 (-KTS) and WT1 (+KTS) is constant in all cell types. Mutations leading to the ratio change between WT1 (-KTS) and WT1 (+KTS) can cause Frasier syndrome in humans which is presented at birth with male pseudohermaphroditism, streak gonads and progressive glomerulonephropathy [69]. WT1 (-KTS) and WT1 (+KTS) have been shown to have different nuclear localization: WT1 (-KTS) isoforms re diffuse in the nuclei as transcription factors, whereas WT1 (+KTS) isoforms colocalize with splicing factors [80]. WT1 (-KTS) isoforms bind to DNA and regulate transcription of the target genes; however, WT1 (+KTS)

isoforms show a higher affinity for RNA as compared to DNA, and play a role in RNA splicing during the post-transcriptional modification [81].

WT1 can either activate or repress gene transcription, depending on cell-context and different target genes. Based on binding site selection and transient transfection, about 20 different genes have been identified as the targets of WT1, including *C-myc*, *TGF- $\beta$ 1*, *IGF2*, *EGF1*, *EGFR*, *Bcl-2*. Results show that WT1 affects the promoter activity of all these target genes [82]. Besides, WT1 enhances the expression of E-cadherin in NIH 3T3 fibroblasts by activation of the murine E-cadherin promoter through a conserved GC-rich sequence similar to an EGR-1 binding site and through a CAAT box sequence [83]. During kidney development, WT1 can target podocalyxin, nephrin and amphiregulin gene expression by binding to their promoters, resulting in potent transcriptional activation [70, 72, 84]. These observations support the role for WT1 in conferring the specific activation of a glomerular differentiation program in renal precursors and provide a molecular basis for some glomerulonephropathies. Recently, a new WT1 transcriptional target gene, *CXXC5* has been identified that negatively regulates Wnt/ $\beta$ -catenin signaling *in vitro* and *in vivo* [85].

#### **1.2.4 Podocyte dysfunction and proteinuria**

In the recent decades, increasing evidence indicates that podocyte dysfunction plays a central role in conferring the defective glomerular filtration and onset of proteinuria. Podocyte dysfunction is characterized by foot process effacement, slit diaphragm loss, and ultimately leading to apoptosis and cell depletion. Proteinuria is an early pathologic feature caused by podocyte dysfunction in many common forms of chronic kidney diseases, such as diabetic nephropathy and focal segmental glomerulosclerosis. On one hand, a large number of genetic

studies have revealed that mutations or deletions of some crucial genes are consequently associated with the development of proteinuria in both animal models and patients; on the other hand, the mechanism that induces podocyte dysfunction in many acquired forms of proteinuric kidney diseases without inherited gene changes remains ambiguous.

As mentioned above, three domains compose the delicate filtration structure of podocyte foot processes: the slit diaphragm, the basal domain attached to the GBM, and the apical domain, which are associated with the actin cytoskeleton. The disruption of domain integrity is a critical event in the development of proteinuria and nephritic syndrome. Foot process effacement may result from disruption of any of these domains and rearrangement of the actin cytoskeleton. Advances in the understanding of the molecular structure of the podocytes have revealed the major role of genetic defects play in the development of podocyte dysfunction and proteinuria. Proteins that are associated with the slit diaphragm (for example, nephrin, podocin,  $\alpha$ -actinin 4, the adaptor protein CD2AP, and trPC6), and those that anchor the foot processes to the GBM (for example,  $\alpha$ 3 $\beta$ 1 integrin,  $\alpha$ -actinin 4, vinculin, talin, and the tetraspanin, CD151), together with those that localize on the apical domain (for example, podocalyxin), and transcription factors (for example WT1 and lim homeobox transcription factor 1 $\beta$ ), all have an important role in the prevention of proteinuria [5]. Mutations and deletions of those genes causing to foot process effacement, podocyte morphology change and proteinuria are involved in various podocyte-associated glomerular diseases in humans and genetic mouse models, as shown in Table 1.



**Table 1. Genes involved in podocyte associated genetic glomerular diseases.**

Disease (OMIM number)	Gene	Protein
Congenital nephrotic syndrome of the Finnish type (256300)	<i>NPHS1</i>	Nephrin
Congenital nephrotic syndrome type 2 (604766)	<i>NPHS2</i>	Podocin
Familial nephrotic syndrome type 3 (610725)	<i>PLCE1</i>	Phospholipase C $\epsilon$ 1
Frasier syndrome and Denys–Drash syndrome (136680 and 194080)	<i>WT1</i>	wilms’ tumor 1
Schimke immuno-osseous dysplasia (242900)	<i>SMARCAL1</i>	hHARP
Nephrotic syndrome caused by mutations in CD2AP (604241)	<i>CD2AP</i>	CD2AP
Nephrotic syndrome caused by mutations in actinin-4 (604638)	<i>ACTN4</i>	$\alpha$ -Actinin-4
Nephrotic syndrome caused by mutations in TRPC6 (603652)	<i>TRPC6</i>	TRPC6
Epstein and Fechtner syndrome (153640 and 153650)	<i>MYH9</i>	NMMHC-A
Nail–patella syndrome (161200)	<i>LMX1B</i>	LMX1B

Table modified from reference [5].

However, genetic causes of podocyte dysfunction explain only a small fraction of proteinuric nephropathies. Mutations are rare in most common forms of chronic kidney diseases such as diabetic nephropathy [86]. In this regard, the exact mechanisms causing podocyte dysfunction in the vast majority of acquired proteinuric kidney diseases are not yet fully delineated. Li et al have proposed that epithelial-mesenchymal transition (EMT) could be a potential pathway leading to podocyte dysfunction and proteinuria under pathological conditions by investigating podocyte EMT after incubation with TGF- $\beta$ 1 *in vitro* [42]. Podocyte EMT is described by loss of epithelial P-cadherin, ZO-1 and podocyte-specific nephrin, and the acquisition of mesenchymal fibroblast-specific protein-1 (Fsp1), desmin, collagen I, fibronectin and transcription factor Snail1, and represents changes consistent with tubular EMT [42]. It is

conceivable that podocytes undergo a range of adaptive changes in response to injury, including hypertrophy, autophagy, dedifferentiation, EMT, detachment and apoptosis. EMT certainly results in podocyte dysfunction, and ultimately leads to podocyte detachment from GBM, onset of proteinuria and glomerulosclerosis [43]. However, this explanation is not without controversy, because these cells possess sophisticated foot processes *in vivo* and express vimentin, characterizing them mesenchymal appearance at baseline. Three major signaling pathways, including TGF- $\beta$ 1, integrin/ILK and Wnt/ $\beta$ -catenin signaling, are involved in conferring podocyte EMT, and these pathways will be discussed in detail in following chapters.

### **1.3 TRANSFORMING GROWTH FACTOR- $\beta$ AND PODOCYTE INJURY**

#### **1.3.1 TGF- $\beta$ structure and activation**

Transforming growth factor-beta (TGF- $\beta$ ), including TGF- $\beta$ 1, TGF- $\beta$ 2 and TGF- $\beta$ 3, is a family of cytokines that regulate cell proliferation, differentiation, adhesion, migration, apoptosis and other functions, during embryogenesis as well as in mature tissues [87].

The three members of the TGF- $\beta$  family have similar peptide structure. They are all encoded as large protein precursors; TGF- $\beta$ 1 contains 390 amino acids, TGF- $\beta$ 2 and TGF- $\beta$ 3 each contains 412 amino acids [88]. Most types of cells secrete TGF- $\beta$  in a biologically inactive form. For example, TGF- $\beta$ 1 has an amino-terminal signal peptide of 29 amino acids that is required for secretion from the cell, a pro-region of the precursor from amino acid 30-278 is cleaved to become 25 kDa latency associated peptide (LAP), and a 112 amino acid carboxy-terminal region that becomes the mature TGF- $\beta$  molecule following its release from the pro-

region by proteolytic cleavage with the endopeptidase furin [88-89]. The proteolysis yields two products that assemble into dimers. Previous analysis has shown that TGF- $\beta$ 1 is secreted as a complex with the active TGF- $\beta$ 1 dimer in a noncovalent interaction with two pro-region polypeptides [90]. The LAP act as chaperones to facilitate the secretion of the mature TGF- $\beta$ 1 and render this complex latent [91]. The cysteines in positions 223 and 225 in the pro-region are important for the association of LAP with TGF- $\beta$ -1 by interchain disulfide bonds. When cysteines are substituted by serines in positions 223 and 225 of the LAP, the TGF- $\beta$ 1 is secreted in an active form [89]. The third cysteine in position 33 is involved in binding to another protein called the latency binding protein (LTBP) [92]. When latent TGF- $\beta$  is associated with an LTBP protein it is referred to as large latent TGF- $\beta$  while latent TGF- $\beta$  alone is referred to as small latent TGF- $\beta$  [88]. The small latent TGF- $\beta$  remains in the cell until it is bound by LTBP to form a Large Latent Complex which can be secreted into the extra cellular matrix [93].

As part of the large latent complex, TGF- $\beta$  is not activated to interact with its receptors, because LAP functions as an inhibitor owing to its noncovalent, high-affinity association with TGF- $\beta$  [94]. Further processing is needed to release active TGF- $\beta$  from the complex. Some of the known activating pathways are cell or tissue specific, while some are seen in multiple cell types and tissues. Since different cellular mechanisms require distinct levels of TGF- $\beta$  signaling, the inactive complex of this cytokine gives the opportunity for proper fine-tuning of TGF- $\beta$  signaling [94]. To activate TGF- $\beta$  proteins, LAP can be removed by several ways *in vitro* and *in vivo* including extremes of pH, heat, chaotropic agents and substances like SDS and urea, proteases, thrombospondin-1(TSP-1), integrins, and reactive oxygen species (ROS). Mild acid treatment (pH 4.5) is sufficient to induce TGF- $\beta$  activation both *in vivo* and *in vitro*. This process may be mediated by denaturing LAP, thereby disturbing the interaction between LAP

and TGF- $\beta$  [95]. Proteases including plasmin, MMP-2 and MMP-9 have been identified *in vitro* as latent TGF- $\beta$  activators, however, mice that have null mutations in the genes that encode the known activating proteases do not demonstrate any phenotypes consistent with TGF- $\beta$  deficiency [94, 96-97]. This may indicate redundancy among the activating enzymes in mice. TSP-1 can activate TGF- $\beta$ 1 through direct binding with LAP *in vivo*. TSP-1 knockout mice show partial overlapping phenotype with TGF- $\beta$ 1 knockout animals, which supports the contention that TSP-1 is an activator of latent TGF- $\beta$  [98]. Integrins including  $\alpha_v\beta_6$  and  $\alpha_v\beta_8$  have been reported as TGF- $\beta$  activators, despite different mechanisms: activation of TGF- $\beta$  by  $\alpha_v\beta_6$  depends on direct interaction with the RGD amino acid sequence present in LAP- $\beta$ 1 and LAP- $\beta$ 3, which plays important role in wound healing and inflammation [99]; and activation by  $\alpha_v\beta_8$  requires the protease MT1-MMP [100]. ROS produced by irradiation *in vitro* and *in vivo* can disable LAP by hydroxyl radical-induced digestion and modification, which reflects important role of TGF- $\beta$  in inflammation and apoptosis due to oxidative stress [101].

### **1.3.2 TGF- $\beta$ signaling pathway**

TGF- $\beta$  exerts its biological activity by binding to transmembrane serine/threonine kinase receptors, which exist in several different homodimeric and heterodimeric isoforms [102]. There are three types of TGF- $\beta$  receptors: I, II, and III, all of which consist of amino-terminal extracellular ligand binding domain, a transmembrane region and a carboxy-terminal serine/threonine kinase domain [87]. Both types I and II receptors have a high affinity for TGF- $\beta$ 1 and low affinity for TGF- $\beta$ 2, while receptor type III has a high affinity for both TGF- $\beta$ 1 and - $\beta$ 2 [103]. TGF- $\beta$ 1 initiates signaling by binding to the constitutively active receptor type II,

leading to the recruitment of receptor type I to form a hetero-oligomeric signaling complex [104]. In contrast, TGF- $\beta$ 2 binds to receptor type III, which presents the cytokine to receptor type II upon oligomerization of both receptor types, since receptor type II has a low affinity for TGF- $\beta$ 2 [105]. Once type II receptor is activated, it recruits and phosphorylates serine residues of receptor type I at its GS domain, and stimulates a ubiquitous intracellular signaling cascade [87, 106].

The canonical signaling of TGF- $\beta$  is transduced by intracellular mediator Smad proteins, which are identified as Mad in *Drosophila*. Upon activation, the type I receptor recruits and phosphorylates a receptor regulated Smad (R-Smad). So far, 10 Smad proteins have been identified, and among which, only Smad2 and Smad3, as R-Smad, respond to signaling by the TGF- $\beta$  subfamily. The R-SMAD then binds to Smad4, the common Smad (CO-Smad), and forms a heterodimeric complex that moves into the nucleus where they interact in a cell-specific manner with various transcription regulators to control the transcription of many pro-fibrogenic genes [87, 107]. On the contrary, Smad6 and Smad7 block the phosphorylation of Smad2 and Smad3, thus inhibiting the TGF- $\beta$  induced inflammatory response [106, 108].

Smad4 and all R-Smad except Smad2 can bind to DNA through the minimal Smad binding element (SBE) which contains only four base pairs, 5'AGAC3' [109]. R-Smad binds to DNA through a highly conserved  $\beta$  hairpin which makes specific contacts with the three bases of the SBE, whereas a unique 30 residue insertion in Smad2 peptide inhibits the formation of  $\beta$  hairpin, resulting in the poor binding of Smad2 to DNA [110]. In addition to the SBE, a G/C rich sequence has also been reported as Smad binding elements [87].

The expression of hundreds of genes is either positively or negatively altered by TGF- $\beta$  stimulation. The same set of Smad complexes is required for both activation and repression of

targeted genes. It is believed that the different responses to TGF- $\beta$  signaling are based on the genetic makeup and environment of the target cell [111]. Due to the relatively low affinity between single copy of SBE and individual Smad proteins, Smads have to cooperate with each other and other DNA binding proteins to elicit specific transcriptional responses. Some of those factors are universal and mediate the same response in all types of cells; however, others are cell type specific leading to cell type dependent response [87]. Many DNA binding proteins, including E-box, Jun/Fos, Runx, CREBP, E2F and homeobox, have been reported as partners of Smad proteins [111].

### **1.3.3 TGF- $\beta$ signaling in kidney diseases**

Renal fibrosis is considered a hallmark and consequence of chronic kidney disease based on experimental and clinical research of the pathophysical processes leading to end-stage renal failure [106]. Renal fibrosis is a condition characterized by excessive accumulation and deposition of extracellular matrix, and results in glomerulosclerosis and tubulointerstitial fibrosis [112-113]. TGF- $\beta$  is one of the most important mediators in this process. Overexpression of TGF- $\beta$  is closely related with pathological condition of renal fibrosis, although its physiological expression is required for normal development [101, 106-107, 111].

The upregulation of TGF- $\beta$  isoforms is found in a variety of human progressive renal diseases, such as diabetic nephropathy, IgA nephropathy, lupus nephritis, focal and segmental glomerulosclerosis and crescentic glomerulonephritis [114]. Diabetic nephropathy, for example, significantly elevated plasma levels of TGF- $\beta$ 1 are found in patients with type 2 diabetes [115], and higher urinary excretion of TGF- $\beta$ 1 is observed in patients with diabetes mellitus than in

normal controls, especially in patients with severe mesangial expansion [116]. In diabetic db/db mice, it has been shown that significantly increased TGF- $\beta$ 1 mRNA and protein expression by in situ hybridization and immunostaining in both glomerular and tubular compartments [117]. The upregulation of TGF- $\beta$  type II receptor and activation of Smad3 in this mouse model also demonstrates the active signaling downstream of the TGF- $\beta$  stimulus [117]. The extracellular matrix proteins, including biglycan, fibronectin, tenascin and collagens are all induced in glomeruli in response to the stimulus of elevated TGF- $\beta$  [118].

Besides diabetic mouse models, TGF- $\beta$  overexpression has been described in several animal experimental models, including nephropathy associated with ureteral obstruction, puromycin aminonucleoside nephrosis, anti-Thy-1 rat model of proliferative glomerulonephritis, anti-GBM glomerulonephritis, and age-related nephropathy [106]. Injection of puromycin aminonucleoside results in focal glomerulosclerosis with proteinuria and stable overexpression of TGF- $\beta$ 1 [119]. In rats with surgical removal of renal mass, TGF- $\beta$  mRNA increases from early stage and induces  $\alpha$ -smooth muscle actin ( $\alpha$ -SMA), leading to renal fibrosis [120]. Also, in this model, overexpression of desmin and loss of synaptopodin in podocytes are associated with an enhanced TGF- $\beta$  mRNA expression [120].

TGF- $\beta$  induces extracellular matrix deposition by both stimulating production of the matrix proteins and reducing the synthesis of matrix degrading protease [121]. *In vitro*, TGF- $\beta$  induces desmin, fibronectin and collagen in podocytes, glomerular mesangial cells and tubular epithelial cells [42, 122]. On the other hand, plasmin generation from plasminogen is regulated by plasminogen activators (PAs) and plasminogen activator inhibitors (PAIs) [123]. Previous studies showed that PA activity was markedly reduced and PAI-1 synthesis dramatically increased in glomeruli treated with TGF- $\beta$  [123]. TGF- $\beta$  signaling is a well-known inducer of

epithelial to mesenchymal transition (EMT), which emerges as an important pathway to generate fibroblasts and myofibroblasts in diseased kidney [43, 124]. TGF- $\beta$ /Smad signaling can regulate the expression of various EMT related genes, including Snail, desmin, Fsp-1, MMP-9, fibronectin, collagen,  $\alpha$ -SMA, PINCH1 and ILK in podocytes and epithelial cells [42, 125-127]. The induction of EMT by TGF- $\beta$  is mediated by induced Snail expression, which is the key EMT regulator [128]. It should be noted that podocytes might respond differently to TGF- $\beta$  stimulation according to its specific concentrations. A high concentration of TGF- $\beta$ 1 causes podocyte apoptosis [129].

Since TGF- $\beta$  plays such an important role in the pathogenesis of glomerulosclerosis and tubulointerstitial fibrosis, it is a significant therapeutic target for the prevention of renal fibrosis. Earlier studies have shown that a natural inhibitor of TGF- $\beta$ , the proteoglycan decorin, can bind to TGF- $\beta$  and neutralize its bioactivity, which leads to suppression of glomerular matrix production and prevents matrix accumulation in the injured glomeruli [130]. More *in vivo* studies of TGF- $\beta$  neutralizing antibodies have demonstrated that antagonism of TGF- $\beta$  can inhibit glomerulosclerosis and tubulointerstitial fibrosis in a variety of mouse models, including unilateral ureteral obstruction (UUO), puromycin aminonucleoside-induced nephrosis, anti-Thy-1 nephritis, cyclosporine-induced nephropathy and mouse model of diabetic nephropathy [131-134]. The suppression of progressive proteinuria and renal damage is associated with decrease in phosphorylation of Smads in the glomeruli and tubular cells [132]. TGF- $\beta$  receptor antagonists can also play the similar role in reducing proteinuria, PAI-1 expression, and phosphorylation and nuclear translocation of Smad2/3 [135]. Also, TGF- $\beta$  short-interfering RNA has been used to suppress target genes type I collagen and PAI-1 in cultured mesangial cells and in UUO mouse model [136].



To sustain the normal immune response by maintaining the physiological level of TGF- $\beta$ , the downstream profibrotic Smads may be a better target in preventing progressive renal injury associated with TGF- $\beta$  signaling. Gene therapy with Smad7, as a natural antagonist of TGF- $\beta$  signaling, has been shown to attenuate renal fibrosis by inhibition the Smad2/3 activation [137]. Hepatocyte growth factor (HGF), as an antifibrotic factor, also has been reported to block Smads signaling by inducing Smad transcriptional corepressor Ski-related novel protein N (SnoN) expression [138].

To summarize, TGF- $\beta$  signaling plays a critical role in progressive renal diseases, which is confirmed by numerous studies in various experimental models and clinical studies. Targeting TGF- $\beta$  signaling as the therapeutic strategy may provide a promising remedy in the treatment of renal disease in humans.

## **1.4 PINCH**

### **1.4.1 IPP complex and integrin signaling pathway**

IPP is a heterotrimeric complex, which contains integrin-linked kinase (ILK), particularly interesting Cys-His-rich protein (PINCH), and parvin. It functions primarily as a signaling platform for integrins by connecting with the actin cytoskeleton and many diverse signaling pathways, and also as a regulator of gene transcription and cell-cell adhesion [139].

The extracellular matrix (ECM) influences various intracellular signal pathways that regulate survival, proliferation, polarity and differentiation by binding to cell surface receptors. Integrins, one of the most important families of adhesion molecules, are heterodimeric

transmembrane molecules consisting of  $\alpha$  and  $\beta$  subunits [140]. Protein-kinase-C can facilitate the conformational change of integrins to promote the binding between integrins and their ligands [139].  $\beta 1$  integrin is widely expressed and contributes to a large number of integrin heterodimers.  $\beta 1$  integrin is the only  $\beta$  subunit expressed in the glomerular cells, where it forms heterodimers with different  $\alpha$  subunits including  $\alpha 1$ ,  $\alpha 2$ ,  $\alpha 3$ ,  $\alpha 5$ , and  $\alpha 8$  [141]. The IPP complex links integrins to the actin cytoskeleton, and mediates signal transduction between the intracellular and extracellular compartments [142-144].

In this complex, ILK is the central component, and it binds to the cytoplasmic tail of  $\beta 1$  integrin [145] and  $\beta 3$  integrin [146]. ILK was originally identified in a yeast-hybridization system for screening the binding partner of  $\beta 1$  cytoplasmic tail in 1996 [145]. Subsequent studies have revealed the structure of ILK: three ankyrin repeats located at the amino-terminus, which mediate protein-protein interactions, and a putative fourth ankyrin repeat that lacks conserved residues; sequence homology to serine/threonine protein kinases located at the carboxy-terminus; a putative pleckstrin homology (PH) domain between these two domains and partially overlaps with them [139, 147]. ILK binds PINCH proteins through the N-terminal ankyrin repeats domain and binds parvin proteins through C-terminal kinase domain [143].

Although ILK is identified as serine/threonine kinase which can phosphorylate  $\beta 1$  integrin, the kinase activity of ILK has remained elusive and controversial. As a kinase, previous studies showed that ILK can directly phosphorylate Glycogen Synthase Kinase 3 (GSK-3) *in vitro* and inhibit GSK-3 activity. In addition, kinase-active ILK can phosphorylate PKB/Akt on serine 473 by a PI3K-dependent fashion, whereas kinase-deficient ILK severely inhibits endogenous phosphorylation of PKB/Akt on serine 473 [148-149]. Mutations on serine or threonine of ILK have been described to abrogate the kinase activity *in vitro*. S343A, R211A,

K220A/M have all been shown to abolish ILK catalytic activity [149-150]. The combination of two inactivating mutations (S343D and K220M) can abolish ATP binding activity, suggesting that these mutations might affect the activation status of downstream substrates such as Akt phosphorylation [151]. ILK deficient mice also displayed that the loss of ILK results in almost complete inhibition of phosphorylation on Ser 473 and significant inhibition of PKB/Akt activity, accompanied by significant stimulation of apoptosis [152]. However, other *in vivo* studies failed to replicate such findings. Studies in *Caenorhabditis elegans* and *Drosophila melanogaster* found that kinase dead ILK mutants were capable of fully rescuing the severe phenotypes caused by ILK deletion in both species, indicating that ILK functions as a scaffold protein and not as a kinase [153-154]. In mouse models, it has been demonstrated that phosphorylation of PKB/Akt and GSK3- $\beta$  is unaffected in ILK-deficient chondrocytes by Fässler's group [155]. Therefore ILK has also been classified as a pseudokinase, a catalytically inactive remnant of an active kinase that uses its substrate recognition motif to interact with other proteins [156].

The assembly of the IPP complex occurs before adhesion, and such an assembly is essential for their localization to cell-extracellular matrix adhesion sites, suggesting that the assembly in the cytoplasm is independent on adhesion signaling [157]. PINCH1 has been shown to be crucial to maintain the expression level of ILK, but not  $\alpha$ -parvin, in this complex and regulate the functions of this complex in cell shape modulation, motility, and survival [158]. Also, in our studies, blocking ILK expression by siRNA can down regulate PINCH1 expression. Interestingly in glomerular cells, TGF- $\beta$ 1 can regulate the IPP complex in a cell type-dependent manner: treatment with TGF- $\beta$ 1 in podocytes inhibits complex formation and promotes apoptosis by activating p38 protein kinase, whereas such treatment promotes the IPP formation

in mesangial cells [159]. It has been demonstrated that the IPP complex is important in controlling podocyte adhesion, morphology, and survival [144]. In this report, elevated levels of the IPP complex is found during podocyte differentiation and disruption of this complex leads to reduction of podocyte–matrix adhesion and foot process formation, and apoptosis [144].

#### **1.4.2 PINCH structure and function**

PINCH1 and PINCH2, also known as LIMS1 and LIMS2, are adaptor proteins that consist of five LIM domains. Both isoforms bind to the N-terminal ankyrin repeat domain (ANK) repeats domain of ILK through their N-terminal LIM1 domain in an identical manner [160-161], so the determination of PINCH1- or PINCH2- containing IPP complex is probably dependent on the competition of available PINCH1 and/or PINCH2 [162].

The LIM domain is now recognized as a tandem zinc-finger structure which is comprised of approximately 55 amino acids with 8 highly conserved cysteine and histidine residues [163]. Each LIM domain binds to two separate zinc ions separately through 4 conserved cysteine and histidine residues [164]. There seems to be no discrete consensus binding sequence or structural element for the LIM domain. Besides ILK, adaptor protein Nck2 is another potential binding partner of PINCH1 whose interaction is mediated by the fourth LIM domain of PINCH and the third SH3 domain of Nck2 [165]. As an adaptor protein, Nck2 is associated with growth factor receptor kinase-signaling pathways, including EGF receptors, PDGF receptor- $\beta$ , and IRS-1, by its SH2/SH3 domains, which indicates that Nck2 may mediate the connection between growth factor receptor-signaling pathways with the integrin-signaling pathways [165]. Nck also connects to the actin cytoskeleton and regulates the organization of actin cytoskeleton [166]. In podocytes, it has been demonstrated that the nephrin phosphorylation event resulted in the

recruitment of Nck and assembly of actin filaments to regulate foot process formation and cell morphology [47-49]. Those reports might provide a pathway which bridges the integrin signaling with slit diaphragm signaling.

The sequence of the C-terminal tail of PINCH reveals a putative leucine-rich nuclear export signal (NES) and an overlapping basic nuclear localization signal (NLS) [167]. It has been shown that PINCH shuttles between the cytoplasm and the nucleus in Schwann cells and dorsal root ganglia neurons, which suggests that PINCH may have an unrecognized function in controlling gene transcription and initiate new protein-protein interactions in the nucleus [167]. Furthermore in Hela cells, PINCH1 C-terminal tail functions not only in the efficient localization of PINCH1 to cell-ECM adhesions but also in cell shape modulation and survival signaling after PINCH1 localizes to the adhesion sites [168].

PINCH1 is ubiquitously expressed during early embryonic development and adult tissues [158]. Homozygous knockout of PINCH1 in mice leads to decreased cell proliferation and excessive cell death by E5.5 [169]. In *Caenorhabditis elegans*, depletion of UNC-97, the homologue of PINCH, results in defects in muscle adherens junctions and the mechanosensory functions of touch neurons [170]. In *Drosophila melanogaster*, muscle cells within embryos bearing mutations in the *steamer duck* (*stck*) gene, which encodes PINCH, show disturbed actin organization and cell-substratum adhesion, and failure of integrin-dependent epithelial cell adhesion in the wing [171]. All those phenotypes resemble the deletion of ILK or  $\beta$ 1-integrin [172] and indicate that PINCH is essential to mediate integrin-dependent signaling during embryogenesis.

### 1.4.3 PINCH in diseases

PINCH plays an important role in the suppression of apoptosis in tumor cells. Upregulation of PINCH has been reported in the initiation and development of several types of tumors, including oral squamous cell carcinoma and high-grade gliomas [173-175]. Depletion of PINCH1 by siRNA in human HeLa cervical carcinoma cells promotes apoptosis [168]. In the PINCH1 null mouse, apoptosis of endodermal cells and neural crest cells was detected in embryos [169, 176]. Mechanistically, PINCH1 promotes the activating phosphorylation of Src family kinases and ERK1/2, and removal of PINCH-1 in cancer cells inhibits SFK and ERK1/2 activation and promotes Bim accumulation, resulting in activation of a Bim-dependent apoptosis pathway [177].

PINCH1 is expressed early in embryonic development and in the adult kidney; however, only a few studies regarding its regulation and function in renal cells is published. Both PINCH1 and PINCH2 have been shown to work with ILK and  $\alpha$ -parvin to play essential roles on the regulation of adhesion, morphology, survival, and fibronectin matrix deposition in glomerular podocytes [144, 178]. PINCH1 has also been demonstrated as a downstream target of TGF- $\beta$ 1/Smad signaling in tubular epithelial cells and to promote tubular epithelial to mesenchymal transition by an ILK dependent mechanism [125]. *In vivo*, PINCH1 upregulation is associated with tubular EMT and renal interstitial fibrogenesis induced by ureteral obstruction [125]. Because LIM domain can bind to many other domains, more binding partners and functions remain to be identified for PINCH.

## 1.5 WNT/ $\beta$ -CATENIN SIGNALING PATHWAY

### 1.5.1 Components of Wnt signaling

Wnt proteins belong to a highly conserved family of secreted growth factors that play an essential role in embryonic development, homeostatic self-renewal in adult tissues and tumor formation [179]. The Wnt family contains 19 members, encoded by distinct genes, which are divided into 12 highly conserved subfamilies on the basis of sequence similarity [180]. They all share common structure features including a signal peptide for secretion, many potential glycosylation sites and multiple cysteine residues responsible for ensuring proper folding and secretion [181].

Wnts are generated as precursors containing an amino-terminal hydrophobic signal peptide that directs the immature protein to the endoplasmic reticulum (ER). In the ER, the signal peptide of Wnt proteins is cleaved and the proteins are palmitoylated on a conserved cysteine residue converting them into hydrophobic proteins. This step is essential for Wnt protein biological activation, and mutation of the modification site results in inactivated proteins [180-181]. Wnt proteins also complex with Wntless in the Golgi to be efficiently mobilized to the outside of the cell [181].

Upon binding of secreted Wnt proteins to specific receptor complexes in target cells, Wnts can activate three different intracellular signaling pathways: the canonical pathway (T-cell factor (Tcf)/  $\beta$ -catenin), the non-canonical pathway (planar cell polarity), and the Wnt/ $\text{Ca}^{2+}$  pathway [182-183]. Each of these pathways has their specific sets of target genes.

### 1.5.2 $\beta$ -catenin in the canonical Wnt pathway

$\beta$ -catenin, the product encoded by *CTNNB1* in humans, is a subunit of the cadherin protein complex. It is an important cytoplasmic component of the classical cadherin adhesion complex that forms the adherens junction in epithelia and mediates cell-cell adhesion in many other tissues, and is a key signaling molecule in the canonical Wnt signaling pathway that controls cell growth and differentiation during both normal development and tumorigenesis.  $\beta$ -catenin expresses a central armadillo-repeat containing domain through which it binds the cytoplasmic tail of classical cadherins. Meanwhile, it also binds  $\alpha$ -catenin, which further links the cadherin complex to the actin cytoskeleton either directly or indirectly [184].

As shown in Figure 4, the activation of  $\beta$ -catenin is a complicated process involved in the interaction between the Wnts and their receptor complex, and the destruction complex, which interacts with  $\beta$ -catenin under inactivation conditions. In the absence of a Wnt signal,  $\beta$ -catenin is associated with a scaffold protein Axin and adenomatous polyposis coli (APC) within the destruction complex, where  $\beta$ -catenin gets phosphorylated on a conserved set of serine and threonine residues at the amino-terminus by the casein kinase 1 (CK-1) and glycogen synthase kinase 3 (GSK-3). This facilitates binding of the  $\beta$ -transducin repeat-containing protein ( $\beta$ -TRCP), which subsequently mediates the ubiquitylation and efficient proteasomal degradation of  $\beta$ -catenin. The degradation of  $\beta$ -catenin ensures the binding of Groucho proteins to Tcf proteins on the promoters and enhancers of Wnt target genes in the nucleus, thereby silencing the expression of the target gene and an array of biological response [181].

When Wnts interact with cell surface receptor complexes that contain a Frizzled family member and low-density lipid receptor 5/6 (LRP5/6), Dishevelled (Dvl) is phosphorylated and



interacts with Frizzled to form a complex. This complex stimulates the aggregation and phosphorylation of LRP by CK-1 at the membrane, leading to the relocation of Axin to the membrane and inactivation of the destruction complex. Finally,  $\beta$ -catenin is free to accumulate and translocate into the nucleus, where it interacts with Tcf and recruits co-activators to facilitate the efficient activation of Wnt target genes [181].

Wnt signaling ultimately controls developmental fates through regulating the transcription of Tcf/ $\beta$ -catenin responsive target genes in specific cell types. Wnt signals not only promote cell proliferation and tissue expansion, but also control fate determination or terminal differentiation of postmitotic cells. These disparate events, proliferation and terminal differentiation, can be activated by Wnt in different cell types within the same structure, such as the hair follicle or the intestinal crypt [185]. The updated list of Wnts target genes can be found on the Wnt homepage ([http://www.stanford.edu/group/nusselab/cgi-bin/wnt/target\\_genes](http://www.stanford.edu/group/nusselab/cgi-bin/wnt/target_genes)). This list contains hundreds of genes regulated by Wnt signaling in humans and other species. Among those genes, we can find that several components of the Wnt signaling pathway, such as Frizzleds, LRP, HSPG, Axin2, and TCF/Lef, are all regulated by the  $\beta$ -catenin/Tcf complex, which demonstrates that Wnt signaling is self regulated at several levels. Mutations in  $\beta$ -catenin phosphorylation sites lead to the constitutive activation of the Wnt pathway and promote proliferation in human cancers [186]. Deregulation of the Wnt pathway is also related to several other types of human cancer and diseases [179].

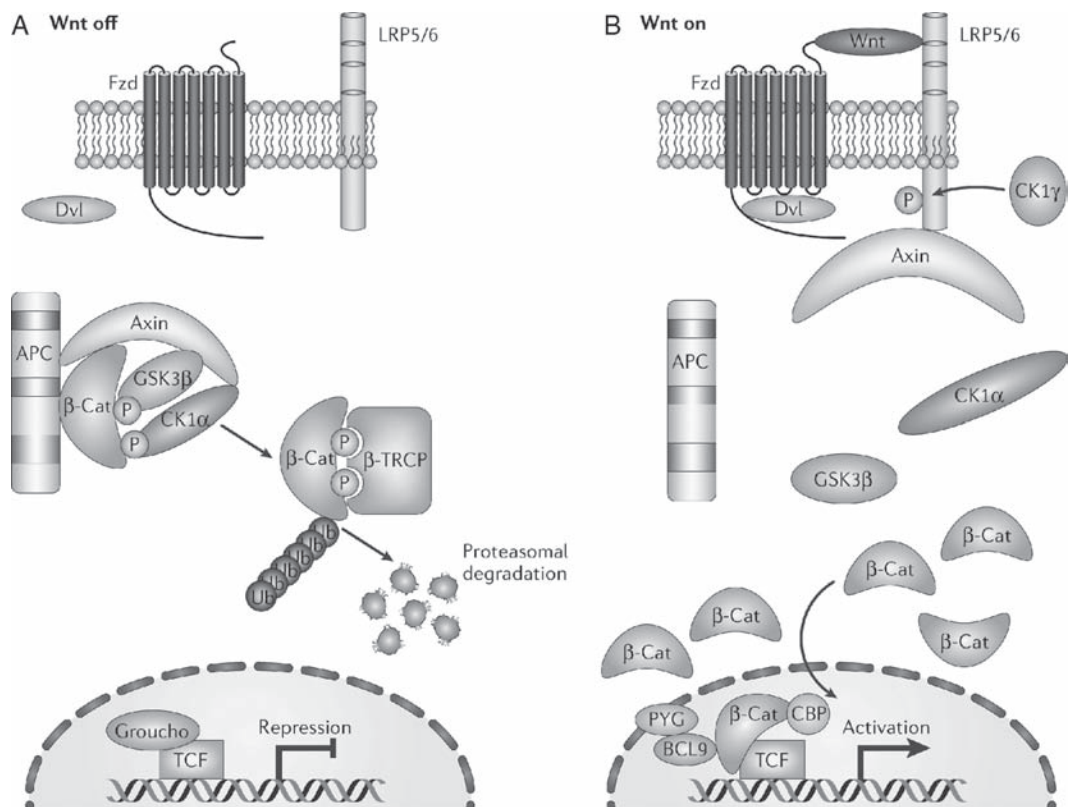


**Figure 4. The overview of Wnt/β-catenin signaling pathway.** Figure taken from reference [181].

### 1.5.3 Regulation of Wnt/β-catenin signaling

The activation of Wnt target genes and stabilization of β-catenin comprises a diverse set of biological processes involving many different proteins working together. Given the complexity, it is easy to understand why aberrant regulation of this signaling activity at any step can affect the embryonic development and tissue renewal in stem cells and cancer cells [179, 185].

Wnt antagonists contain two functional classes, the sFRP class and the Dickkopf class. Members of the sFRP class bind directly to Wnts, thereby altering their ability to bind to the Wnt receptor complex; members of the Dickkopf (DKK) class inhibit Wnt signaling by binding to the LRP5/LRP6 component of the Wnt receptor complex. Thus, in theory, those antagonists of the

sFRP class will inhibit both canonical and noncanonical pathways, whereas those of the DKK class specifically inhibit the canonical pathway [187]. The DKK family comprises four members (DKK-1 to DKK-4). DKKs contain two characteristic cysteine-rich domains (Cys-1 and Cys-2) separated by a linker region of variable length. Cys-2, in particular, is highly conserved among all members of the family and contains 10 conserved cysteine residues [188]. DKK-1, as a secretory protein, binds to the Wnt binding domain of LRP6 and forms a ternary complex with LRP-6 and Kremen (KRM) to lead to the endocytosis of the whole receptor complex [189-190]. DKK-1 inhibits Wnt-induced stabilization of  $\beta$ -catenin and  $\beta$ -catenin/Tcf-dependent transcription of both artificial and endogenous genes in mammalian and amphibian cells, respectively [191-192]. In the kidney, DKK-1 blocks the expression of Wnt target genes, such as Twist, LEF1, c-myc and fibronectin and ameliorates renal fibrosis after obstructive injury *in vivo* [193]. On the other hand, DKK-1 is also a target of the  $\beta$ -catenin/TCF pathway and highly regulated on the transcriptional level as the direct feed back control of Wnt stimulation [194].

#### **1.5.4 Wnt/ $\beta$ -catenin signaling in kidney diseases and podocyte injury**

Wnt/ $\beta$ -catenin signaling is intimately involved in kidney development. The genetic deletions of Wnt9b or Wnt4 in mice lead to severe kidney hypoplasia and an arrest of tubulogenesis at the stage of the pretubular aggregate with incomplete nephron formation [195-196]. Conditional  $\beta$ -catenin knockout in the metanephric mesenchyme results in marked renal hypoplasia, reduction of nephron numbers, and down regulation of  $\beta$ -catenin/TCF target genes, including *pax8*, *Wnt4*, *Fgf8* and *Lhx1* [197]. Together, the data indicate that Wnt/ $\beta$ -catenin signaling is crucial for nephron development.

In normal adult kidney, Wnt signaling turns to be silenced [193]. However, overexpression of diverse Wnts and  $\beta$ -catenin are observed in a variety of kidney diseases originated from both the glomeruli and tubulointerstitium [198]. Patients treated with lithium, a pharmacologic activator of  $\beta$ -catenin, have shown increased proteinuria, nephritic syndrome and progressive nephropathy, which is closely associated with the duration and cumulative dose [199-200]. Moreover, increased expressions of Wnt1 and  $\beta$ -catenin are found in the podocytes of patients with diabetic nephropathy and focal segmental glomerulosclerosis (FSGS) [201]. In mouse models, all of Wnt family members except Wnt5b, Wnt8b and Wnt9b are upregulated in fibrotic kidneys after unilateral ureteral obstruction (UUO), compared with sham normal kidney [193]. Consistently, the expression of  $\beta$ -catenin and its targets genes, such as c-Myc, Twist, LEF-1, and fibronectin are all upregulated in this model [193]. In the murine model of podocyte injury, adriamycin can induce proteinuria and activation of Wnt/ $\beta$ -catenin signaling, and ectopic expression of exogenous Wnt1 gene can exacerbate podocytes injury and proteinuria [201]. Moreover, in the same report, it was shown that podocyte-specific deletion of  $\beta$ -catenin protects against development of albuminuria after podocyte injury induced by adriamycin. Similarly, recent studies also demonstrate an induction of Wnt2 expression in a rat model of podocyte injury induced by puromycin aminonucleoside [202]. In both reports, the expression level of Snail1 is induced and associated with upregulation of Wnts and  $\beta$ -catenin in injured podocytes, which leads to the suppression of nephrin and podocytes dysfunction. Together with the data from UUO model, it is conceivable that Wnt/ $\beta$ -catenin signaling may play a critical role in the pathogenesis of both podocyte injury and interstitial fibrosis, and therefore targeting this signaling could represent a novel class of therapeutic remedies for the treatment of proteinuric and fibrotic nephropathies.



## **2.0 PINCH1 IS TRANSCRIPTIONAL REGULATOR THAT INTERACTS WITH WT1 AND REPRESSES PODOCALYXIN EXPRESSION**

### **2.1 ABSTRACT**

PINCH1, an adaptor protein containing five LIM domains, plays an important role in regulating the integrin-mediated cell adhesion, migration and epithelial-mesenchymal transition. Here we show that expression of PINCH1 in cultured podocytes was induced by TGF- $\beta$ 1, a fibrogenic cytokine that promotes podocyte dysfunction and proteinuria. Interestingly, increased expression of PINCH1 not only localized at the sites of focal adhesions, but also underwent nuclear translocation after TGF- $\beta$ 1 stimulation. This nuclear translocation of PINCH1 was apparently dependent on the putative nuclear export/localization signals (NES/NLS) at its C-terminus, as deletion or site-directed mutation of this sequence abolished its cytoplasmic-nuclear shuttling. Co-immunoprecipitation and pull-down experiments revealed that PINCH1 interacted with WT1, a transcription factor that is essential for directing podocyte-specific gene expression in adult kidney. Interaction of PINCH1 and WT1 was mediated by the LIM1 domain of PINCH1 and C-terminal zinc-finger domain of WT1, which led to the suppression of the WT1-mediated podocalyxin expression in podocytes. PINCH1 also repressed podocalyxin gene transcription in a promoter-luciferase reporter assay. In vivo, ectopic expression of TGF- $\beta$ 1 in mice also promoted nuclear translocation of PINCH1 and its interaction with WT1. These results indicate

that PINCH1 can shuttle into the nucleus from cytoplasm in podocytes, wherein it interacts with WT1, leading to suppression of the podocyte-specific podocalyxin gene expression. Our studies reveal that PINCH1 could act as a transcriptional regulator through interacting with nuclear WT1.

## **2.2 MATERIALS AND METHODS**

### **2.2.1 Cell culture and treatment**

The conditionally immortalized human podocyte cell line was kindly provided by Dr. M. Saleem (University of Bristol, Bristol, UK) [203]. To propagate podocytes, cells were cultured at 33°C in RPMI-1640 medium supplemented with 10% fetal bovine serum and a mixture of insulin, transferrin and sodium selenite (ITS) (cat. no. I3146; Sigma, St. Louis, MO). To induce differentiation, podocytes were grown under nonpermissive conditions at 37°C to inactivate the SV40 large T antigen. Podocytes were treated with recombinant TGF- $\beta$ 1 at the concentration of 2 ng/ml, unless otherwise indicated. For some studies, podocytes were transiently transfected with various PINCH1 expression vectors by using Lipofectamine 2000 reagent (Invitrogen, Carlsbad, CA), as described previously [204]. Of note, pilot experiments indicated that human podocytes were relatively more efficient for transfection, compared to their mouse counterparts.

### **2.2.2 Animal models**

Male BALB/c mice that weighed approximately 18 to 20 g were purchased from Harlan Sprague Dawley (Indianapolis, IN). For delivery of mouse TGF- $\beta$ 1 gene, constitutively active TGF- $\beta$ 1 expression plasmid (pCA-TGF- $\beta$ 1), in which two cysteines at the positions 223 and 225 were mutated into serines, was injected intravenously at 0.3 mg/kg body wt by use of a hydrodynamics-based *in vivo* gene transfer approach, as described previously [205-206]. Control mice were administered an injection of empty vector pcDNA3 plasmid in an identical manner. Mice were sacrificed at day 1 and day 2 after injection, and kidney tissues were collected for various analyses. Animal protocols were approved by the Institutional Animal Care and Use Committee at the University of Pittsburgh.

### **2.2.3 Isolation of glomeruli**

Glomeruli were isolated using a differential sieving technique from mouse kidneys according to the method described elsewhere [207]. Briefly, the kidneys were excised and pressed with a spatula through a stainless steel screen of # 100 mesh and rinsed with 1% albumin in cold phosphate-buffered saline (PBS-A) through successive screens of #200 mesh and #282 mesh, respectively. The glomeruli were collected on the #282-mesh screen and suspended in PBS-A. After centrifugation at 200g for 10 min, the isolated glomeruli (purity, ~80%) were collected for subsequent analyses.



#### **2.2.4 Construction of various expression vectors**

Various expression vectors with different epitope-tags were constructed using routine molecular cloning techniques. Flag- and GFP-tagged PINCH1 expression vectors (pFlag-PINCH1 and pGFP-PINCH1), as well as GFP-tagged WT1 (pGFP-WT1) were constructed in the pcDNA3-based expression vector under the control of CMV promoter. The expression vector for WT1 (-KTS) without KTS was kindly provided by Dr. D. Haber (Massachusetts General Hospital, Charlestown, MA). The expression vector for truncated PINCH1 without NES/NLS (pFlag-PINCH1- $\Delta$ NES) was constructed by PCR using the wild-type PINCH1 expression plasmid (pFlag-PINCH1-wt) as a template. The expression vectors for mutant PINCH1 with either a single amino acid mutation (pFlag-PINCH1-M1) or three amino acid mutation in the NES/NLS motif (pFlag-PINCH1-M3) were made by using QuikChange II XL site-directed mutagenesis kit (Stratagene, La Jolla, CA). The expression plasmid harboring constitutively active TGF- $\beta$ 1 (pCA-TGF- $\beta$ 1) contained two cysteine to serine mutations at the positions 223 and 225 (C223S/C225S). This expression vector was made by using QuikChange II XL site-directed mutagenesis kit, and it produces bioactive TGF- $\beta$ 1 that does not require acid activation, as previously reported [208]. The correct sequences of different expression vectors were confirmed by sequencing at the DNA Sequencing Core Facility of the University of Pittsburgh.

#### **2.2.5 RT-PCR and real-time PCR**

Total RNA was extracted using the TRIzol RNA isolation system (Invitrogen, Carlsbad, CA). The first strand of cDNA was synthesized using 2  $\mu$ g of RNA in 20  $\mu$ l of reaction buffer by reverse transcription using AMV-RT (Promega, Madison, WI) and random primers at 42°C for

30 min. PCR was carried out using a standard PCR protocol with 1 µl aliquot of cDNA, HotStarTaq polymerase (Qiagen, Valencia, CA) and specific primer pairs. The sequences of the primer pairs were as shown in Table 2. For quantitative determination of mRNA levels, a real-time RT-PCR was performed on ABI PRISM 7000 Sequence Detection System (Applied Biosystems, Foster City, CA), as described previously [209]. The PCR reaction mixture in a 25 µl volume contained 12.5 µl of 2x SYBR Green PCR Master Mix (Applied Biosystems), 10 µl of diluted RT product (1: 10), and 0.5 µM sense and antisense primer sets. PCR reaction was run by using standard conditions[209]. After sequential incubations at 50°C for 2 min and 95°C for 10 min, respectively, the amplification protocol consisted of 40 cycles of denaturing at 95°C for 15 sec, and annealing and extension at 60°C for 60 sec. The mRNA levels of various genes were calculated after normalizing with β-actin.

**Table 2. Nucleotide sequences of the primers used for RT-PCR**

Human gene	Primer sequence of sense	Primer sequence of anti-sense
PINCH1	CCGCTGAGAAGATCGTGAAC	GGGCAAAGAGCATCTGAAAG
podocalyxin	GAGCAGTCAAAGCCACCTTC	TGGTCCCCTAGCTTCATGTC
WT1	GCGGAGCCCAATACAGAATA	TTATTGCAGCCTGGGTAAGC
GAPDH	TGAAGGTCGGAGTCAACGGA TTTGGT	CATGTGGGCCATGAGGTCCA CCAC
β-actin	AGGCATCCTCACCCTGAAGTA	CACACGCAGCTCATTGTAGA

### **2.2.6 Western blot analysis**

Cultured human podocytes were lysed in SDS sample buffer. The isolated glomeruli were pooled and lysed with radioimmunoprecipitation assay buffer containing 1% NP-40, 0.1% sodium dodecyl sulfate, 100 µg/ml phenylmethylsulfonyl fluoride, 1% protease inhibitor cocktail, and 1% phosphatase I and II inhibitor cocktail (Sigma) in phosphate buffered saline on ice. The supernatants were collected after centrifugation at  $13,000 \times g$  at 4 °C for 20 min. Protein expression was analyzed by Western blot analysis as described previously [210]. The primary antibodies used were as follows: anti-PINCH1 (cat. no. 612711; BD Transduction, San Jose, CA), anti-Flag M2 (cat. no. F1804; Sigma), anti-GFP (cat. no. ab290; Abcam, Cambridge, MA), anti-WT1 (cat. no. sc-192; Santa Cruz Biotechnology, Santa Cruz, CA), anti-podocalyxin (cat. no. 39-3800; Invitrogen), anti-Histone H3 (cat. no. ab1791; Abcam), anti-TBP (TATA binding protein) (cat. no. ab181-100; Abcam), anti-actin (cat. no. sc-1616; Santa Cruz Biotechnology) and anti- $\alpha$ -tubulin (cat. no. T9026; Sigma).

### **2.2.7 Immunoprecipitation**

Immunoprecipitation experiments were performed using similar methods as described previously [211]. Briefly, human podocyte lysates or mouse glomerular lysates were centrifuged at  $12,000 \times g$  for 10 min at 4°C. The supernatants were collected for immunoprecipitation. After preclearing with normal host IgG, the lysates were immunoprecipitated overnight at 4°C with 4 µg antibodies of anti-GFP, anti-Flag, anti-WT1, or normal rabbit or mouse IgG as controls, followed by precipitation with 60 µl protein A/G Plus-Agarose (Santa Cruz Biotechnology) for 3

h at 4°C. The precipitated complexes were washed three times with lysis buffer and boiled for 5 min in SDS sample buffer, followed by immunoblotting with various antibodies as indicated.

### **2.2.8 Nuclear and cytoplasmic fractionation**

For preparation of nuclear protein, human podocytes were washed twice with cold phosphate-buffered saline (PBS) and scraped off the plate with a rubber policeman. After centrifugation, cell pellets were resuspended in Buffer A (10 mM HEPES pH 7.9, 1.5 mM MgCl<sub>2</sub>, 10 nM KCl, 0.5% NP-40 and 1% protease inhibitor cocktail (Sigma)) and lysed with homogenizer. Cell nuclei were collected by centrifugation at 5,000 rpm for 15 min, and the supernatants were saved as cytoplasmic protein preparation. After washing with Buffer B (10 mM HEPES pH 7.9, 1.5 mM MgCl<sub>2</sub>, 10 nM KCl and 1% protease inhibitor cocktail), nuclei were lysed in SDS sample buffer. Isolated mouse glomeruli were collected and washed twice with cold phosphate-buffered saline (PBS). Nuclear protein preparation was made with NE-PER Nuclear and Cytoplasmic Extraction Reagents (Thermo Scientific, Rockford, IL).

### **2.2.9 Purification of GST fusion protein and pull down assay**

Bacterial BL21 competent cells were transformed with GST and GST-WT1 fusion protein expression vectors, respectively. Bacterial cells were cultured in LB medium containing ampicillin until the OD<sub>600</sub> reaches 0.6-0.8, followed by adding 100 µM IPTG to induce recombinant protein expression. After shaking at room temperature for 3 h, cell pellets were collected by spinning at 5,000 g for 10 min at 4°C. Bacterial cell lysis was prepared with Rapid GST Inclusion Body Solubilization and Renaturation Kit (Cell Biolabs, Inc., San Diego, CA).

Gluthinoe-agarose beads were used to incubate with bacterial cell lysis overnight at 4°C. Beads were washed three times with PBS containing 1% Triton X-100, and then incubated with podocyte lysates overnight at 4°C. The precipitated complex were washed three times with lysis buffer and boiled for 5 min in SDS sample buffer, followed by immunoblotting with various antibodies as indicated.

#### **2.2.10 Luciferase reporter assay**

The reporter construct pGL3-podocalyxin, which contains the human podocalyxin promoter sequence and the sequence for firefly luciferase, was constructed as described elsewhere [70]. After co-transfection with pGL3-podocalyxin and PINCH1 or/and WT1 expression vectors using Lipofectamine 2000 reagent (Invitrogen), podocytes were incubated for 48 h. The supernatants of cell lysates were collected for the luciferase assay. Luciferase activity was determined using the Dual Luciferase Assay System kit as described by the manufacturer's protocols (Promega). Relative luciferase activity of each group was reported as fold induction over the controls.

#### **2.2.11 Urinary albumin and creatinine assay**

Urine albumin level was measured by using a mouse Albumin ELISA Quantification kit, according to the manufacturer's protocol (Bethyl Laboratories, Montgomery, TX, USA). Urine creatinine was determined by a routine procedure as described previously [204].

### **2.2.12 Statistical analysis**

All data examined were expressed as mean  $\pm$  SEM. Statistical analysis was performed using SigmaStat software (Jandel Scientific Software, San Rafael, CA, USA). Comparison between groups was made using one-way analysis of variance (ANOVA), followed by Student-Newman-Keuls test. A *P* value of less than 0.05 was considered significant.

## **2.3 RESULTS**

### **2.3.1 Induction of PINCH1 expression by TGF- $\beta$ 1 in glomerular podocyte**

We first examined the expression of PINCH1 in human podocytes after incubation with TGF- $\beta$ 1, a potent fibrogenic cytokine that is shown to induce podocyte dysfunction in a wide variety of proteinuric chronic kidney diseases [210, 212]. As shown in Figure 5A, PINCH1 mRNA was significantly induced in cultured human podocytes following TGF- $\beta$ 1 stimulation, as demonstrated by a quantitative, real-time RT-PCR assay. This induction of PINCH1 mRNA started at 6 h, reached the peak at 24 h and sustained at least to 48 h after TGF- $\beta$ 1 treatment. Consistent with the mRNA expression, PINCH1 protein expression was also induced by TGF- $\beta$ 1 in podocytes, as illustrated by Western blot analyses of the whole cell lysates (Figure 5, B and C). TGF- $\beta$ 1 induced PINCH1 protein in a time-dependent manner, detected at 24 h and sustained at least to 72 h after treatment, time points that significantly lagged behind the mRNA induction. The induction of PINCH1 expression also occurred in a dose-dependent fashion; and TGF- $\beta$ 1 induced its protein level at the concentration as low as 0.5 ng/ml, which reached the

peak at 2 ng/ml. Further increase in TGF- $\beta$ 1 concentration did not result in additional induction of PINCH1 in podocytes.

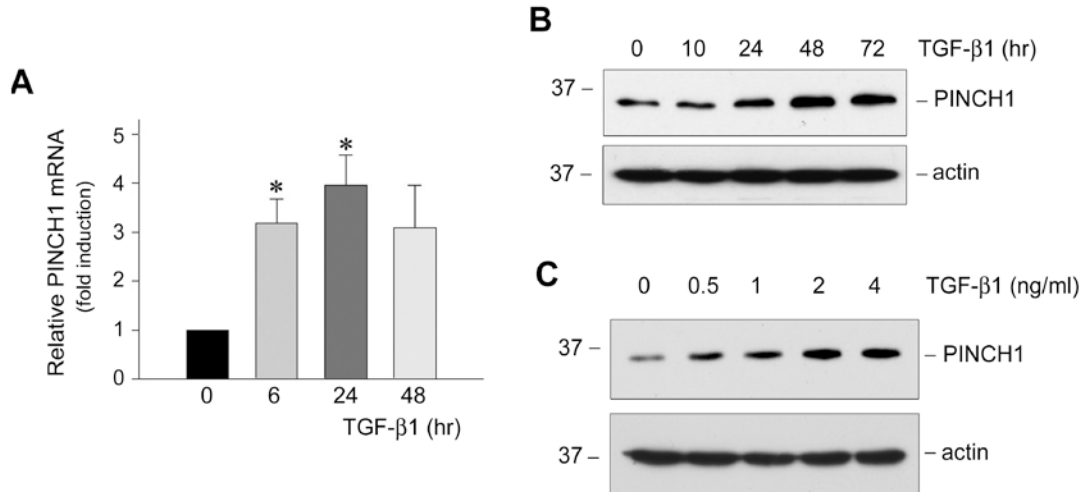


**Figure 5. TGF- $\beta$ 1 induces PINCH1 mRNA and protein expression in human podocytes.** A, Quantitative real-time RT-PCR reveals that TGF- $\beta$ 1 induced PINCH1 mRNA expression in a time-dependent manner. PINCH1 mRNA levels were assessed by quantitative real-time RT-PCR in human podocytes after TGF- $\beta$ 1 treatment (2 ng/ml) for various periods of time as indicated. Data are presented as mean  $\pm$  SEM of three experiments. \* $P$  < 0.05 versus controls. B and C, Western blot analyses demonstrate that TGF- $\beta$ 1 induced PINCH1 protein expression in a time- and dosage-dependent manner. Human podocytes were treated with a fixed amount of TGF- $\beta$ 1 (2 ng/ml) for various periods of time as indicated (B) or with various concentrations of TGF- $\beta$ 1 for 48 h (C). Total cell lysates were immunoblotted with specific antibodies against PINCH1 and actin, respectively.

### 2.3.2 Nuclear translocation of PINCH1 in podocytes after TGF- $\beta$ 1 stimulation

As an adaptor protein that binds to ILK, PINCH1 is primarily localized at the cell focal adhesion sites [213]. However, we found that PINCH1 was increasingly accumulated in the nuclei of podocytes after TGF- $\beta$ 1 stimulation. Subcellular fractionation experiments revealed that nuclear PINCH1 was dramatically increased in a dose-dependent fashion, while its levels in the cytoplasmic preparation declined after TGF- $\beta$ 1 treatment (Figure 6A). Quantitative

determination of the ratio of nuclear/cytoplasmic PINCH1 in podocytes after TGF- $\beta$ 1 treatment is presented in Figure 6B. These results indicate that TGF- $\beta$ 1 not only induces PINCH1 expression, but also triggers it to undergo nuclear translocation in podocytes.

To rule out the possibility that an increased nuclear accumulation of PINCH1 is a consequence of its over-expression, we next tested whether TGF- $\beta$ 1 directly promotes the nuclear translocation of endogenous PINCH1. To this end, we examined the nuclear accumulation of PINCH1 after a short incubation with TGF- $\beta$ 1, as it did not significantly induce PINCH1 protein expression until 24 h of incubation (Figure 5B). As shown in Figure 7A, incubation with TGF- $\beta$ 1 for 1 to 3 h was sufficient to induce nuclear translocation of endogenous PINCH1, indicating that TGF- $\beta$ 1-induced nuclear translocation of PINCH1 is regulated by a mechanism independent of its abundance.

To further confirm the nuclear translocation of PINCH1, we constructed an expression vector of GFP-PINCH1 fusion protein driven under CMV promoter. After transfection of this GFP-PINCH1 expression vector for 24 h, podocytes were treated with TGF- $\beta$ 1 for 24 h. We examined GFP-tagged PINCH1 subcellular distribution in podocytes using microscopy. As shown in Figure 7B, under basal conditions, GFP-PINCH1 was mainly localized in the peri-nuclear region of the cytoplasm, as well as at the focal adhesion sites in the periphery of spreading podocytes (Figure 7B, left panel, arrows), but little in the nuclei (Figure 7B, left panel, arrowhead). However, GFP-tagged PINCH1 diminished in the peri-nuclear region and accumulated in the nuclei of podocytes after TGF- $\beta$ 1 treatment (Figure 7B, right panel, arrowhead), although it remained present at the focal adhesion sites (Figure 7B, right panel, arrow). Quantitative calculation showed more than 60% of podocytes that exhibited GFP-PINCH1 in the nuclei after TGF- $\beta$ 1 stimulation, a significant increase over the controls (Figure



7C). To analyze this in a more quantitative way, we assessed nuclear and cytosol GFP-PINCH1 abundance by Western blotting. As shown in Figure 7D, nuclear GFP-PINCH1 was increased while its level in the cytoplasm declined, leading to a significant shift in the ratio of nuclear/cytoplasm GFP-PINCH1 after TGF- $\beta$ 1 treatment. Since GFP-tagged PINCH1 is controlled under CMV promoter, which is not regulated by TGF- $\beta$ 1, these results indicate that TGF- $\beta$ 1 is able to induce nuclear translocation of PINCH1 apparently by an active process independent of its protein abundance.

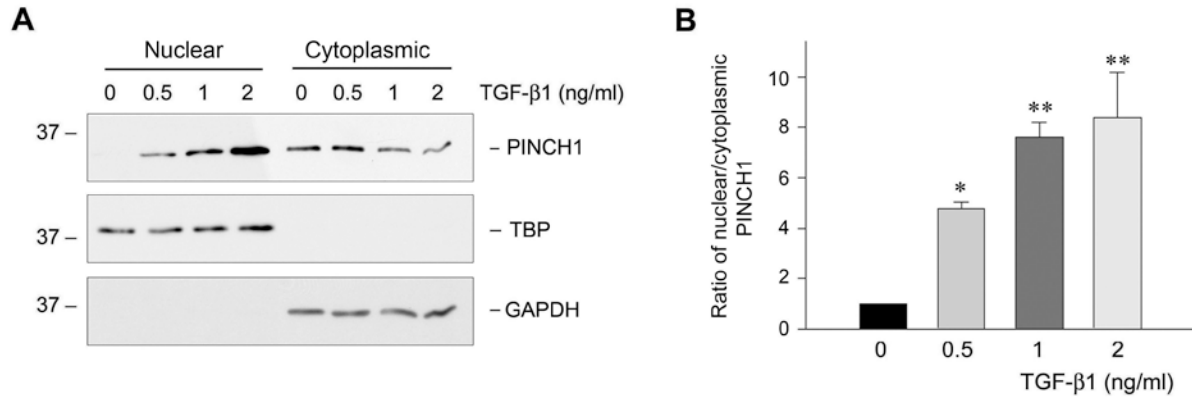


**Figure 6. TGF- $\beta$ 1 induces nuclear translocation of PINCH1 in human podocytes.** A, Western blot analyses show marked induction of PINCH1 protein in the nuclei of podocytes after TGF- $\beta$ 1 treatment. Podocytes were incubated with TGF- $\beta$ 1 at various concentrations as indicated for 72 h. Nuclear and cytoplasmic preparations were made and immunoblotted with specific antibodies against PINCH1, TATA box binding protein (TBP) and GAPDH, respectively. B, Graphic presentation shows the relative ratio of the nuclear/cytoplasmic PINCH1 protein in podocytes after TGF- $\beta$ 1 treatment. The value of the nuclear/cytoplasmic ratio of PINCH1 in the control group was set as 1.0. Data are presented as mean  $\pm$  SEM of four experiments. \* $P$  < 0.05, \*\* $P$  < 0.01 versus controls.

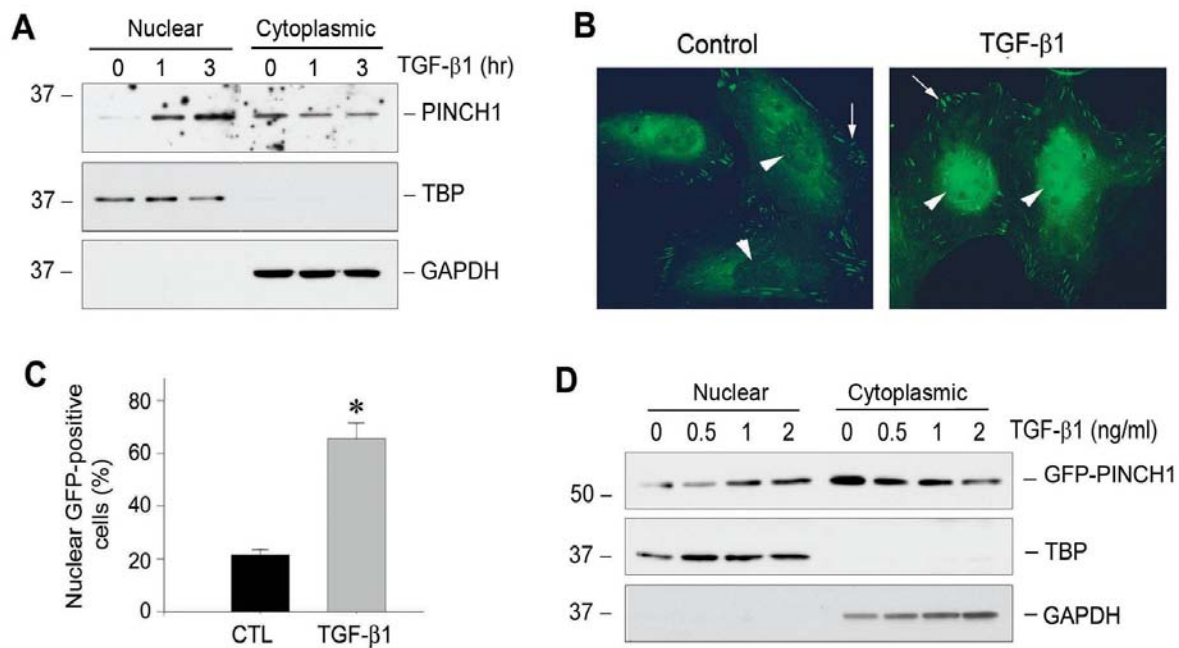


**Figure 7. PINCH1 nuclear translocation induced by TGF-β1 is regulated by a mechanism independent of its abundance.** A, Western blot analyses show nuclear accumulation of endogenous PINCH1 protein in podocytes after a short period of TGF-β1 treatment. Podocytes were incubated with TGF-β1 (2 ng/ml) for short periods of time as indicated. Nuclear and cytoplasmic proteins were separated and immunoblotted with specific antibodies against PINCH1, TBP and GAPDH, respectively. B, Representative micrographs show the sub-cellular localization of GFP-PINCH1 fusion protein in control or TGF-β1-treated podocytes. Podocytes were transfected with GFP-PINCH1 expression plasmid driven under CMV promoter for 24 h, and then incubated with TGF-β1 for additional 24 h at 2ng/ml. Arrows indicate the localization of PINCH1 in the focal adhesion, while arrowheads denote the nuclear localization of PINCH1. C, Graphic presentation shows the percentage of the podocytes with positive nuclear GFP protein after TGF-β1 treatment. Data are presented as mean  $\pm$  SEM of three experiments. \* $P < 0.05$  versus controls. D, Western blot analyses show an induction of GFP-PINCH1 protein in the nuclei of podocytes by TGF-β1. Nuclear and cytoplasmic proteins were separated and immunoblotted with specific antibodies against PINCH1, TBP and GAPDH, respectively.

### 2.3.3 Nuclear translocation of PINCH1 requires its putative NES/NLS motif

Bioinformatics analysis revealed that PINCH1 harbors a leucine-rich, putative nuclear export signal (NES) and an overlapping nuclear localization signal (NLS), consisting of charged, mostly

basic amino acids such as lysine and arginine in its C-terminus, as previously reported [167, 214]. Alignment of PINCH1 sequences derived from different species indicated that this region was highly conserved during evolution (Figure 8A). To test whether this putative NES/NLS is responsible for mediating cytoplasmic-nuclear shuttling of PINCH1, we generated the truncated, Flag-tagged PINCH1 expression vector (pFlag-PINCH1- $\Delta$ NES) in which the putative NES/NLS was deleted. In addition, we also constructed a Flag-tagged, wild-type PINCH1 (pFlag-PINCH1-wt), as well as two mutant PINCH1 expression vectors (pFlag-PINCH1-M1 and pFlag-PINCH1-M3) by site-directed mutagenesis, as illustrated in Figure 8B. These mutant PINCH1 vectors contained either one or three leucine to alanine (L/A) point mutations in its putative NES/NLS motif, respectively (Figure 8B). As shown in Figure 8C, deletion of putative NES/NLS almost completely blocked nuclear translocation of PINCH1, compared with the wild type PINCH1 controls. Furthermore, mutations at three leucine positions (M3) in the NES/NLS motif also rendered PINCH1 unable to undergo cytoplasmic-nuclear shuttling (Figure 8C). However, a single mutation at one leucine position (M1) only marginally reduced the nuclear accumulation of PINCH1 (Figure 8C). We further examined whether the putative NES/NLS is required for TGF- $\beta$ 1-induced nuclear translocation of PINCH1 by transfecting either wild-type or mutant PINCH1. As demonstrated in Figure 8D, TGF- $\beta$ 1 could induce wild-type, but not mutant (M3), PINCH1 nuclear translocation in podocytes. Therefore, it appears that the putative NES/NLS motif is required for mediating cytoplasmic-nuclear shuttling of PINCH1 under both basal and TGF- $\beta$ 1-stimulated conditions.

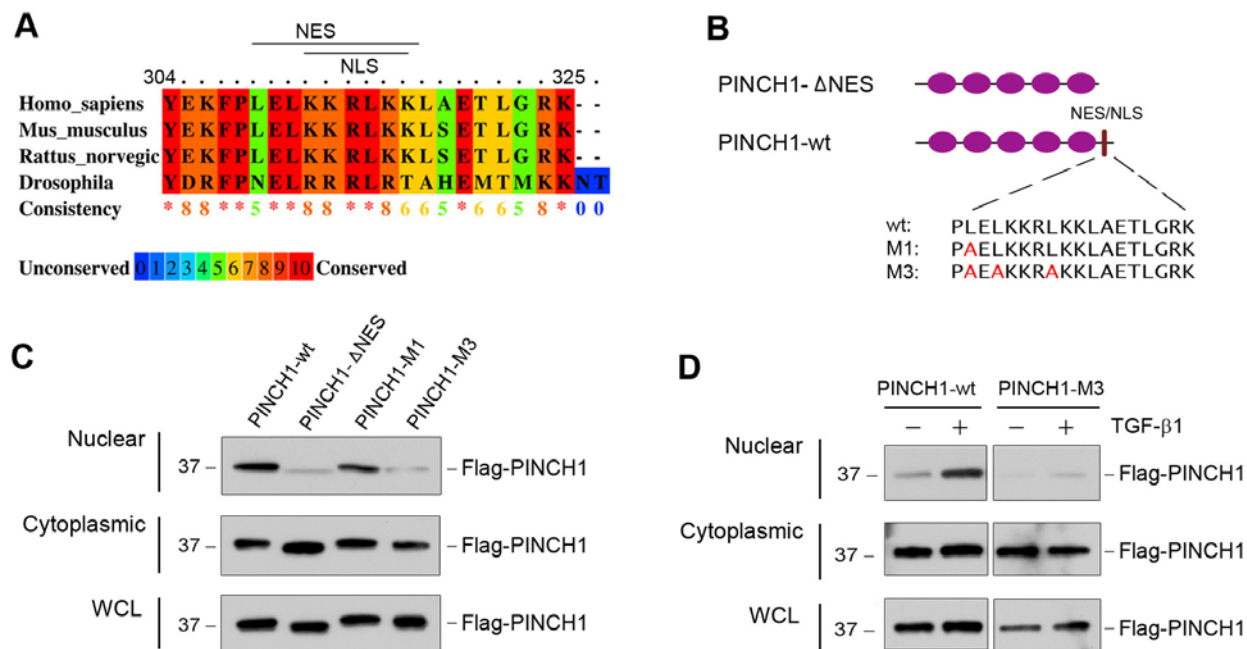


**Figure 8. Subcellular localization of PINCH1 is dictated by a putative motif in its C-terminus.** A, Amino acid sequence comparison reveals a conserved, overlapped, putative NES/NLS motif in the C-terminus of PINCH1 among different species including human, mouse, rat, and Drosophila. Alignments of the deduced amino acid sequences were performed by using PRALINE program. Color bar is a strength histogram that denotes the least to most conserved amino acids (least: dark blue, light blue, green, orange, red: most). B, Schematic diagram shows the structural domains of PINCH1 and construction of various PINCH1 mutants. Purple ovals indicate the five LIM domains. The position of a putative NES/NLS motif is shown by a bar, and the sequences of wild-type and mutant NES/NLS are given. C, Deletion or mutation of the putative NES/NLS blocks nuclear translocation of PINCH1 in podocytes. Human podocytes were transfected for 48 h with Flag-tagged wild-type PINCH1 (pFlag-PINCH1-wt), truncated PINCH1 without NES/NLS (pFlag-PINCH1-ΔNES), PINCH1 with single amino acid mutation in the NES/NLS motif (pFlag-PINCH1-M1) and PINCH1 with three amino acids mutation in the NES motif (pFlag-PINCH1-M3), respectively. Nuclear and cytoplasmic proteins were separated and immunoblotted with antibodies against Flag. D, TGF-β1 treatment fails to induce nuclear translocation of PINCH1 with mutant NES/NLS. Podocytes were transfected with wild-type PINCH1 (pFlag-PINCH1-wt) or mutant PINCH1 (pFlag-PINCH1-M3) for 48 h, respectively, and then treated TGF-β1 (2 ng/ml) for 3 h. Nuclear and cytoplasmic proteins were separated and immunoblotted with antibodies against Flag.

### **2.3.4 PINCH1 interacts with nuclear transcription factor WT1**

The finding that PINCH1 can shuttle into the nucleus prompted us to investigate its potential function in podocytes. In view of the structural characteristics of PINCH1, which contains five LIM domains that mediate protein-protein interactions, we reasoned that PINCH1 might interact with other nuclear proteins that are important for podocyte biology. Along this line, we revealed that PINCH1 could interact with WT1, a transcription factor that is exclusively expressed in podocytes in adult kidney. As shown in Figure 9A, when Flag-tagged PINCH1 and GFP-tagged WT1 were co-expressed in podocytes, PINCH1 could be detected in the immunocomplexes precipitated by anti-GFP antibody. In reciprocal experiments, after transfection of podocytes with Flag-tagged PINCH1 expression vector, endogenous WT1 was found in the immunocomplexes precipitated with anti-Flag antibody (Figure 9B). These interactions between PINCH1 and WT1 appeared specific, as replacing specific antibodies with control IgG did not result in any binding (Figure 9, A and B). Furthermore, physical interaction between endogenous PINCH1 and WT1 was detectable in podocytes after TGF- $\beta$ 1 stimulation (Figure 9C), suggesting that PINCH1/WT1 complex formation actually occurs in patho-physiologically relevant conditions.

To further confirm the specificity of PINCH1/WT1 interaction, we employed a GST-fusion protein pull down experiment to examine the interaction between PINCH1 and WT1. To this end, we generated a GST-WT1 fusion protein using a bacterial expression system. As shown in Figure 9D, GST-WT1 fusion protein as well as GST control protein was purified. When these purified proteins were immobilized on glutathione-agarose beads and incubated with podocyte lysates, PINCH1 was pulled down and detected in the assay (Figure 9E), indicating a specific interaction between PINCH1 and WT1. Of note, PINCH2, a protein that is closely

related to and shares a high degree of structural homology with PINCH1, also interacted with WT1 (Figure 9F).

### **2.3.5 Delineation of the structural domains mediating PINCH1/WT1 interaction**

To define the structural domains responsible for mediating PINCH1/WT1 interaction, we generated a series of Flag-tagged, truncated PINCH1 expression vectors containing different LIM domains (Figure 10A). After these constructs were co-transfected with GFP-tagged WT1 expression vector into podocytes, physical interaction between different domains of PINCH1 and WT1 were assessed by co-immunoprecipitation. As shown in Figure 10B, all truncated PINCH1 proteins that contained LIM1 domain were detected in the immunocomplexes precipitated by anti-GFP antibody, whereas those PINCH1 proteins without LIM1 were not found in the immunoprecipitates under the same conditions. These results indicate that the LIM1 domain of PINCH1 mediates its interaction with WT1 (Figure 10B).

We also sought to determine the structural domain of WT1 that is involved in its interaction with PINCH1. To this end, we generated two GFP-tagged expression vectors that contained either N-terminal, proline/glutamine-rich regulatory domain (1-315 aa) (WT1-NT) or C-terminal, DNA-binding domain (280-429 aa) (WT1-CT) containing four zinc fingers of the Kruppel-type (Figure 10C), respectively. When these expression vectors were co-transfected with Flag-tagged PINCH1 construct in podocytes, potential interaction between truncated WT1 and PINCH1 was examined by co-immunoprecipitation. As shown in Figure 10, D and E, PINCH1 was only detected in the immunocomplexes in podocytes over-expressing GFP-tagged C-terminus of WT1 (WT1-CT), but not in the cells transfected with expression vector encoding

N-terminus of WT1 (WT1-NT). Therefore, it appears clear that the C-terminal zinc-finger domains of WT1 mediate its interaction with PINCH1.

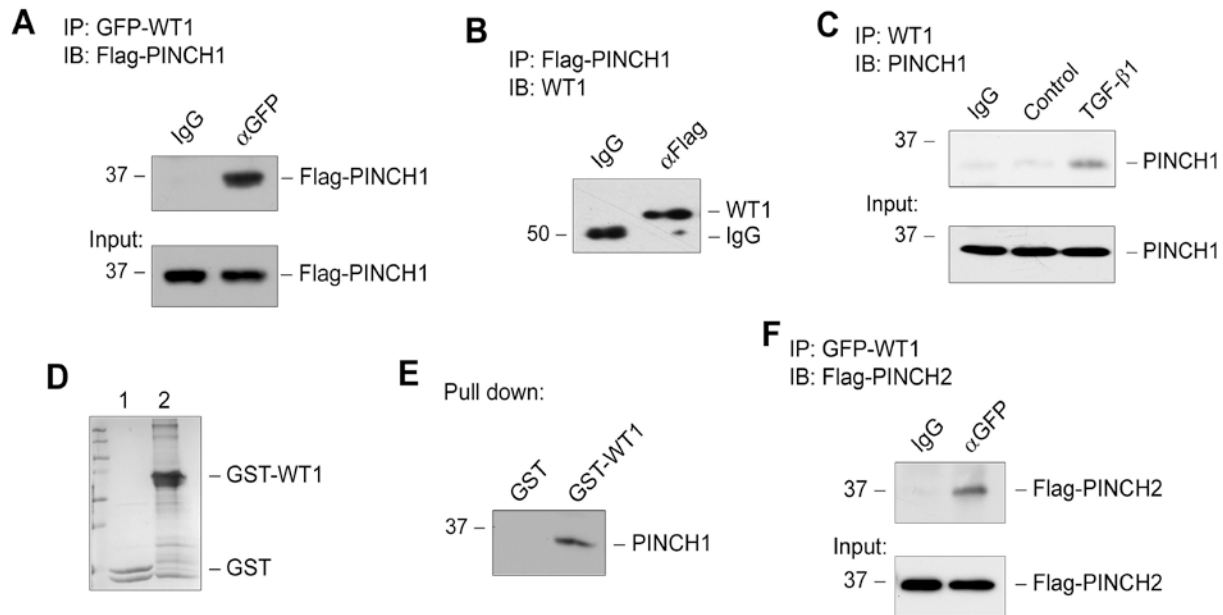


**Figure 9. PINCH1 physically interacts with nuclear transcription factor WT1 in human podocytes.** A, Co-immunoprecipitation demonstrates a complex formation between PINCH1 and WT1. Human podocytes were transfected with Flag-PINCH1 and GFP-WT1 for 48 h. Cell lysates were immunoprecipitated with specific antibody against GFP, followed by immunoblotting with antibody against Flag. IgG, control rabbit IgG. B, Co-immunoprecipitation shows a complex formation between PINCH1 and WT1. Human podocytes were transfected with Flag-PINCH1 for 48 h. Cell lysates were immunoprecipitated with specific antibody against Flag, followed by immunoblotting with antibody against endogenous WT1. IgG, control mouse IgG. C, Endogenous WT1 and PINCH1 interact after TGF-β1 treatment in podocytes. Human podocytes were treated with TGF-β1 (2 ng/ml) for 24 h. Cell lysates were immunoprecipitated with anti-WT1 antibody, followed by immunoblotting with anti-PINCH1. D, Coomassie blue staining shows the purified GST tagged proteins expressed in bacterial BL21. Lane 1, purified GST. Lane 2, purified GST-WT1 fusion protein. E, Pull-down assay revealed a complex formation between PINCH1 and WT1. Purified GST-WT1 protein as well as control GST protein was incubated with podocyte lysate overnight, followed by immunoblotting with antibody against PINCH1. F, PINCH2 also interacts with WT1. Cells were transfected with Flag-PINCH2 and GFP-WT1 for 48 h. IgG, control rabbit IgG.

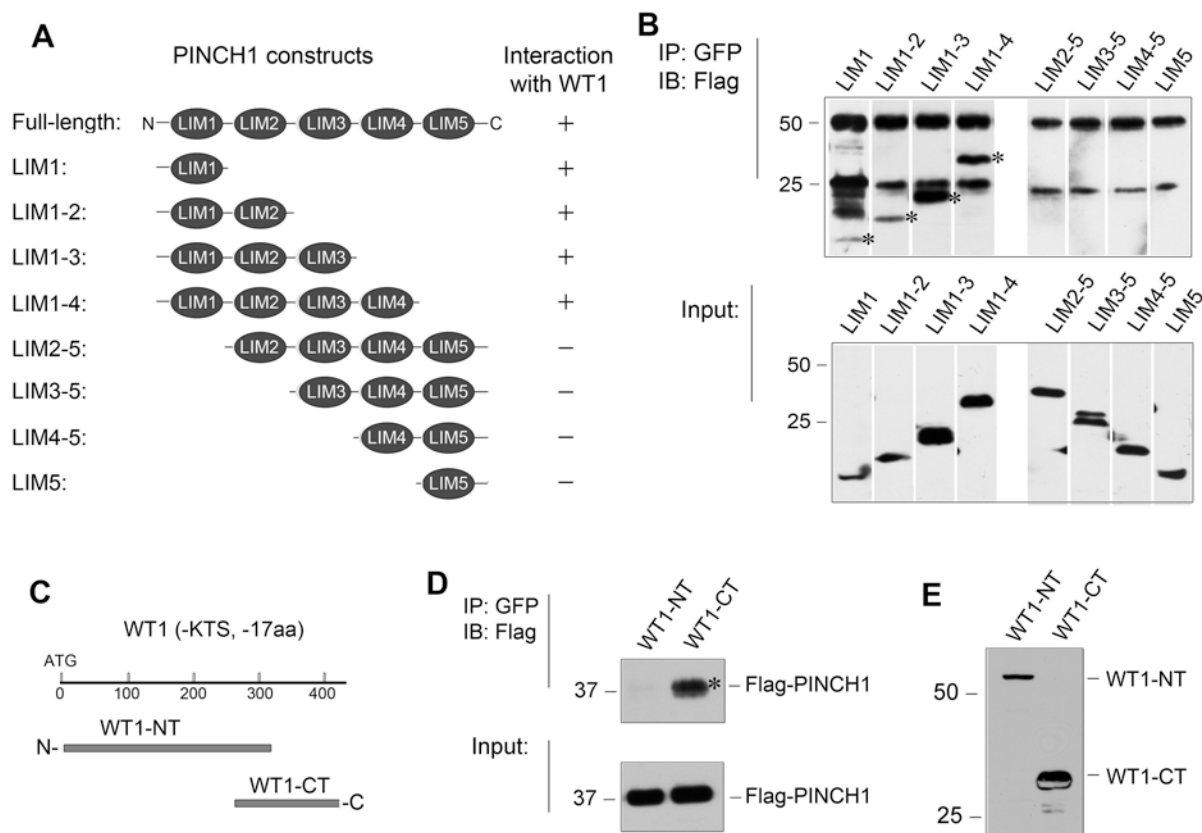


**Figure 10. Delineation of the structural domains that mediate PINCH1/WT1 interaction.**

A, Schematic diagram shows the construction of various Flag-tagged PINCH1 expression vectors containing different LIM domains. B, Co-immunoprecipitation indicates that the LIM1 domain of PINCH1 mediates the interaction with WT1. Human podocytes were co-transfected with various Flag-tagged PINCH1 LIM domains and GFP-WT1 for 48 h. Cell lysates were immunoprecipitated with specific antibody against GFP, followed by immunoblotting with antibody against Flag. Asterisk (\*) indicate positive interactions. C, Diagram shows the constructions of GFP tagged WT1 fragments. The WT1 used is the isoform without KTS and 17 aa encoded by exon 5 (WT1, -KTS, -17 aa). WT1-NT, N-terminal fragment of WT1 (1-315 aa); WT1-CT, C-terminal fragment of WT1 (280-429 aa). D, Co-immunoprecipitation shows that PINCH1 interacted with WT1-CT, but not WT1-NT. Human podocytes were transfected with Flag-PINCH1 and either GFP-tagged WT1-NT or GFP-tagged WT1-CT for 48 h. Cell lysates were immunoprecipitated with specific antibody against GFP, followed by immunoblotting with anti-Flag. E, Expression of GFP-tagged WT1 fragments in podocytes after transfection were confirmed by Western blot analysis.



### **2.3.6 PINCH1 represses WT1-mediated podocalyxin expression**

To examine the potential consequence of PINCH1/WT1 interaction, we investigated the effects of PINCH1 on WT1-mediated gene expression. Podocalyxin, a transmembrane protein that plays a crucial role in the maintenance of podocyte morphology and foot processes [215], is well characterized as a WT1 target gene. Indeed, we found that ectopic expression of WT1 in podocytes significantly induced podocalyxin mRNA and protein expression (Figure 11, A through C). However, co-transfection of PINCH1 largely abolished WT1-mediated podocalyxin induction. Of note, PINCH1 had the tendency, although not significantly, to inhibit basal podocalyxin mRNA expression in the absence of exogenous WT1 (Figure 11, A and B), suggesting that podocalyxin is also controlled by endogenous WT1 in podocytes. Likewise, knockdown of PINCH1 increased podocalyxin mRNA expression in podocytes (Figure 11, D and E). Therefore, it becomes clear that PINCH1 interacts with WT1, which leads to suppression of the WT1-mediated gene expression in podocytes.

We further investigated the effects of PINCH1 on podocalyxin gene transcription using a promoter-luciferase reporter assay. A podocalyxin promoter luciferase reporter vector containing a putative WT1 response element at the nucleotide positions -1213 to -1227 was constructed, as previously reported [70]. We found that co-transfection of the WT1 expression vector significantly stimulated the podocalyxin promoter luciferase activity in podocytes, compared to empty vector pcDNA3 (Figure 11F). However, when PINCH1 was co-expressed, the WT1-mediated podocalyxin promoter-luciferase activity was suppressed, compared with transfection with WT1 alone (Figure 11F). Therefore, consistent with the suppression of podocalyxin protein and mRNA, PINCH1 also abolishes the WT1-mediated transcription of podocalyxin gene.

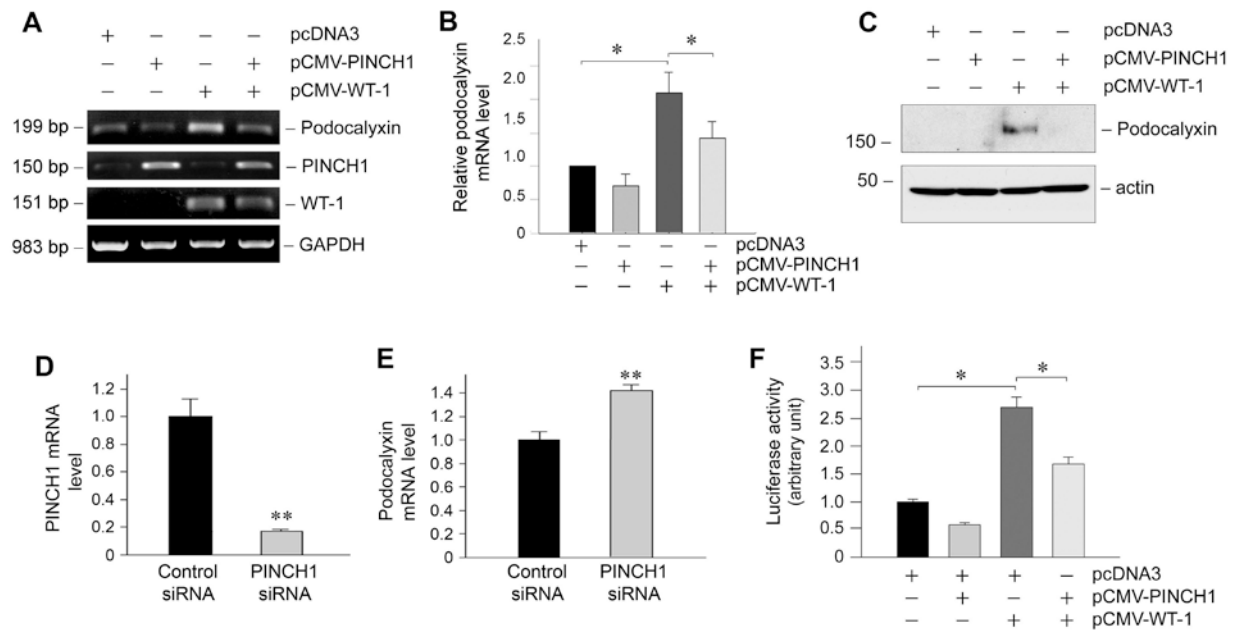


**Figure 11. PINCH1 blocks WT1-mediated podocalyxin expression in human podocytes.** A, RT-PCR analyses demonstrate that PINCH1 blocked WT1-stimulated podocalyxin mRNA expression in podocytes. Cells were transfected with expression vectors for PINCH1, WT1 or both, respectively. RT-PCR amplification of housekeeping GAPDH was performed in an identical manner to serve as controls. B, Graphic presentation shows the relative PINCH1 mRNA abundance in different groups after normalization with GAPDH. Data are presented as mean  $\pm$  SEM of three independent experiments.  $*P < 0.05$ . C, Western blot analyses show that PINCH1 blocked WT1-mediated podocalyxin protein expression. Human podocytes were transfected with different plasmids as indicated for 48 h. Total cell lysates were immunoblotted with specific antibodies against podocalyxin and actin, respectively. D and E, Knockdown of PINCH1 in podocytes promotes podocalyxin expression. Human podocytes were transfected with either control or PINCH1-specific siRNA at 100nM. The expression of PINCH1 (D) and podocalyxin (E) was assessed by quantitative RT-PCR.  $**P < 0.01$  ( $n = 3$ ). F, PINCH1 represses WT1-activated podocalyxin gene promoter activity. Human podocytes were co-transfected with different plasmids as indicated with luciferase - podocalyxin gene promoter reporter construct (pGL3-podocalyxin) for 48 h. Equal amounts of DNA were present in each transfection. Data are presented as mean  $\pm$  SEM of three independent experiments.  $*P < 0.05$ .

### 2.3.7 PINCH1/WT1 interaction occurs *in vivo* and is associated with proteinuria

To explore the pathophysiological relevance of PINCH1 nuclear translocation *in vivo*, we examined the endogenous PINCH1/WT1 interaction in mouse glomeruli after TGF- $\beta$ 1 stimulation. Expression plasmid encoding constitutively active TGF- $\beta$ 1 was administrated into mice through a single intravenous injection by using a hydrodynamic-based gene delivery approach, as previously described [205-206]. As shown in Figure 12A, PINCH1 also underwent nuclear translocation in the glomerular cells *in vivo* after TGF- $\beta$ 1 stimulation. Furthermore, co-immunoprecipitation demonstrated a physical interaction between endogenous PINCH1 and WT1 in the isolated glomeruli *in vivo*, which was induced by TGF- $\beta$ 1 in a time-dependent manner (Figure 12B). Notably, PINCH1 abundance in the glomerular lysates was also slightly increased at 24 hours after pCA-TGF- $\beta$ 1 injection (Figure 12B, Input). Of note, such a PINCH1/WT1 interaction was associated with proteinuria in mice (data not shown). Taken together, it is clear that after stimulation with TGF- $\beta$ 1, endogenous PINCH1 also undergoes nuclear translocation and interacts with WT1 *in vivo*, which is associated with onset of proteinuria.

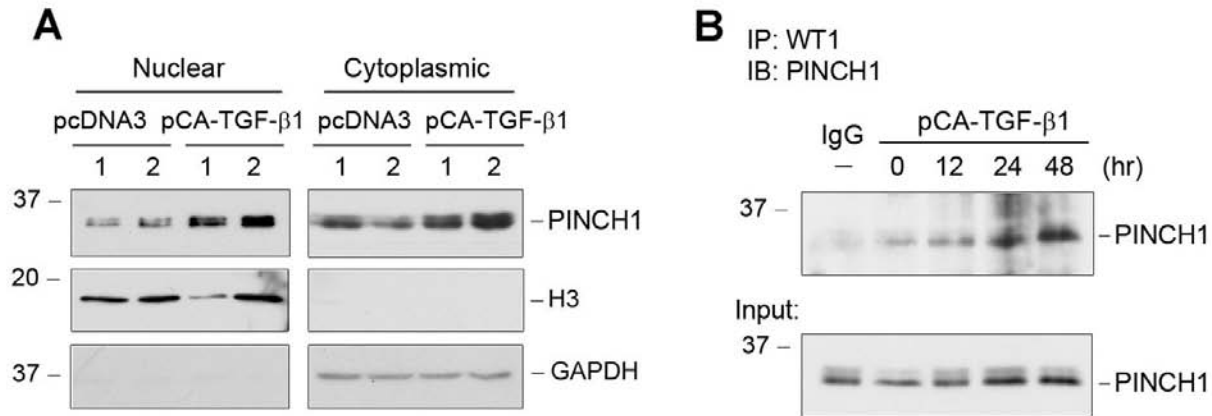


**Figure 12. PINCH1 undergoes nuclear translocation and forms interaction with WT1 *in vivo*.** A, PINCH1 undergoes nuclear translocation in glomerular cells. Glomeruli were isolated from mouse kidneys at 24 hours after injection of plasmids (pcDNA3 or pCA-TGF- $\beta$ 1). Nuclear and cytoplasmic proteins from the isolated glomeruli were prepared and immunoblotted with antibodies against PINCH1, histone H3 (H3) or GAPDH, respectively. Numbers (1 and 2) indicate each individual glomerular preparation, which was made from a pool of kidneys from two mice. B, PINCH1 interacts with WT1 *in vivo*. Glomerular lysates at different time points after injection of TGF- $\beta$ 1 expression plasmid were immunoprecipitated with anti-WT1 antibody, followed by immunoblotting with anti-PINCH1. Whole glomerular lysates were also immunoblotted with anti-PINCH1.

## 2.4 DISCUSSION

PINCH1 is an adaptor/scaffolding protein that constitutively interacts with ILK and localizes at focal adhesion sites. In this study, we provide evidence demonstrating that PINCH1 also functions as a transcriptional regulator by interacting with nuclear WT1, a podocyte-specific transcription factor that plays a pivotal role in the establishment and maintenance of the unique differentiated features of podocytes in adult kidney. We show that PINCH1 is up-regulated in podocytes after stimulation with TGF- $\beta$ 1, translocates into the nucleus, wherein it binds to WT1

and suppresses the WT1-mediated gene transcription. Our results uncover a novel pathway in which PINCH1 controls gene transcription by interacting with the nuclear transcription factor WT1 in podocytes.

As a LIM-only adaptor protein, PINCH1 is a well known to interact with cytoplasmic ILK and modulates integrin signaling [216-217]. In glomerular podocytes, PINCH1 likely plays an imperative role in bridging the cell-cell slit diaphragm and cell-matrix integrin signaling by participating in the nephrin/ILK complex formation [211]. It is well established that PINCH1 through its LIM1 domain binds to the ankyrin repeat domain of ILK [160], while its LIM4 domain interacts with the third SH3 domain of Nck [165], another cytoplasmic adaptor protein that binds to nephrin through its SH2 domain [218-219]. As a result, PINCH1, together with Nck, essentially builds a physical connection between nephrin and ILK. This notion is supported by an earlier observation that ILK is physically linked to nephrin, as shown by co-immunoprecipitation and co-localization [211]. Conditional ablation of ILK in a podocyte-specific fashion leads to aberrant nephrin distribution by disrupting this multi-component complex formation, thereby causing podocyte dysfunction, proteinuria, kidney failure and premature animal death [211]. Interestingly, ILK/PINCH1 complex formation is decreased in glomerular podocytes after treatment with TGF- $\beta$ 1 [159], although both ILK and PINCH1 are upregulated in these cells. These observations support our present results that PINCH1 undergoes nuclear translocation in podocytes after stress/injury.

In view of the presence of a putative NES/NLS motif in its C-terminus, it is not completely surprising that PINCH1 undergoes cytoplasmic-nuclear shuttling. Indeed, this NES/NLS motif is evolutionarily conserved, functionally important and obligatory for mediating nuclear translocation of PINCH1, as deletion or site-directed mutations of this motif effectively

prevents cytoplasmic-nuclear shuttling of PINCH1 in podocytes under basal and TGF- $\beta$ 1-stimulated conditions (Figure 8). However, at this stage we cannot exclude the possibility that deletion or mutation of NES/NLS motif may cause a structural perturbation, leading to disruption of the PINCH1 function, as leucine residues in the motif may play a critical role in stabilizing the overall structure of the protein.

It is conceivable that a small fraction of PINCH1 may be localized constitutively in the nuclei under basal conditions. Along that line, there are three possible sub-cellular, nuclear, cytoplasmic and focal adhesion-associated, pools of PINCH1 in podocytes. Each specific pool of PINCH1 may have different functions. While the focal adhesion-associated PINCH1 may play a critical role in modulating cell adhesion, cell shape and survival [168], we show here that nuclear PINCH1 is instrumental in regulating gene transcription via its interaction with WT1. Cellular stress/injury after TGF- $\beta$ 1 treatment accelerates the rate of its cytoplasmic-nuclear shuttling, resulting in an increased accumulation of PINCH1 in the nuclei, but it does not appear to significantly affect the focal adhesion-associated PINCH1 (Figure 7B). Nuclear accumulation of PINCH1 is unlikely a passive consequence of an increased overall level of its protein, since TGF- $\beta$ 1 also promotes nuclear translocation of PINCH1 after a short period of incubation (1-3 hours) (Figure 7A) when significant PINCH1 induction was not evident (Figure 5B). Such a PINCH1 shuttling between cytoplasm and nucleus is also reported in Schwann cells after chronic constriction injury in adult rats [167]. Consistently, several other LIM-containing proteins are found to be able to undergo cytoplasmic-nuclear shuttling [163, 220-221]. In this context, it is reasonable to conclude that PINCH1 is able to translocate into the nuclei, thereby initiating new protein-protein interactions and participating in the control of gene transcription in diverse circumstances.

One of the novel findings in the present study is the identification of WT1 transcription factor as the binding partner for PINCH1 in the nuclei. Through defining the molecular details of PINCH1/WT1 interaction, it is revealed that the LIM1 domain of PINCH1 mediates its interaction with WT1, whereas the C-terminal zinc-finger domains of WT1 are responsible for its binding to PINCH1 (Figure 10). Notably, the same LIM1 domain mediates PINCH1 interaction with ILK in the cytoplasm at the focal adhesion sites. Therefore, LIM1 domain of PINCH1 is practically responsible for its interaction with either cytoplasmic ILK or nuclear WT1, depending on its specific localization within podocytes at a given setting. Because WT1, a key transcription factor that is exclusively expressed in glomerular podocytes in adult kidney, plays a critical role in establishing the unique features of podocytes by inducing specific gene expression, such a PINCH1/WT1 interaction likely has a detrimental consequence. Indeed, endogenous PINCH1/WT1 interaction actually occurs in podocytes after TGF- $\beta$ 1 stimulation both *in vitro* (Figure 9C) and *in vivo* (Figure 12B). It should be noted that it remains to be determined what consequence can be caused directly by PINCH1/WT1 interaction. Similarly, interaction between WT1 and the WT1-interacting protein (WTIP), another LIM-containing protein, is previously shown to lead to the suppression of WT1-mediated gene expression and podocyte dysfunction [220-221].

PINCH1 cytoplasmic-nuclear shuttling and subsequent interaction with WT1 might influence the WT1-mediated gene expression in podocytes. In that regard, it is revealed that PINCH1 regulates the expression of podocalyxin, a well-characterized podocyte-specific protein that is transcriptionally controlled by WT1. Earlier *in vivo* and *in vitro* studies demonstrate that WT1 level and activity directly dictate podocalyxin expression in glomerular podocytes [70, 73, 215]. Indeed, ectopic expression of WT1 in cultured podocytes induces podocalyxin mRNA and

protein expression (Figure 11). Given that PINCH1 binds to the zinc-finger domains of WT1, it is not unexpected that over-expression of PINCH1 abolishes WT1-mediated podocalyxin expression, while knockdown of PINCH1 induced podocalyxin expression (Figure 11). Podocalyxin is a CD34-related, transmembrane, sialoglycoprotein that contains a highly charged cytoplasmic tail [215]. It is connected to the cortical actin cytoskeleton via ezrin and Na<sup>+</sup>/H<sup>+</sup>-exchanger regulatory factor 2 (NHERF2) and plays an essential role in maintaining the foot process structure and filtration function. Disruption of podocalyxin/NHERF2/ezrin/actin interactions leads to pathologic conditions associated with changes in podocyte foot processes [222]. Consistently, podocalyxin-deficient mice fail to form foot processes and slit diaphragm and die within 24 hours after birth with anuric renal failure [64]. Therefore, suppression of WT1-mediated gene expression by PINCH1 could be a potential pathway leading to podocyte dysfunction.

In summary, we have shown that PINCH1, an adaptor protein that is associated with ILK at the focal adhesion site, can undergo cytoplasmic-nuclear shuttling in podocytes. Nuclear PINCH1 via its LIM1 domain interacts with a new partner WT1. By interacting with the zinc finger domains of WT1, PINCH1 effectively blocks WT1-mediated gene transcription. Our data provide a proof of principle that PINCH1 can function as a transcriptional regulator by repressing WT1-mediated gene expression, and these studies could set a foundation for future investigations.



### **3.0 WNT/ $\beta$ -CATENIN SIGNALING MEDIATES TGF- $\beta$ 1-DRIVEN PODOCYTE INJURY AND PROTEINURIA**

#### **3.1 ABSTRACT**

TGF- $\beta$ 1, a potent fibrogenic cytokine, is upregulated in virtually all kinds of chronic kidney diseases, and its over-expression in transgenic mice is associated with podocyte injury and proteinuria. However, how TGF- $\beta$ 1 induces podocyte dysfunction and proteinuria *in vivo* remains poorly understood. Here we show that Wnt/ $\beta$ -catenin signaling plays a critical role in mediating podocyte injury and proteinuria induced by TGF- $\beta$ 1. *In vitro*, treatment with TGF- $\beta$ 1 induced the expression of several Wnts, predominantly Wnt1, and activated  $\beta$ -catenin in mouse podocytes. Wnt antagonist Dickkopf-1 (DKK1) blocked TGF- $\beta$ 1-induced  $\beta$ -catenin activation and preserved nephrin expression. *In vivo*, ectopic expression of constitutively active TGF- $\beta$ 1 induced Wnt1 expression, activated glomerular  $\beta$ -catenin, and upregulated its downstream target genes such as Snail1, MMP-7, MMP-9, desmin and fibroblast-specific protein 1 (Fsp1), which led to podocyte injury and proteinuria. Consistently, concomitant expression of DKK1 gene abolished  $\beta$ -catenin activation in mouse glomeruli, inhibited the TGF- $\beta$ 1-triggered Wnt/ $\beta$ -catenin target genes including Snail1, MMP-7, MMP-9, LEF-1 and plasminogen activator inhibitor-1, and reduced albuminuria. These results establish a role for Wnt/ $\beta$ -catenin signaling

in the pathogenesis of podocyte injury. Our data also suggest that this signaling pathway could be exploited as a therapeutic target for the treatment of proteinuric kidney diseases.

## **3.2 MATERIALS AND METHODS**

### **3.2.1 Cell culture and treatment**

The conditionally immortalized mouse podocyte cell line was kindly provided by Dr. Peter Mundel (Mount Sinai School of Medicine, New York, NY), as described previously [42]. To propagate podocytes, cells were cultured at 33°C in RPMI-1640 medium supplemented with 10% fetal bovine serum (FBS) and recombinant IFN- $\gamma$  (Invitrogen, Carlsbad, CA). To induce differentiation, podocytes were grown under nonpermissive conditions at 37°C in the absence of IFN- $\gamma$ . Podocytes were treated with recombinant TGF- $\beta$ 1 (R & D Systems, Minneapolis, MN) at the concentration of 2 ng/ml, unless otherwise indicated. Recombinant mouse DKK1 (R&D Systems, Inc., Minneapolis, MN) was used for pretreatment at 40 or 200 ng/ml for 1 h, followed by incubation with TGF- $\beta$ 1 for 24 h. For some studies, podocytes were transiently transfected with either HA-tagged Wnt1 expression vector (pHA-Wnt1; Upstate Biotechnology, Lake Placid, NY), or Flag-tagged N-terminal truncated, stabilized  $\beta$ -catenin expression vector (pDel- $\beta$ -cat) by using Lipofectamine 2000 reagent (Invitrogen, Carlsbad, CA), as described previously [204].

### 3.2.2 Animal models

Male BALB/c mice that weighed approximately 18 to 20 g were purchased from Harlan Sprague Dawley (Indianapolis, IN). For delivery of mouse TGF- $\beta$ 1 gene, constitutively active TGF- $\beta$ 1 expression plasmid (pCA-TGF- $\beta$ 1), in which two cysteines at the positions 223 and 225 were mutated into serines, was injected intravenously at 0.3 mg/kg body wt by using of a hydrodynamics-based *in vivo* gene transfer approach, as described previously [205-206]. For delivery of human DKK1 gene, naked DKK1 expression plasmid (pFlag-DKK1; provided by Dr. Xi He, Harvard Medical School, Boston, MA) was injected intravenously at 2 mg/kg body wt by using the same approach with or without pCA-TGF- $\beta$ 1 plasmid. Control mice were administered an injection of empty vector pcDNA3 plasmid in an identical manner. Mice were sacrificed at day 1 and day 2 after injection, and kidney tissues were collected for various analyses. One part of the kidneys was fixed in 10% phosphate-buffered formalin for histologic and immunohistochemical studies after paraffin embedding. Another part was immediately frozen in OCT compound for cryosection. The remaining kidneys were snap-frozen in liquid nitrogen and stored at -80°C for protein extractions. Animal protocols were approved by the Institutional Animal Care and Use Committee at the University of Pittsburgh.

### 3.2.3 Isolation of glomeruli

Glomeruli were isolated by differential sieving technique according to the method described elsewhere [207]. Briefly, the kidneys were excised and pressed with a spatula through a stainless steel screen of #100 mesh and rinsed with 1% albumin in cold phosphate-buffered saline (PBS-A) through successive screens of #200 mesh and #282 mesh, respectively. The glomeruli were

collected on the #282-mesh screen and suspended in PBS-A. After centrifugation at 200 g for 10 min, the isolated glomeruli (purity, ~80%) were collected for subsequent analyses.

#### **3.2.4 Urinary albumin and creatinine assay**

Urinary albumin level was measured by using a mouse Albumin ELISA Quantification kit, according to the manufacturer's protocol (Bethyl Laboratories, Montgomery, TX, USA). Urine creatinine was determined by a routine procedure as described previously [204].

#### **3.2.5 Construction of pCA-TGF- $\beta$ 1 vector**

The expression plasmid vectors containing mouse wild-type TGF- $\beta$ 1 (pWT-TGF- $\beta$ 1), N-terminus truncated TGF- $\beta$ 1 (pNT-TGF- $\beta$ 1) and constitutively active TGF- $\beta$ 1 (pCA-TGF- $\beta$ 1) were constructed by using standard molecular cloning techniques. The pCA-TGF- $\beta$ 1 vector contained two cysteine to serine mutations at the positions 223 and 225 (C223S/C225S). This expression vector was made by using QuikChange II XL site-directed mutagenesis kit, and it produces bioactive TGF- $\beta$ 1 that does not require acid activation, as previously reported [208]. The correct sequences of different expression vectors were confirmed by sequencing at the DNA Sequencing Core Facility of the University of Pittsburgh.

#### **3.2.6 RT-PCR and real-time PCR**

Total RNA was extracted using the TRIzol RNA isolation system (Invitrogen, Carlsbad, CA). The first strand of cDNA was synthesized using 2  $\mu$ g of RNA in 20  $\mu$ l of reaction buffer by

reverse transcription using AMV-RT (Promega, Madison, WI) and random primers at 42°C for 30 min. PCR was carried out using a standard PCR protocol with 1 µl aliquot of cDNA, HotStarTaq polymerase (Qiagen, Valencia, CA) and specific primer pairs. The sequences of the primer pairs were shown in Table 3. For quantitative determination of mRNA levels, a real-time RT-PCR was performed on ABI PRISM 7000 Sequence Detection System (Applied Biosystems, Foster City, CA), as described previously [209]. The PCR reaction mixture in a 25 µl volume contained 12.5 µl of 2x SYBR Green PCR Master Mix (Applied Biosystems), 10 µl of diluted RT product (1: 10), and 0.5 µM sense and antisense primer sets. PCR reaction was run by using standard conditions [209]. After sequential incubations at 50°C for 2 min and 95°C for 10 min, respectively, the amplification protocol consisted of 40 cycles of denaturing at 95°C for 15 sec, and annealing and extension at 60°C for 60 sec. The mRNA levels of various genes were calculated after normalizing with  $\beta$ -actin.

**Table 3. Nucleotide sequences of the primers used for RT-PCR**

<b>Mouse gene</b>	<b>Primer sequence of sense</b>	<b>Primer sequence of anti-sense</b>
nephrin	CCCAACACTGGAAGAGGTGT	CTGGTCGTAGATTCCCCTTG
Snail	ATTCTCCTGCTCCCACTGC	ACTCTTGGTGCTTGTGGAG
MMP9	CACCACCACAACTGAACCAC	CTCAGAAGAGCCCGCAGTAG
MMP7	TAGGCGGAGATGCTCACTTT	TTCTGAATGCCTGCAATGTC
FSP-1	AGCTACTGACCAGGGAGCTG	TCATTGTCCCTGTTGCTGTC
PAI-1	TCATCAATGACTGGGTGGAA	TGCTGGCCTCTAAGAAAGGA
LEF-1	AAATGGGTCCCTTTCTCCAC	CATCTGACGGGATGTGTGAC

β-actin	CAGCTGAGAGGGGAAATCGTG	CGTTGCCAATAGTGATGACC
Wnt1	GCCCTAGCTGCCAACAGTAGT	GAAGATGAACGCTGTTTCTCG
Wnt2	AGAGTGCCAACACCAGTTCC	TACAGGAGCCACTCACACCA
Wnt2b	TTGTGTCAACGCTACCCAGA	ACCACTCCTGCTGACGAGAT
Wnt3	GGGGCGTATTCAAGTAGCTG	GTAGGGACCTCCCATTGGAT
Wnt3a	TTCTTACTTGAGGGCGGAGA	CTGTCGGGTCAAGAGAGGAG
Wnt4	CGAGGAGTGCCAATACCACT	GTCACAGCCACACTTCTCCA
Wnt5a	CCCAGTCCGGACTACTGTGT	TTTGACATAGCAGCACCAGTG
Wnt5b	TCTCCGCCTCACAAAAGTCT	CACAGACACTCTCAAGCCCA
Wnt6	TTCGGGGATGAGAAGTCAAG	CGGCACAGACAGTTCTCCTC
Wnt7a	GACAAATACAACGAGGCCGT	GGCTGTCTTATTGCAGGCTC
Wnt7b	ACAGGAGGGTGGGGATAGA	GAAACAGCCCAGGAAACCGT
Wnt8a	CTGACTACTGCAACCGCAAC	TGACAGTGCAACACCACTGA
Wnt8b	CCAGAGTTCCGGGAGGTAG	GAGATGGAGCGGAAGGTGT
Wnt9a	CCCCTGACTATCCTCCCTCT	GATGGCGTAGAGGAAAGCAG
Wnt9b	GGGTGTGTGTGGTGACAATC	TCCAACAGGTACGAACAGCA
Wnt10a	GCGCTCCTGTTCTTCCTACT	ATGCCCTGGATAGCAGAGG
Wnt10b	TCAGTCGGGCTCTAAGCAAT	TGGTGCTGACACTCGTGAAC
Wnt11	TGCTTGACCTGGAGAGAGGT	AGCCCGTAGCTGAGGTTGT
Wnt16	CCCTCTTTGGCTATGAGCTG	TACTGGACATCATCCGAGCA

### **3.2.7 Western blot analysis**

Cultured mouse podocytes were lysed in SDS sample buffer. The isolated glomeruli were pooled and lysed with radioimmunoprecipitation assay buffer containing 1% NP-40, 0.1% sodium dodecyl sulfate, 100 µg/ml phenylmethylsulfonyl fluoride, 1% protease inhibitor cocktail, and 1% phosphatase I and II inhibitor cocktail (Sigma) in phosphate buffered saline on ice. The supernatants were collected after centrifugation at  $13,000 \times g$  at 4 °C for 20 min. Protein expression was analyzed by Western blot analysis as described previously [210]. The primary antibodies used were as follows: anti- $\beta$ -catenin (cat. no. 6101541; BD Transduction, San Jose, CA), anti-dephosphorylated, active  $\beta$ -catenin (cat. no. 05-665; Millipore, Billerica, MA), anti-GFP (cat. no. ab290; Abcam, Cambridge, MA), anti-phospho-Smad3 (Ser<sup>423/425</sup>) (cat. no. 9514; Cell Signaling, Boston, MA), anti-Smad1/2/3 (cat. no. sc-7960; Santa Cruz Biotechnology, Santa Cruz, CA), anti-PAI-1 (sc-5297; Santa Cruz Biotechnology), anti-WT1 (ab15249; Abcam), anti-Histone H3 (ab1791; Abcam), anti-actin (sc-1616; Santa Cruz Biotechnology) and anti- $\alpha$ -tubulin (T9026; Sigma).

### **3.2.8 Nuclear and cytoplasmic fractionation**

For preparation of nuclear protein, isolated mouse glomeruli were collected and washed twice with cold phosphate-buffered saline (PBS). Nuclear protein preparation was made with NE-PER Nuclear and Cytoplasmic Extraction Reagents, according to the protocols specified by the manufacturer (Thermo Scientific, Rockford, IL).

### **3.2.9 Immunofluorescent and Immunohistochemical staining**

Kidney cryosections at 3- $\mu$ m thickness were fixed for 15 min in 4% paraformaldehyde, followed by permeabilization with 0.2% Triton X-100 in PBS for 10 min at room temperature. After blocking with 10% donkey serum for 60 min, slides were immunostained with primary antibodies against nephrin (Fitzgerald Industries International, Concord, MA, USA), or phosphorylated Smad3 (Ser423/425) (cat. no. 9514, Cell Signaling). To visualize the primary antibodies, cells were stained with Cy2 or Cy3-conjugated secondary antibodies (Sigma). Slides were viewed with a Nikon Eclipse E600 Epi-fluorescence microscope equipped with a digital camera (Melville, NY). In each experimental setting, images were captured with identical light exposure times. Immunohistochemical staining of kidney sections was performed by an established protocol [223]. Paraffin-embedded sections were stained with polyclonal rabbit anti- $\beta$ -catenin antibody (ab-15180; Abcam, Cambridge, MA). Slides were viewed with a Nikon Eclipse E600 microscope equipped with a digital camera (Melville, NY).

### **3.2.10 Statistical analysis**

All data examined were expressed as mean  $\pm$  SEM. Statistical analysis was performed using SigmaStat software (Jandel Scientific Software, San Rafael, CA, USA). Comparison between groups was made using one-way analysis of variance (ANOVA), followed by Student-Newman-Keuls test. A *P* value of less than 0.05 was considered significant.



### 3.3 RESULTS

#### 3.3.1 Induction of Wnt expression by TGF- $\beta$ 1 in podocytes

We first performed a systematic analysis of the mRNA expression of all Wnt genes in cultured mouse podocytes after incubation with TGF- $\beta$ 1 by RT-PCR approach. As shown in Figure 13A, a comprehensive survey of all 19 Wnts showed that the induction of mRNA expression of several Wnts, including Wnt1, Wnt2, Wnt9a, Wnt10b and Wnt11, was detected at different time points. Slight inhibition of Wnt5b and Wnt16 was also observed, particularly at late time points. Notably, the expression of Wnt3a, Wnt4 and Wnt9b was undetectable in cultured podocytes throughout the experiments (data not shown). Compared with other Wnts, the induction of Wnt1 mRNA by TGF- $\beta$ 1 was most predominant. Quantitative, real-time RT-PCR (qRT-PCR) results revealed that Wnt1 mRNA expression was induced by approximately 14-fold at 8 h after TGF- $\beta$ 1 treatment in mouse podocytes (Figure 13B). The induction of Wnt1 mRNA expression also occurred in a dose-dependent fashion; and TGF- $\beta$ 1 induced its mRNA level at the concentration as low as 0.5 ng/ml, which reached the peak at 2 ng/ml (Figure 13C).

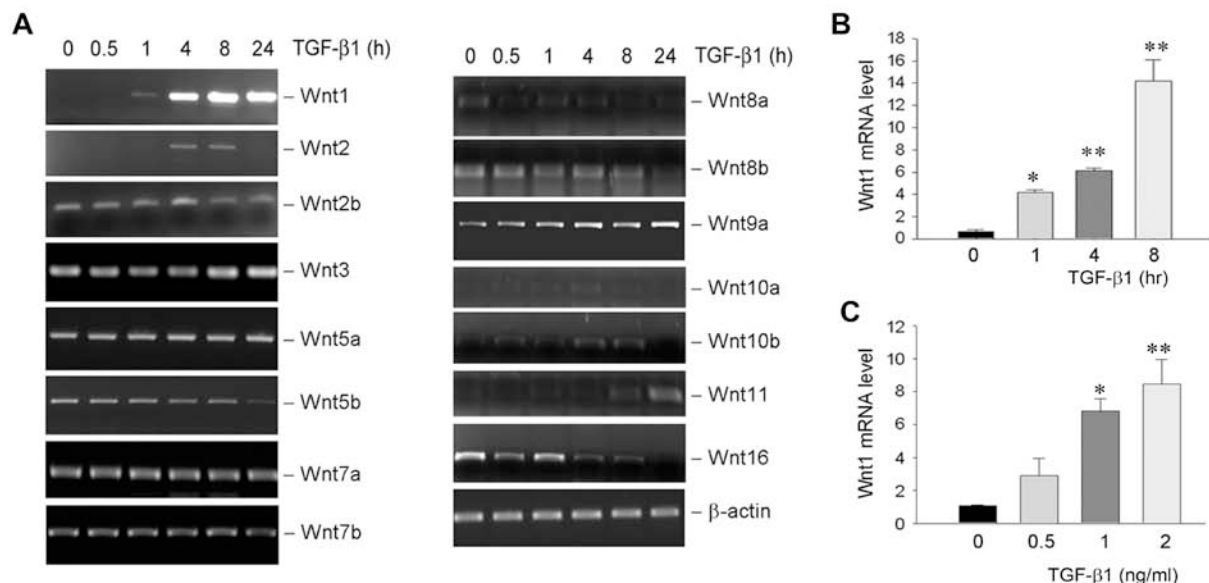


**Figure 13. Expression of Wnt genes is induced by TGF-β1 in podocytes.** A, RT-PCR demonstrates an altered expression of various Wnts mRNA in cultured mouse podocytes after treatment with TGF-β1 at 2 ng/ml for various periods of time as indicated. B and C, Quantitative real-time RT-PCR reveals that TGF-β1 induced Wnt1 mRNA expression in a time- and dosage- dependent manner. Wnt1 mRNA levels were assessed by quantitative real-time RT-PCR in mouse podocytes after treatment with a fixed amount of TGF-β1 (2 ng/ml) for various periods of time as indicated (B) or with various concentrations of TGF-β1 for 24 h (C). Data are presented as mean  $\pm$  SEM of three experiments. \* $P < 0.05$  versus control. \*\* $P < 0.01$  versus control.

### 3.3.2 Activation of β-catenin in podocytes by TGF-β1

To examine the biological consequence of Wnt induction in podocytes, we next investigated the activation of β-catenin, the principal downstream mediator of canonical Wnt signaling, in podocytes after TGF-β1 treatment. As shown in Figure 14A, active, dephosphorylated form of β-catenin protein was induced in cultured mouse podocytes at 24 h after incubation with TGF-β1, which sustained to 48 h. This activation of β-catenin significantly lagged behind the Wnt1 induction by TGF-β1. The induction of active β-catenin protein was also dose-dependent; and

TGF- $\beta$ 1 induced active  $\beta$ -catenin at a concentration as low as 0.5 ng/ml, which reached the peak at 2 ng/ml (Figure 14B). We further examined  $\beta$ -catenin activation and its subcellular distribution in podocytes after incubation with TGF- $\beta$ 1 for 24 h. As illustrated in Figure 14C,  $\beta$ -catenin predominantly displayed a plasma membrane-associated staining pattern in the resting, control podocytes (Figure 14C, arrowhead). However, upon stimulation by TGF- $\beta$ 1,  $\beta$ -catenin underwent nuclear translocation, with disappearance of the plasma membrane-associated staining and concomitant emergence of nuclear  $\beta$ -catenin (Figure 14C, arrowheads). This nuclear translocation of  $\beta$ -catenin, together with the Western blot results (Figure 14, A and B), clearly indicates the activation of canonical Wnt/ $\beta$ -catenin signaling in podocytes after TGF- $\beta$ 1 treatment.

### **3.3.3 DKK1 blocks Wnt/ $\beta$ -catenin signaling in podocytes**

To further corroborate the activation of Wnt/ $\beta$ -catenin signaling by TGF- $\beta$ 1, we sought to inhibit Wnt/ $\beta$ -catenin signaling by using DKK1, a secreted Wnt antagonist that specifically blocks the canonical pathway of Wnt signaling. As shown in Figure 15A, transfection of podocytes with expression vector encoding constitutively active TGF- $\beta$ 1 (pCA-TGF- $\beta$ 1) induced  $\beta$ -catenin activation, as illustrated by an increased expression of active  $\beta$ -catenin. However, co-transfection with DKK1 expression vector (pFlag-DKK1) abolished  $\beta$ -catenin activation (Figure 15A), suggesting that DKK1 is sufficient to antagonize the Wnt/ $\beta$ -catenin signaling activated by TGF- $\beta$ 1 in podocytes.

We further investigated the potential downstream targets of TGF- $\beta$ 1/Wnt/ $\beta$ -catenin signaling that are relevant to podocyte dysfunction. To this end, we examined the expression of

slit diaphragm protein nephrin and transcription factor Snail1. As shown in Figure 15B, either incubation with TGF- $\beta$ 1 or transient transfection with Flag-tagged N-terminal truncated, stabilized  $\beta$ -catenin expression vector (pDel- $\beta$ -cat) or HA-tagged Wnt1 expression vector (pHA-Wnt1) was sufficient to suppress nephrin expression and concomitantly induced Snail1 expression.

We next tested whether blockade of Wnt/ $\beta$ -catenin signaling by DKK1 can attenuate TGF- $\beta$ 1-mediated podocyte dysfunction. As shown in Figure 15, C and D, TGF- $\beta$ 1 suppressed nephrin expression in cultured mouse podocytes at different time points. However, pre-incubation with recombinant DKK1 protein was able to preserve nephrin expression in a dose-dependent manner. Taken together, it becomes clear that DKK1 is sufficient to impede Wnt/ $\beta$ -catenin signaling and protect podocytes against TGF- $\beta$ 1-induced injury.

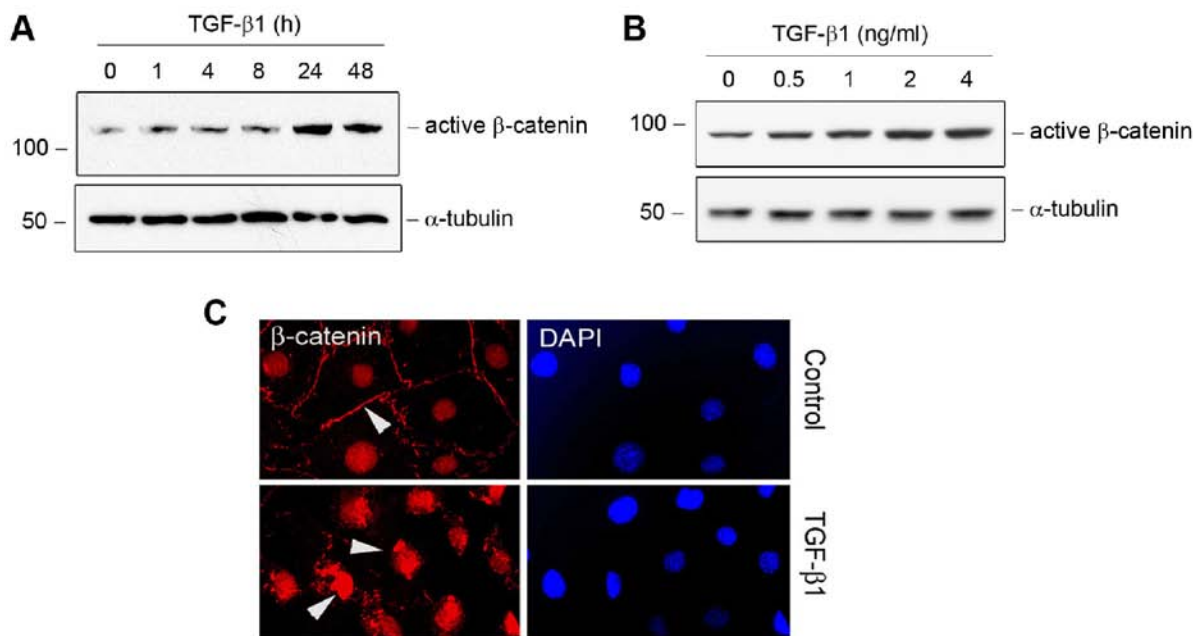


**Figure 14.  $\beta$ -catenin is activated by TGF- $\beta$ 1 in podocytes.** A and B, Western blot analyses demonstrate that TGF- $\beta$ 1 induced active  $\beta$ -catenin protein expression in a time- and dosage-dependent manner. Podocytes were treated with a fixed amount of TGF- $\beta$ 1 (2 ng/ml) for various periods of time as indicated (A) or with various concentrations of TGF- $\beta$ 1 for 48 h (B). Total cell lysates were immunoblotted with specific antibodies against active  $\beta$ -catenin and  $\alpha$ -tubulin, respectively. C, Immunofluorescence staining demonstrates the activation of  $\beta$ -catenin and nuclear translocation in mouse podocytes after treatment with TGF- $\beta$ 1 at 2 ng/ml for 24 h. Arrowheads indicate  $\beta$ -catenin staining.

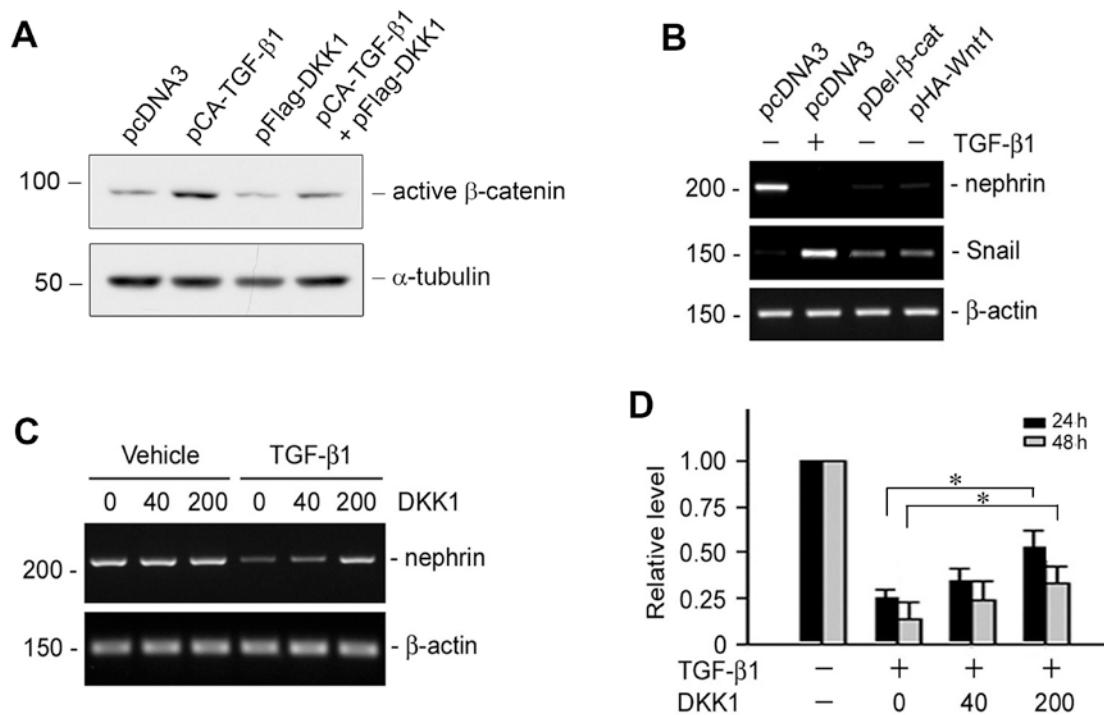


**Figure 15. Exogenous Wnt antagonist DKK1 blocks Wnt signaling induced by TGF-β1 in podocytes.** A, Western blot analysis demonstrates that exogenous DKK1 blocks the activation of β-catenin induced by TGF-β1. Podocytes were transfected with constitutively active TGF-β1 expression vector (pCA-TGF-β1), DKK1 expression vector (pFlag-DKK1) or empty vector pcDNA3, as indicated, for 48 h. Total cell lysates were immunoblotted with specific antibodies against active β-catenin and α-tubulin, respectively. B, TGF-β1/Wnt1/β-catenin cascade is sufficient for triggering nephrin suppression and Snail induction in podocytes. Mouse podocytes were transiently transfected with expression vector pHA-Wnt1, pDel-β-cat or pcDNA, respectively, followed by incubation with TGF-β1 at 2 ng/ml for 48h. Representative RT-PCR results demonstrated the mRNA expression of nephrin and Snail. C and D, treatment of DKK1 preserves nephrin mRNA expression repressed by TGF-β1. Podocytes were pre-treated with recombinant protein DKK1 at 40 or 200 ng/ml for 1 h, followed with the treatment of TGF-β1 at 2 ng/ml for 24 h or 48h. Representative RT-PCR results (C) and quantitative data (D) demonstrate the mRNA expression of nephrin. Data are presented as mean ± SEM of three experiments. \* $P < 0.05$  versus control. † $P < 0.05$  versus group treated with TGF-β1 alone.

### 3.3.4 Ectopic TGF- $\beta$ 1 expression targets podocyte *in vivo* and induces proteinuria

To assess the potential role of Wnt/ $\beta$ -catenin activation in podocyte dysfunction induced by TGF- $\beta$ 1, we sought to express bioactive, exogenous TGF- $\beta$ 1 *in vivo* by use of a hydrodynamic-based gene delivery approach [224-225]. As shown in Figure 16A, several mammalian expression plasmid vectors were constructed, which contained the coding region of mouse wild type TGF- $\beta$ 1 full length cDNA (pWT-TGF- $\beta$ 1), C-terminus truncated TGF- $\beta$ 1 (pCT-TGF- $\beta$ 1) and constitutively active TGF- $\beta$ 1 (pCA-TGF- $\beta$ 1), respectively. The pCA-TGF- $\beta$ 1 vector contained two cysteine to serine mutations at the positions 223 and 225 (C223S/C225S), which produces bioactive TGF- $\beta$ 1 that does not require acid activation [208], rendering it constitutively active. To test the bioactivity of these TGF- $\beta$ 1 expression vectors, we examined their potential in inducing the expression of plasminogen activator inhibitor-1 (PAI-1), a sensitive TGF- $\beta$ 1 target gene. As shown in Figure 16B, little PAI-1 induction was observed in podocytes after transient transfection with either pWT-TGF- $\beta$ 1 or pCT-TGF- $\beta$ 1, compared with empty vector pcDNA3. However, transfection with pCA-TGF- $\beta$ 1 dramatically induced PAI-1 expression, corroborating the bioactivity of this mutant, constitutively active TGF- $\beta$ 1 (Figure 16B).

We next investigated the functional consequence of delivery of the expression plasmid encoding constitutively active TGF- $\beta$ 1 (pCA-TGF- $\beta$ 1) *in vivo* by single intravenous injection in mice. As shown in Figure 16C, single administration of pCA-TGF- $\beta$ 1 plasmid markedly induced Smad3 phosphorylation, a surrogate marker for TGF- $\beta$  receptor activation, in the glomerular lysates of the kidneys at 1 or 2 days after injection. Double immunofluorescence staining for both phosphorylated Smad3 and nephrin revealed that podocytes in the glomeruli

were preferentially responsive to TGF- $\beta$ 1, with a positive staining for phosphorylated Smad3 after TGF- $\beta$ 1 gene delivery (Figure 16D, arrowheads).

Analysis of urine samples revealed that urinary albumin levels were substantially increased in mice that received TGF- $\beta$ 1 plasmid injection, compared to pcDNA3 controls (Figure 17A). SDS-PAGE analysis demonstrated that albumin was the major constituent of urine proteins in these mice after ectopic expression of exogenous TGF- $\beta$ 1 (Figure 17B), suggesting defective glomerular filtration. Consistently, exogenous TGF- $\beta$ 1 induced an altered nephrin distribution, from a linear staining along GBM to granular pattern, as illustrated by immunofluorescence staining, although it did not significantly affect nephrin abundance (Figure 17C). The expression of Wilms tumor 1 (WT1), an important transcription regulator that is exclusively expressed in podocytes in adult kidney, was significantly suppressed after exogenous TGF- $\beta$ 1 plasmid injection (Figure 17D). Hence, single injection of the expression vector encoding constitutively active TGF- $\beta$ 1 is sufficient to cause podocyte injury and induce proteinuria in normal and healthy mice.

### **3.3.5 Activation of Wnt/ $\beta$ -catenin signaling *in vivo* by TGF- $\beta$ 1**

We next examined the effects of TGF- $\beta$ 1 on Wnt/ $\beta$ -catenin signaling pathway in podocytes *in vivo*. Quantitative real-time RT-PCR result revealed an increased expression of Wnt1 gene in glomeruli, which was detected at day 1 and sustained at day 2 after TGF- $\beta$ 1 plasmid injection (Figure 18A). Subcellular fractionation of the isolated glomeruli, followed by Western blot analyses, indicated that  $\beta$ -catenin in both cytoplasmic and nuclear compartments was markedly induced after TGF- $\beta$ 1 gene delivery *in vivo* (Figure 18B). Compared with pcDNA3 controls,



ectopic expression of TGF- $\beta$ 1 clearly promoted  $\beta$ -catenin to undergo nuclear translocation (Figure 18B), suggesting the activation of the canonical Wnt signaling. We further studied the expression of several putative target genes of Wnt/ $\beta$ -catenin in the glomeruli after TGF- $\beta$ 1 gene delivery. As shown in Figure 18, C through E, numerous well characterized Wnt/ $\beta$ -catenin target genes including Snail1, MMP-9, MMP-7, desmin and Fsp1 were upregulated in mouse glomeruli after ectopic expression of exogenous TGF- $\beta$ 1.

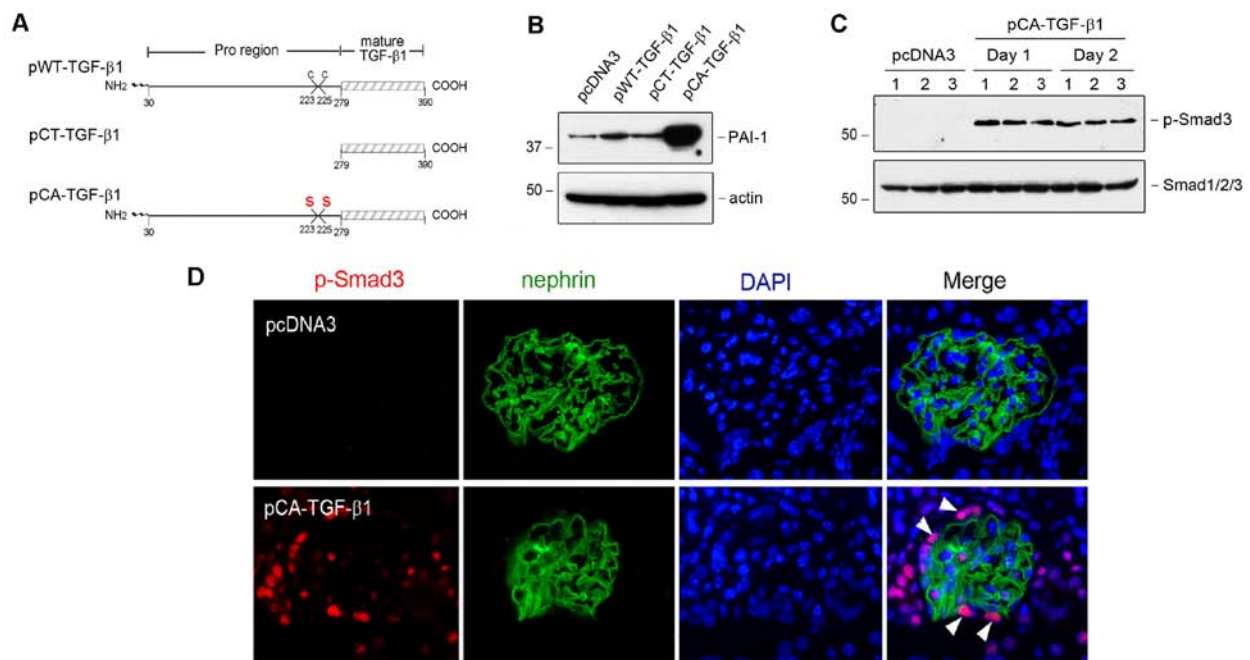


**Figure 16. Ectopic expression of TGF- $\beta$ 1 targets glomerular podocytes *in vivo*.** A, diagram depicts the construction of wild type TGF- $\beta$ 1 (pWT-TGF- $\beta$ 1), C-terminus truncated TGF- $\beta$ 1 (pCT-TGF- $\beta$ 1) and constitutively active TGF- $\beta$ 1 (pCA-TGF- $\beta$ 1) expression vectors. B, Expression vector pCA-TGF- $\beta$ 1 dramatically induces PAI-1 gene expression in podocytes. Mouse podocyte were transiently transfected with expression vector pWT-TGF- $\beta$ 1, pCT-TGF- $\beta$ 1 and pCA-TGF- $\beta$ 1 and pcDNA3 for 48 h, respectively. Total cell lysates were immunoblotted with specific antibodies against PAI-1 and actin, respectively. C and D, Delivery of constitutively active TGF- $\beta$ 1 gene induces Smad3 phosphorylation in glomerular podocytes *in vivo*. One or two days after a single intravenous injection of either TGF- $\beta$ 1-expressing plasmid (pCA-TGF- $\beta$ 1) or empty vector (pcDNA3), glomerular lysates were prepared and immunoblotted with anti-phospho-Smad3 and anti-Smad1/2/3 antibodies. Mouse kidney sections were immunostained with antibodies against phospho-specific Smad3 (red) and nephrin (green) (D). Arrowheads indicate phospho-Smad3-positive podocytes.

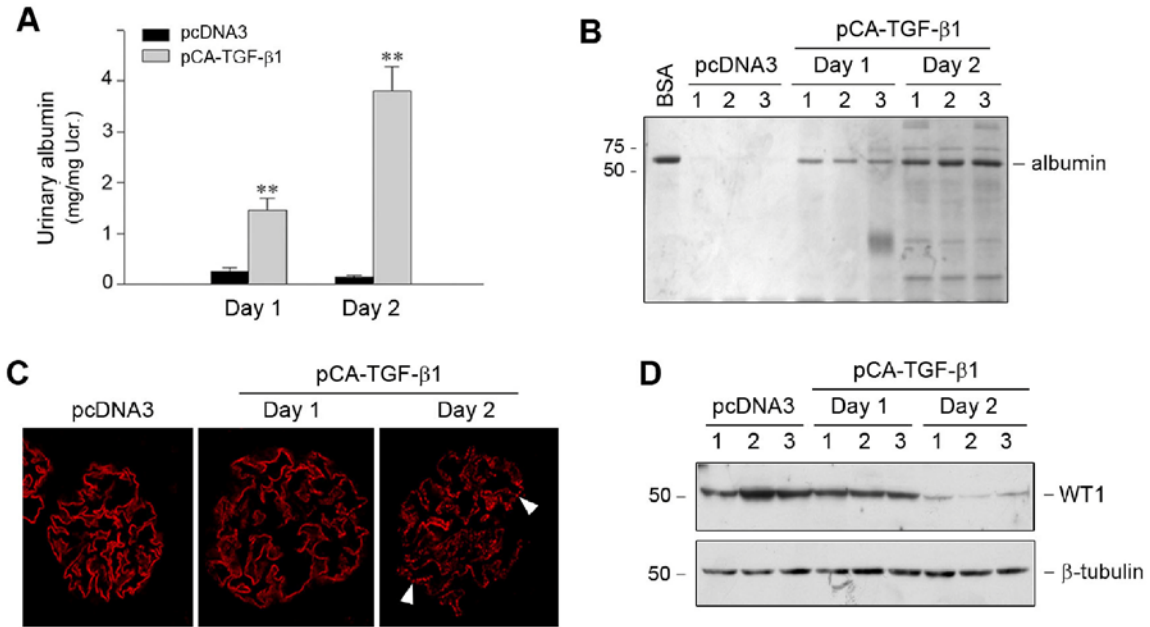


**Figure 17. Ectopic expression of TGF-β1 causes proteinuria and podocyte dysfunction.** A, Urinary albumin levels in mice after ectopic expression of exogenous TGF-β1. Male BALB/c mice were injected intravenously with TGF-β1-expression plasmid (pCA-TGF-β1) or empty vector (pcDNA3). Urinary albumin was determined at 1 or 2 days after injection, and expressed as mg per mg creatinine. \*\* $P < 0.01$  versus pcDNA3 control ( $n = 6$ ). B, Representative SDS-PAGE shows the urinary proteins at day 1 and day 2 after pCA-TGF-β1 plasmid injection. C, Immunofluorescence staining shows the expression and distribution pattern of nephrin in different groups as indicated. Arrowheads indicate a dot-like pattern of nephrin after TGF-β1 plasmid injection. D, Western blot analysis demonstrates the suppression of WT1 by TGF-β1 *in vivo*. Whole glomerular lysates were immunoblotted with anti-WT1 and  $\alpha$ -tubulin, respectively.

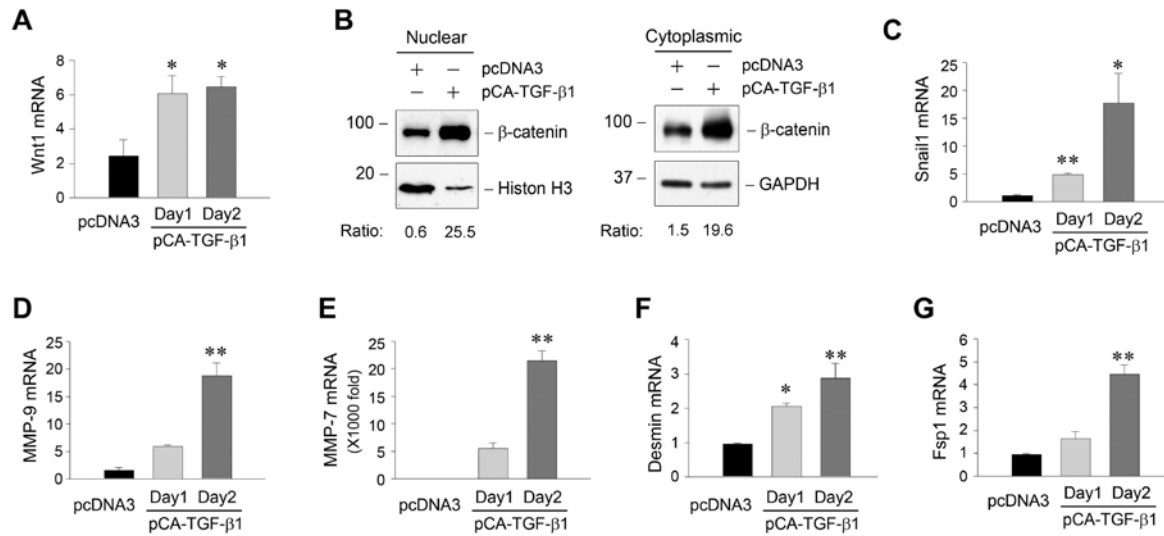


**Figure 18. Ectopic expression TGF-β1 activates Wnt/β-catenin signaling and induces its downstream target gene expression *in vivo*.** A, Quantitative real-time RT-PCR reveals that TGF-β1 induced Wnt1 mRNA expression in mouse glomeruli. B, TGF-β1 induces cytoplasmic β-catenin accumulation and its nuclear translocation in mouse glomeruli. Glomeruli were isolated from mouse kidneys at 1 day after injection of TGF-β1 expression plasmid (pCA-TGF-β1) or empty vector (pcDNA3). Nuclear and cytoplasmic proteins from the isolated glomeruli were prepared and immunoblotted with antibodies against β-catenin, histone H3 (H3) or GAPDH, respectively. The ratios of β-catenin per control proteins (histone H3 for nuclear protein and GAPDH for cytoplasmic protein) are shown. C through G, Quantitative real-time RT-PCR reveals that TGF-β1 induces the mRNA expression of Wnt/β-catenin downstream genes such as Snail1, MMP-9, MMP-7, desmin and Fsp-1. Various mRNA levels were assessed by quantitative real-time RT-PCR in the isolated glomeruli in different groups as indicated. Data are presented as mean  $\pm$  SEM of three glomerular preparations, each of them contains a pool of two animals. \* $P < 0.05$  versus control group. \*\* $P < 0.01$  versus control group.

### **3.3.6 Ectopic expression of DKK1 gene blocks Wnt/ $\beta$ -catenin signaling and reduces proteinuria**

To further investigate the role of Wnt/ $\beta$ -catenin signaling in mediating TGF- $\beta$ 1-induced podocyte injury and proteinuria, we sought to block Wnt signaling *in vivo* by its natural antagonist DKK1. To this end, mice were injected concurrently with TGF- $\beta$ 1 expression vector (pCA-TGF- $\beta$ 1) in the presence or absence of DKK1 expression vector (pFlag-DKK1). As shown in Figure 19A, ectopic expression of constitutively active TGF- $\beta$ 1 induced both active and total  $\beta$ -catenin expression in the glomeruli, as demonstrated by Western blot analyses of glomerular lysates. However, concomitant expression of DKK1 gene evidently abolished  $\beta$ -catenin induction and activation. Immunohistochemical staining produced similar results. As shown in Figure 19B, renal  $\beta$ -catenin protein was increased in glomerular podocytes and tubular cells after ectopic expression of exogenous TGF- $\beta$ 1 (Figure 19B, arrowheads). The positive  $\beta$ -catenin staining localized in the cytoplasmic and nuclear compartments was significantly diminished when DKK1 gene was concurrently administered. Interestingly, delivery of DKK1 gene significantly mitigated albuminuria induced by exogenous TGF- $\beta$ 1 (Figure 19C), indicating an important role for Wnt/ $\beta$ -catenin signaling in mediating TGF- $\beta$ 1-induced podocyte injury and proteinuria.

We next examined the expression of Wnt/ $\beta$ -catenin downstream target genes in the glomeruli of these mice. As shown in Figure 20, A through D, administration of DKK1 gene resulted in significant inhibition of the Wnt/ $\beta$ -catenin targets genes. Quantitative RT-PCR revealed that DKK1 significantly inhibited the mRNA expression of Snail1, MMP-9, MMP-7 and LEF-1 genes, which were induced in mouse glomeruli after TGF- $\beta$ 1 expression (Figure 20).

Notably, albeit not statistically significant, DKK1 seemed also to block the induction of PAI-1 expression by TGF- $\beta$ 1 (Figure 20E).

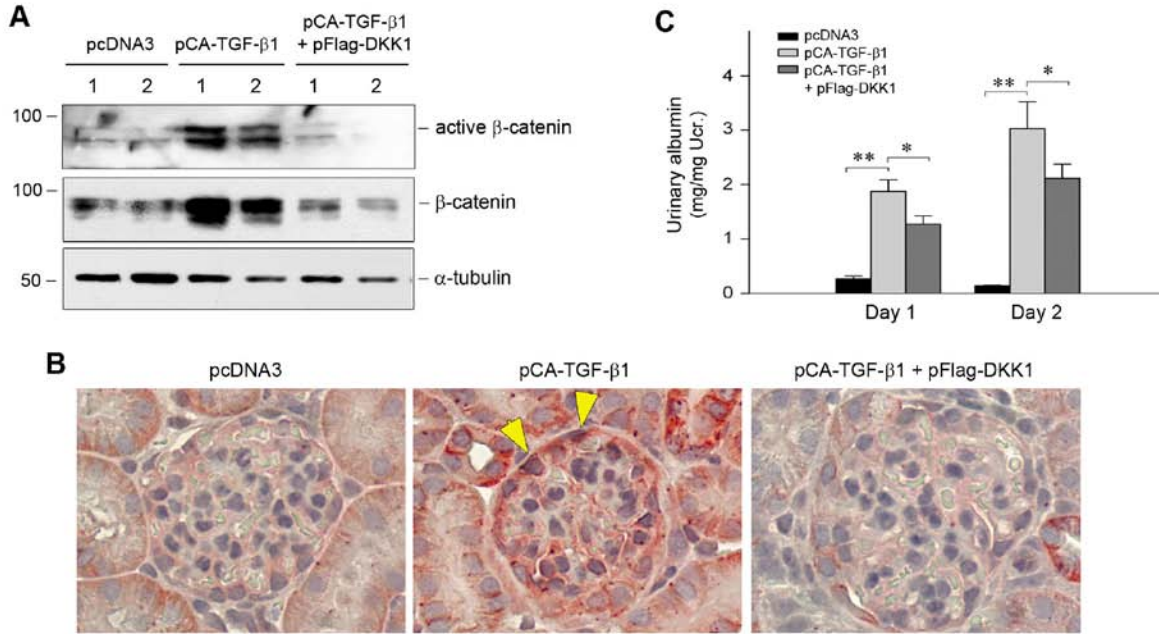


**Figure 19. Ectopic expression of DKK1 blocks  $\beta$ -catenin activation and reduces albuminuria induced by TGF- $\beta$ 1 *in vivo*.** A, Western blot analyses demonstrate that DKK1 blocks the TGF- $\beta$ 1-induced active and total  $\beta$ -catenin expression in mouse glomeruli. Whole glomerular lysates were immunoblotted with anti-active  $\beta$ -catenin,  $\beta$ -catenin and  $\alpha$ -tubulin antibodies, respectively, at day 2 after intravenous plasmid injection. B, Representative micrographs demonstrate  $\beta$ -catenin expression and localization in different groups at day 2. Mouse kidney sections were immunostained with antibody against  $\beta$ -catenin. Arrowheads indicate  $\beta$ -catenin-positive podocytes. C, Urinary albumin levels in different group as indicated. Data are presented as mean  $\pm$  SEM of six animals. \* $P < 0.05$ ; \*\* $P < 0.01$ .

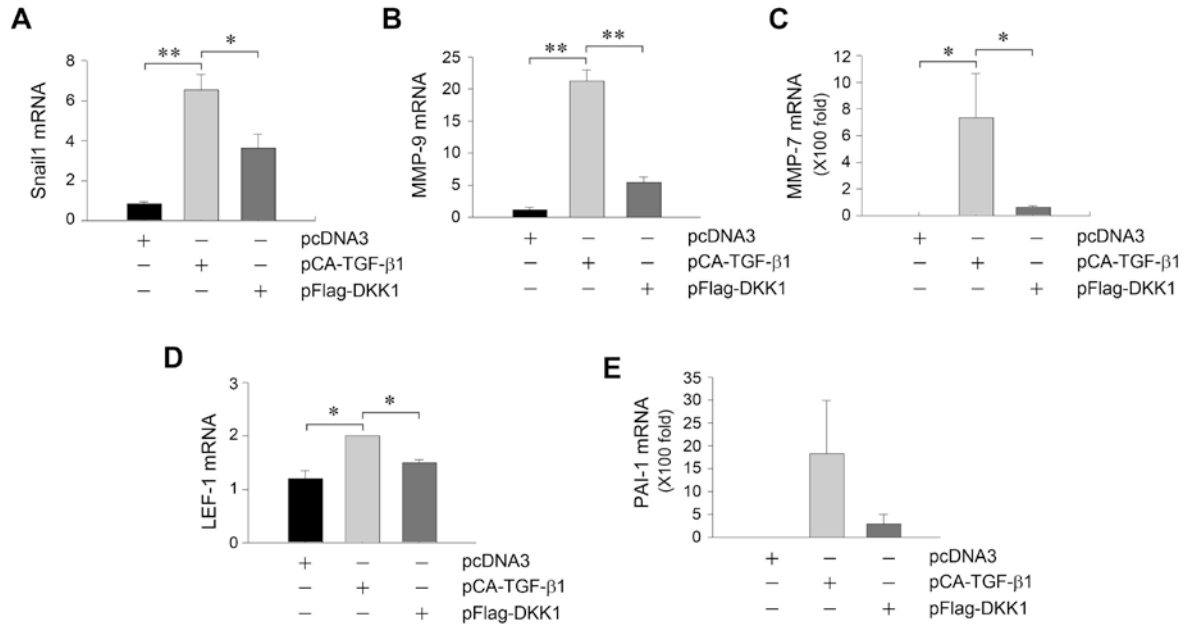


**Figure 20. Exogenous DKK1 blocks Wnt/ $\beta$ -catenin target gene expression induced by TGF- $\beta$ 1 *in vivo*.** Quantitative real-time RT-PCR reveals that exogenous DKK1 inhibits TGF- $\beta$ 1-induced the mRNA expression of Wnt/ $\beta$ -catenin target genes, including Snail1 (A), MMP-9 (B), MMP-7 (C), LEF-1 (D), and PAI-1 (E). Various mRNA levels were assessed in the isolated glomeruli from mice injected with different expression vectors as indicated at day2. Data are presented as mean  $\pm$  SEM of three glomerular preparations, each of them contains a pool of two animals. \* $P < 0.05$ ; \*\* $P < 0.01$  ( $n = 3$ ).

### 3.4 DISCUSSION

The results presented here clearly illustrate a critical role for Wnt/ $\beta$ -catenin signaling in mediating the pathogenesis of podocyte injury and proteinuria *in vivo* after ectopic expression of fibrogenic TGF- $\beta$ 1. We demonstrate that Wnt1 is upregulated and  $\beta$ -catenin is activated in the glomeruli after exogenous TGF- $\beta$ 1 expression through a hydrodynamic-based gene delivery approach, which leads to the over-expression of several key Wnt target genes including Snail1, resulting in podocyte injury and onset of proteinuria. Moreover, Wnt antagonist DKK1 is

effective in blocking TGF- $\beta$ 1-mediated  $\beta$ -catenin activation *in vivo* and *in vitro*, leading to significant inhibition of Wnt target genes and mitigation of albuminuria in mice. These studies establish a simple mouse model in which ectopic expression of TGF- $\beta$ 1, *per se*, is sufficient to cause podocyte injury *in vivo* and results in proteinuric kidney disease. Our data also underscore that targeting Wnt/ $\beta$ -catenin could be a promising novel therapeutic strategy for the treatment of a variety of proteinuric kidney disease in humans.

TGF- $\beta$ 1, as a fibrogenic factor, is up-regulated in the injured kidneys in experimental animal models and in humans of virtually every type of chronic kidney diseases [226]. Although exaggerated TGF- $\beta$  signaling is considered to be a major profibrotic stimulus in mesangial injury and expansion, little is known about its pathobiology in podocytes *in vivo*. Earlier studies on transgenic mice over-expressing TGF- $\beta$ 1 under albumin promoter (Alb/TGF- $\beta$ 1 mice) have pointed toward a causative role of TGF- $\beta$ 1 in the pathogenesis of nephropathies, as these mice spontaneously develop proteinuria, progressive glomerulosclerosis and interstitial fibrosis, with advanced kidney failure leading to approximately 50% animal death at 5-12 weeks of age [129]. However, because of the tremendous heterogeneity in renal pathology, these mice have not been widely used as an animal model of chronic kidney diseases. In this study, by a single injection of naked plasmid vector encoding constitutively active TGF- $\beta$ 1, we have established a simple, quick, reproducible and accessible mouse model of podocyte injury and proteinuria (Figure 17). As TGF- $\beta$ 1 is the sole culprit of kidney injury in this model, these mice could also serve as an *in vivo* model to dissect the cellular and molecular mechanism of TGF- $\beta$ 1 action in the kidneys. Interestingly, of three major cell types in the glomeruli, podocytes seem to be the most susceptible cells that are readily responsive to TGF- $\beta$ 1 stimulation *in vivo*, as illustrated by Smad3 phosphorylation, a surrogate marker for TGF- $\beta$  receptor activation (Figure 16). Such an

activation of TGF- $\beta$ 1 evidently leads to induction of numerous Wnt genes in podocytes, particularly Wnt1 (Figure 13), which results in the stabilization and accumulation of  $\beta$ -catenin, as well as its nuclear translocation. In addition, TGF- $\beta$ 1 and Wnt ligands may work in concert to regulate gene expression [227], as previous studies suggest that  $\beta$ -catenin can form a complex with Smad4 [228]. In short, TGF- $\beta$ 1 is categorically linked to the activation of Wnt/ $\beta$ -catenin, a developmental signaling that is recently implicated in podocyte injury and proteinuria [201].

Wnt/ $\beta$ -catenin signaling is highly conserved during the evolution and plays important role in controlling many biologic processes during the embryogenesis and tumorigenesis. At the cellular level, this signaling regulates morphology, proliferation, motility and cell fate. Inappropriate activation of this signaling has been linked to tumorigenesis in humans [229]. At least two Wnt ligands, Wnt9b and Wnt4, are intimately involved in the epithelial differentiation of metanephric mesenchymal progenitors during nephron formation [230], whereas their signaling is considered to be silent in adult kidney. Depending on different receptors and cellular context, Wnt proteins can activate three intracellular signaling pathways, including the canonical  $\beta$ -catenin-dependent pathway, the non-canonical,  $\beta$ -catenin-independent planar cell polarity (PCP) pathway and Wnt/ $\text{Ca}^{2+}$  pathway [179]. However, it appears that the signaling elicited by Wnts in podocytes after TGF- $\beta$ 1 expression in this study is mediated by the canonical pathway. It is worthwhile to point out that aberrant expression of Wnts and activation of  $\beta$ -catenin are common findings in a wide variety of kidney diseases in animal models and in humans, including unilateral ureteral obstruction (UUO), adriamycin nephropathy, ischemia-reperfusion induced acute kidney injury and diabetic nephropathy [193, 201, 231-232].

How activation of Wnt/ $\beta$ -catenin signaling causes podocyte injury remains elusive, but it could be related to its ability to regulate epithelial-mesenchymal transition (EMT), a cell



phenotypic alteration process taking place in embryonic development, cancer metastasis and tissue fibrosis [233-235]. Earlier studies demonstrate that podocytes also undergo EMT *in vitro* after TGF- $\beta$ 1 stimulation, and this process could be a potential pathway leading to podocyte dysfunction and proteinuria under pathological conditions [42]. In agreement with this notion, EMT has been reported as a potential explanation for podocyte dysfunction, detachment and depletion in human diabetic nephropathy. It is of interest to point out that Snail1, a key transcription factor controlling EMT [128, 236], is a downstream target gene of Wnt/ $\beta$ -catenin signaling [235]. Snail1, in turn, could directly suppress nephrin expression in podocytes [202] and induces the expression of other mesenchymal markers. Indeed, either incubation with TGF- $\beta$ 1 or over-expression of Wnt1 or stabilized  $\beta$ -catenin by transient transfection is sufficient to induce Snail1 expression and suppress nephrin expression in podocytes (Figure 15). *In vivo* TGF- $\beta$ 1/Wnt/ $\beta$ -catenin cascade also induces glomerular expression of Snail1 as well as mesenchymal marker Fsp1 (Figure 18). Taken together, by inducing Snail1 expression, Wnt/ $\beta$ -catenin signaling suppresses podocyte-specific protein nephrin and promotes podocyte dedifferentiation and mesenchymal transition, leading to the onset of proteinuria.

Besides Snail1, numerous downstream target genes of Wnt/ $\beta$ -catenin are identified to be activated in the glomeruli upon TGF- $\beta$ 1 expression, such as MMP-9, MMP-7, LEF-1, Fsp1 and PAI-1. Among these genes, induction of LEF-1, a DNA-binding transcription regulator that interacts with  $\beta$ -catenin by forming a trans-activation protein complex [237], clearly favors a positive feedback loop that re-enforces Wnt signaling. Matrix metalloproteinases (MMPs) are a family of extracellular proteases that are responsible for the degradation of the extracellular matrix and other substrates during tissue remodeling [238-239]. Although the exact action of MMPs in podocyte injury is unclear, MMP-mediated extracellular domain shedding of nephrin

could play a role. PAI-1, a well characterized fibrogenic factor, is another direct downstream target of Wnt/ $\beta$ -catenin signaling, and its induction may also contribute to the development of nephropathy in mice after TGF- $\beta$ 1 expression. It is conceivable that each of these target genes activated by Wnt/ $\beta$ -catenin could promote podocyte injury and proteinuria in their own ways. However, it is interesting to note that many of these genes including Snail1, MMPs, Fsp1 and PAI-1 share the same action by promoting cell migration. An increased podocyte migration could render them from stationary to motile state, which could reduce their adhesions to GBM and promote detachment. This view is in line with previous observation that EMT leads to an increased podocyte detachment and depletion in diabetic nephropathy.

Our present study also indicates that targeting Wnt/ $\beta$ -catenin signaling might be an effective strategy to mitigate podocyte injury and proteinuria. DKK1, a secreted Wnt antagonist, specifically binds to the Wnt co-receptors LRP-5/6, leading to blockade of the canonical Wnt pathway [194]. Because delivery of exogenous DKK1 gene via intravenous injection is sufficient to lead to substantial expression of DKK1 in kidney as previously reported [193], it is not unexpected that DKK1 gene therapy blocks  $\beta$ -catenin activation, suppresses Wnt/ $\beta$ -catenin target gene expression and mitigates albuminuria. Therefore, these studies underscore a pivotal role of the canonical Wnt/ $\beta$ -catenin signaling in mediating TGF- $\beta$ 1-triggered podocyte injury and proteinuria *in vivo*.

#### 4.0 GENERAL DISCUSSION AND FUTURE DIRECTIONS

In the first project, we demonstrated the induction of PINCH1 by fibrogenic factor TGF- $\beta$ 1 in glomerular podocytes. We then revealed the nuclear-cytoplasmic shuttling of PINCH1, which is dependent on its putative NES/NLS motif. More importantly, we have identified WT1 as a novel binding partner of PINCH1 in podocytes and showed that such binding of PINCH1/WT1 affects the podocyte-specific podocalyxin gene expression. In summary, we established that PINCH1, adaptor protein that localizes at the focal adhesions and is important for mediating integrin signaling, is acting as a novel, nuclear transcription regulator that interacts with WT1 to affect gene expression in podocytes.

In the second project, we investigated the role of Wnt/ $\beta$ -catenin signaling in podocyte injury induced by TGF- $\beta$ 1. We showed that among all 19 Wnt genes, Wnt1 expression was dramatically induced by TGF- $\beta$ 1 in cultured podocytes. We further demonstrated that Wnt canonical pathway was activated by TGF- $\beta$ 1 and Wnt antagonist DKK1 was able to block such activation *in vitro*. By intravenous injection of naked plasmid encoding constitutively active TGF- $\beta$ 1, we established a simple mouse model of podocyte injury and proteinuria. Using this model, we showed that TGF- $\beta$ 1 activated Wnt/ $\beta$ -catenin signaling and induced its downstream target genes *in vivo*. Furthermore, we showed that DKK1 gene therapy effectively blocked Wnt/ $\beta$ -catenin signaling, inhibited the expression of Wnt target genes, and mitigated proteinuria *in vivo*.

Taken together, we have identified and delineated two important but separate signaling pathways downstream of TGF- $\beta$ 1, which lead to podocytes injury and proteinuria. As shown in Figure 21, on one hand, TGF- $\beta$ 1 induces PINCH1 expression and its nuclear translocation, wherein it interacts with transcriptional factor WT1 and blocks the WT1-mediated gene expression, leading to podocyte dysfunction. On the other hand, TGF- $\beta$ 1 is able to trigger podocyte injury *via* canonical Wnt/ $\beta$ -catenin signaling. At this stage, the relative contribution of PINCH1/WT1 and Wnt/ $\beta$ -catenin pathways to podocyte injury remains unknown. However, it is highly likely that both pathways are necessary and indispensable for mediating TGF- $\beta$ 1-induced podocyte dysfunction and proteinuria. This notion is corroborated by the observation that Wnt antagonist DKK1 only partially blocks TGF- $\beta$ 1-induced proteinuria, indicating that PINCH1/WT1 or other signaling besides Wnt/ $\beta$ -catenin plays a role in this pathogenic process. Whether Wnt/ $\beta$ -catenin and PINCH1/WT1 signaling can cross-talk with each other remains a fascinating question awaiting further investigation.

## **4.1 GENERAL DISCUSSION**

### **4.1.1 Conditionally immortalized podocyte cell lines**

Podocytes are terminally differentiated glomerular epithelial cells, which play a critical role in maintaining the filtration barrier with complex structure of foot processes. The development of immortalized podocytes cell lines is a major impetus to the study of podocytes *in vitro*. In our study, we used both human and mouse podocytes cell lines which were derived with the use of

conditional immortalization techniques with a temperature-sensitive transgene [203, 240]. These cells can proliferate at the “permissive” temperature (33°C) and enter growth arrest and start to differentiate after transferring to the “nonpermissive” temperature (37°C). Although they express multiple markers of differentiated podocytes, including nephrin, podocin, CD2AP and synaptopodin, after differentiation [203, 240], there is no evidence for imitating the sophisticated three-dimensional structure of foot processes and the slit diaphragm in the monolayer culture of podocytes *in vitro*. Despite these pitfalls, here we used these cell lines to investigate the subcellular pathways, gene transcription and the effects of established and novel therapeutic agents in podocytes. To validate the *in vitro* results, we have developed and adopted TGF- $\beta$ 1 mouse model for investigating the functional effects of different intracellular signaling and mediators in podocytes *in vivo*.

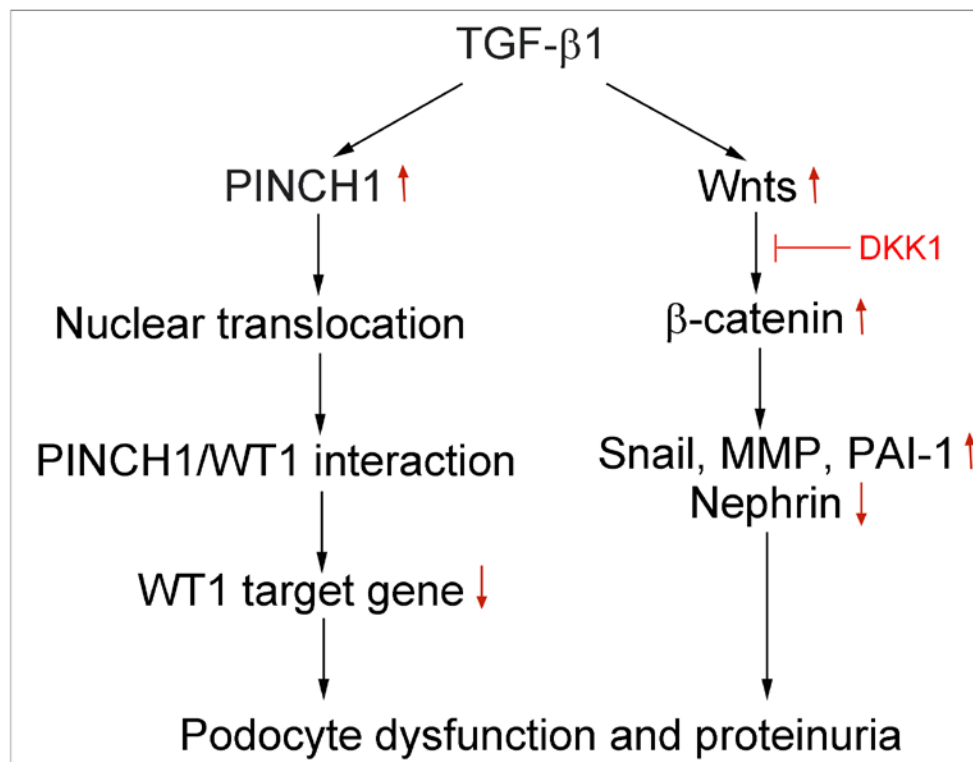


**Figure 21.** Diagram of two signaling pathways under TGF- $\beta$ 1 stimulation leading to podocyte dysfunction and proteinuria.

#### **4.1.2 TGF- $\beta$ 1 mouse model**

Although hyperactive TGF- $\beta$  signaling is observed in the injured kidneys in experimental animal models and in humans of virtually every type of chronic kidney diseases [226], little is known about its pathobiology in podocytes in vivo. Earlier studies on transgenic Alb/TGF- $\beta$ 1 mice revealed the causative role of TGF- $\beta$ 1 in the pathogenesis of nephropathies, as these mice spontaneously developed proteinuria, progressive glomerulosclerosis and interstitial fibrosis, with advanced kidney failure leading to approximately 50% animal death at 5-12 weeks of age [129, 241]. In addition, these studies demonstrated that progressive depletion of podocytes was associated with a robust increase in podocyte apoptosis from transgenic animals and indicated that podocyte depletion may be an initial lesion in the development of chronic kidney disease [130]. However, previous studies in our lab have suggested that the EMT process of podocytes, rather than their loss, is the primary cause of podocyte dysfunction leading to proteinuria in many common glomerular diseases [42]. We speculated that podocytes respond to injurious stimuli in different ways, depending on the severity and duration of the injury. In our studies, we used a simple, quick, reproducible and accessible mouse model to investigate podocyte injury induced by TGF- $\beta$ 1. Because it was much easier to regulate the expression level of TGF- $\beta$ 1 by controlling the concentration of naked plasmid vector compared to TGF- $\beta$ 1 transgenic mice, we were able to observe the cellular and molecular changes in podocytes before the presence of apoptosis. Importantly, among the three major cell types in the glomeruli, podocytes are the most susceptible target in vivo as illustrated by Smad3 phosphorylation, a surrogate marker for TGF- $\beta$  receptor activation (Figure 16). Therefore we propose that the TGF- $\beta$ 1 mouse model

established in this study is a valuable model to investigate the role of TGF- $\beta$ 1 and its downstream signaling in podocytes injury.

#### **4.1.3 Potential drawbacks**

In the first part of my studies, *in vitro* results demonstrated that PINCH1 undergoes nuclear translocation, interacts with WT1 and blocks WT1-regulated gene expression in cultured podocytes. Although nuclear translocation of PINCH1 and increased interaction between PINCH1 and WT1 have been shown in TGF- $\beta$ 1 mouse model, the direct biological consequences of these new findings *in vivo* remains to be explored. Due to the limitation of our mouse model, we cannot draw the conclusion that the interaction of PINCH1/WT1 directly causes podocyte dysfunction and proteinuria; however, the prediction that PINCH1 plays a role in regulating WT1-dependent podocytes differentiation can be made based on *in vitro* data. Consistent with this notion, another LIM domain containing protein, Wilms tumor 1 interacting protein (WTIP), has been reported to undergo nuclear translocation and interact with WT1 in podocytes, although there is also no direct evidence for WTIP-dependent repression of WT1 transcriptional activity *in vivo* [220, 242]. This raises a general theme that focal adhesion-associated proteins such as PINCH1 and WTIP are able to translocate into the nucleus and participate in gene regulation. In future, genetic approaches can be use in this study. Transgenic mouse overexpressing PINCH1 or its mutant version with disrupted nuclear localization in a podocyte-specific fashion will be an elegant and valuable approach to investigate the direct function of PINCH1 as transcription regulator *in vivo*.

As shown in Figure 8, we identified a putative NES/NLS region at the C-terminus of PINCH1, which is required for mediating cytoplasmic-nuclear shuttling of PINCH1 under both

basal and TGF- $\beta$ 1 stimulated conditions. Deletion of this region or mutations of leucine to alanine in this region impairs PINCH1 nuclear translocation, which was demonstrated by Western blot analysis of the nuclear and cytoplasmic fractions. Since leucine as a hydrophobic residue often acts as a core residue to stabilize protein structure, we cannot rule out the possibility that the failure of nuclear translocation of mutant and truncated PINCH1 is due to the overall structural perturbation. Mutating surrounding residues such as lysine may provide a negative control, however there is still the possibility that mutation of leucine may affect the whole structure of PINCH1. Another way to demonstrate the importance of a putative NES/NLS is to fuse the NES/NLS sequence to a heterologous protein, such as GFP, and then show that the putative NES/NLS drives the nuclear import of the heterologous protein by imaging studies. Using a similar approach, fusion of the mutant NES/NLS sequence to a heterologous protein should block its nuclear import.

In the second part of my studies, we investigated the role for Wnt/ $\beta$ -catenin signaling in mediating the pathogenesis of podocyte injury and proteinuria *in vivo* after ectopic expression of fibrogenic TGF- $\beta$ 1. Multiple signaling pathways can be activated by TGF- $\beta$ 1 stimulation, including Smad-dependent and Smad-independent signaling; and transcription levels of hundreds of genes are expected to change either positively or negatively. The activation of Wnt/ $\beta$ -catenin induced by TGF- $\beta$ 1 may be one of several signal pathways which are responsible for the onset of proteinuria and podocyte dysfunction. Gene therapy with DKK1 only partially mitigates albuminuria, which can be explained by two different reasons: TGF- $\beta$ 1 induces podocyte dysfunction and proteinuria by activating other signaling pathways independent of Wnt/ $\beta$ -catenin signaling; or  $\beta$ -catenin is activated by other upstream proteins besides Wnt proteins. It should be noted that although we cannot exclude the possibility of the involvement of other



pathways leading to podocyte dysfunction in this mouse model, the critical role of Wnt/ $\beta$ -catenin signaling in mediating podocyte injury has been confirmed in  $\beta$ -catenin knockout mice. Earlier studies in our lab have demonstrated that Wnt/ $\beta$ -catenin is activated in the podocytes of mouse and human kidneys with primary glomerular disorders; that ectopic expression of Wnt1 gene in mice exacerbates podocyte injury and albuminuria; and that mice with podocyte-specific ablation of  $\beta$ -catenin are protected against the development of albuminuria after adriamycin injury [201].

#### **4.1.4 Therapeutic implication and future directions**

My studies and recent reports from our lab suggest a critical role of Wnt/ $\beta$ -catenin signal pathway in podocyte dysfunction and renal fibrosis [193, 201]. The results of gene therapy with DKK1 suggest that targeting Wnt/ $\beta$ -catenin signaling might be an effective strategy to hinder the progression of podocyte injury and renal interstitial fibrosis. As a Wnt antagonist, DKK1 specifically blocks Wnt ligands binding to LRP5/6, the co-receptors that are obligatory for transmitting the canonical pathway of Wnt/ $\beta$ -catenin signaling [187]. Blocking Wnt/ $\beta$ -catenin signaling leads to the reduction of  $\beta$ -catenin accumulation, suppression of Wnt/ $\beta$ -catenin target genes, attenuation of proteinuria and podocyte injury, and reduction of renal matrix deposition and fibrosis. This conclusion is in line with a previous report that secreted frizzled-related protein 4 (sFRP4) blocks  $\beta$ -catenin signaling in tubular epithelial cells and suppressed the progression of renal fibrosis in UUO model [243]. In addition, recent studies from our lab indicate that administration of the vitamin D analog (paricalcitol) also suppresses  $\beta$ -catenin-mediated gene transcription through inducing a physical interaction between the vitamin D receptor and  $\beta$ -catenin in podocytes, and leads to amelioration of established proteinuria [244].

Therefore, it appears that targeting canonical Wnt/ $\beta$ -catenin signaling could be a novel strategy for therapeutic intervention of a variety of proteinuric and fibrotic kidney diseases.

Two independent pathways associated with podocyte dysfunction under TGF- $\beta$ 1 stimulation have been revealed by this study. Although both of them are shown to play important and distinct roles in regulating gene expression and podocytes biological functions, further studies are needed to fully understand their relative contributions as well as their pathogenic mechanisms *in vivo*. Toward this end, transgenic mouse model with overexpression of wild-type and mutant PINCH1 in a podocyte-specific fashion can be utilized to investigate the biological consequences induced by PINCH1 nuclear translocation and its interaction with WT1 *in vivo*. The mechanism of podocyte dysfunction caused by nuclear translocation can be examined by studies on WT1 targeted gene expressions and cytoskeleton changes related to PINCH1 translocation. Furthermore, the mechanism of PINCH1 nuclear translocation needs to be determined. The nuclear translocation of WTIP has been shown to require JNK activity to assemble a multiprotein complex of the scaffolding protein JNK-interacting protein 3 and the motor dynein [245]. The proteins involved in promoting PINCH1 shuttling are still unknown. In addition, further studies are warranted to investigate the potential interaction between PINCH1 and ILK after nuclear translocation. A previous report has shown that TGF- $\beta$ 1 inhibits the formation of IPP complex in podocytes [159], despite that the expressions of both ILK and PINCH1 are upregulated in that setting. As ILK is also found in the nucleus in some reports, whether nuclear ILK can interact with PINCH1 (or/and WT1) in podocytes remains to be explored [246]. Finally, the exact mechanism how  $\beta$ -catenin activation leads to podocyte dysfunction remains elusive. Key target genes which lead to the change of slit diaphragm, foot processes effacement and proteinuria can be identified and functionally validated *in vivo* by

“knock in” and “knock out” approaches. Inhibitors for  $\beta$ -catenin activity can be used to demonstrate the direct biological function of active  $\beta$ -catenin in podocytes dysfunction, and exploited as novel therapeutic agents for treatment of proteinuric and fibrotic kidney diseases.

## BIBLIOGRAPHY

1. Abrahamson, D.R., *Structure and development of the glomerular capillary wall and basement membrane*. Am J Physiol, 1987. **253**(5 Pt 2): p. F783-94.
2. J. Ashley Jefferson, S.J.S., *Glomerular Disease: The Podocyte is Ready for Prime Time and May Already Be Center Stage*. Nephrology Self-Assessment Program, 2006. **Vol 5**(No 6).
3. Ohse, T., et al., *The enigmatic parietal epithelial cell is finally getting noticed: a review*. Kidney Int, 2009. **76**(12): p. 1225-38.
4. Schlondorff, D. and B. Banas, *The mesangial cell revisited: no cell is an island*. J Am Soc Nephrol, 2009. **20**(6): p. 1179-87.
5. Chiang, C.K. and R. Inagi, *Glomerular diseases: genetic causes and future therapeutics*. Nat Rev Nephrol, 2010. **6**(9): p. 539-54.
6. Comper, W.D. and L.M. Russo, *The glomerular filter: an imperfect barrier is required for perfect renal function*. Curr Opin Nephrol Hypertens, 2009. **18**(4): p. 336-42.
7. Haraldsson, B. and M. Jeansson, *Glomerular filtration barrier*. Curr Opin Nephrol Hypertens, 2009. **18**(4): p. 331-5.
8. Yamada, E., *The fine structure of the renal glomerulus of the mouse*. J Biophys Biochem Cytol, 1955. **1**(6): p. 551-66.
9. Patrakka, J. and K. Tryggvason, *New insights into the role of podocytes in proteinuria*. Nat Rev Nephrol, 2009. **5**(8): p. 463-8.
10. Patrakka, J. and K. Tryggvason, *Molecular make-up of the glomerular filtration barrier*. Biochem Biophys Res Commun, 2010. **396**(1): p. 164-9.
11. Satchell, S.C. and F. Braet, *Glomerular endothelial cell fenestrations: an integral component of the glomerular filtration barrier*. Am J Physiol Renal Physiol, 2009. **296**(5): p. F947-56.
12. Venkatachalam, M.A., R.S. Cotran, and M.J. Karnovsky, *An ultrastructural study of glomerular permeability in aminonucleoside nephrosis using catalase as a tracer protein*. J Exp Med, 1970. **132**(6): p. 1168-80.
13. Karnovsky, M.J. and S.K. Ainsworth, *The structural basis of glomerular filtration*. Adv Nephrol Necker Hosp, 1972. **2**: p. 35-60.
14. Rodewald, R. and M.J. Karnovsky, *Porous substructure of the glomerular slit diaphragm in the rat and mouse*. J Cell Biol, 1974. **60**(2): p. 423-33.
15. Ichimura, K., et al., *Glomerular endothelial cells form diaphragms during development and pathologic conditions*. J Am Soc Nephrol, 2008. **19**(8): p. 1463-71.
16. Hjalmarsson, C., B.R. Johansson, and B. Haraldsson, *Electron microscopic evaluation of the endothelial surface layer of glomerular capillaries*. Microvasc Res, 2004. **67**(1): p. 9-17.

17. Singh, A., et al., *Glomerular endothelial glycocalyx constitutes a barrier to protein permeability*. J Am Soc Nephrol, 2007. **18**(11): p. 2885-93.
18. Henry, C.B. and B.R. Duling, *Permeation of the luminal capillary glycocalyx is determined by hyaluronan*. Am J Physiol, 1999. **277**(2 Pt 2): p. H508-14.
19. Jeansson, M. and B. Haraldsson, *Morphological and functional evidence for an important role of the endothelial cell glycocalyx in the glomerular barrier*. Am J Physiol Renal Physiol, 2006. **290**(1): p. F111-6.
20. Kuwabara, A., et al., *Deterioration of glomerular endothelial surface layer induced by oxidative stress is implicated in altered permeability of macromolecules in Zucker fatty rats*. Diabetologia, 2010. **53**(9): p. 2056-65.
21. Eremina, V., et al., *VEGF inhibition and renal thrombotic microangiopathy*. N Engl J Med, 2008. **358**(11): p. 1129-36.
22. Eremina, V., et al., *Glomerular-specific alterations of VEGF-A expression lead to distinct congenital and acquired renal diseases*. J Clin Invest, 2003. **111**(5): p. 707-16.
23. Veron, D., et al., *Overexpression of VEGF-A in podocytes of adult mice causes glomerular disease*. Kidney Int, 2010. **77**(11): p. 989-99.
24. Quaggin, S.E. and J.A. Kreidberg, *Development of the renal glomerulus: good neighbors and good fences*. Development, 2008. **135**(4): p. 609-20.
25. Miner, J.H., *Renal basement membrane components*. Kidney Int, 1999. **56**(6): p. 2016-24.
26. Tamsma, J.T., et al., *Expression of glomerular extracellular matrix components in human diabetic nephropathy: decrease of heparan sulphate in the glomerular basement membrane*. Diabetologia, 1994. **37**(3): p. 313-20.
27. van den Born, J., et al., *Distribution of GBM heparan sulfate proteoglycan core protein and side chains in human glomerular diseases*. Kidney Int, 1993. **43**(2): p. 454-63.
28. Shimomura, H. and R.G. Spiro, *Studies on macromolecular components of human glomerular basement membrane and alterations in diabetes. Decreased levels of heparan sulfate proteoglycan and laminin*. Diabetes, 1987. **36**(3): p. 374-81.
29. Raats, C.J., et al., *Reduction in glomerular heparan sulfate correlates with complement deposition and albuminuria in active Heymann nephritis*. J Am Soc Nephrol, 1999. **10**(8): p. 1689-99.
30. van den Born, J., et al., *A monoclonal antibody against GBM heparan sulfate induces an acute selective proteinuria in rats*. Kidney Int, 1992. **41**(1): p. 115-23.
31. Morita, H., et al., *Heparan sulfate of perlecan is involved in glomerular filtration*. J Am Soc Nephrol, 2005. **16**(6): p. 1703-10.
32. Harvey, S.J., et al., *Disruption of glomerular basement membrane charge through podocyte-specific mutation of agrin does not alter glomerular permselectivity*. Am J Pathol, 2007. **171**(1): p. 139-52.
33. Goldberg, S., et al., *Glomerular filtration is normal in the absence of both agrin and perlecan-heparan sulfate from the glomerular basement membrane*. Nephrol Dial Transplant, 2009. **24**(7): p. 2044-51.
34. Asgeirsson, D., et al., *Increased glomerular permeability to negatively charged Ficoll relative to neutral Ficoll in rats*. Am J Physiol Renal Physiol, 2006. **291**(5): p. F1083-9.
35. R, C.S. and M. Rao, *Tilt texture domains on a membrane and chirality induced budding*. Phys Rev Lett, 2002. **88**(8): p. 088101.
36. Tanjore, H. and R. Kalluri, *The role of type IV collagen and basement membranes in cancer progression and metastasis*. Am J Pathol, 2006. **168**(3): p. 715-7.

37. Hudson, B.G., et al., *Alport's syndrome, Goodpasture's syndrome, and type IV collagen*. N Engl J Med, 2003. **348**(25): p. 2543-56.
38. Noakes, P.G., et al., *The renal glomerulus of mice lacking  $\alpha$ -laminin/laminin beta 2: nephrosis despite molecular compensation by laminin beta 1*. Nat Genet, 1995. **10**(4): p. 400-6.
39. Zenker, M., et al., *Human laminin beta2 deficiency causes congenital nephrosis with mesangial sclerosis and distinct eye abnormalities*. Hum Mol Genet, 2004. **13**(21): p. 2625-32.
40. Jarad, G., et al., *Proteinuria precedes podocyte abnormalities in  $\text{Lamb2}^{-/-}$  mice, implicating the glomerular basement membrane as an albumin barrier*. J Clin Invest, 2006. **116**(8): p. 2272-9.
41. Ciechanowicz, A., et al., *"Treasure your exceptions": recent advances in molecular genetics of glomerular disease*. J Appl Genet, 2008. **49**(1): p. 93-9.
42. Li, Y., et al., *Epithelial-to-mesenchymal transition is a potential pathway leading to podocyte dysfunction and proteinuria*. Am J Pathol, 2008. **172**(2): p. 299-308.
43. Liu, Y., *New insights into epithelial-mesenchymal transition in kidney fibrosis*. J Am Soc Nephrol, 2010. **21**(2): p. 212-22.
44. Sawada, H., et al., *Epithelial polyanion (podocalyxin) is found on the sides but not the soles of the foot processes of the glomerular epithelium*. Am J Pathol, 1986. **125**(2): p. 309-18.
45. Faul, C., et al., *Actin up: regulation of podocyte structure and function by components of the actin cytoskeleton*. Trends Cell Biol, 2007. **17**(9): p. 428-37.
46. Kestila, M., et al., *Positionally cloned gene for a novel glomerular protein--nephrin--is mutated in congenital nephrotic syndrome*. Mol Cell, 1998. **1**(4): p. 575-82.
47. Jones, N., et al., *Nck adaptor proteins link nephrin to the actin cytoskeleton of kidney podocytes*. Nature, 2006. **440**(7085): p. 818-23.
48. Li, H., et al., *Rat nephrin modulates cell morphology via the adaptor protein Nck*. Biochem Biophys Res Commun, 2006. **349**(1): p. 310-6.
49. Verma, R., et al., *Nephrin ectodomain engagement results in Src kinase activation, nephrin phosphorylation, Nck recruitment, and actin polymerization*. J Clin Invest, 2006. **116**(5): p. 1346-59.
50. Putaala, H., et al., *The murine nephrin gene is specifically expressed in kidney, brain and pancreas: inactivation of the gene leads to massive proteinuria and neonatal death*. Hum Mol Genet, 2001. **10**(1): p. 1-8.
51. Boute, N., et al., *NPHS2, encoding the glomerular protein podocin, is mutated in autosomal recessive steroid-resistant nephrotic syndrome*. Nat Genet, 2000. **24**(4): p. 349-54.
52. Huber, T.B., et al., *Interaction with podocin facilitates nephrin signaling*. J Biol Chem, 2001. **276**(45): p. 41543-6.
53. Roselli, S., et al., *Early glomerular filtration defect and severe renal disease in podocin-deficient mice*. Mol Cell Biol, 2004. **24**(2): p. 550-60.
54. Shih, N.Y., et al., *CD2AP localizes to the slit diaphragm and binds to nephrin via a novel C-terminal domain*. Am J Pathol, 2001. **159**(6): p. 2303-8.
55. Schwarz, K., et al., *Podocin, a raft-associated component of the glomerular slit diaphragm, interacts with CD2AP and nephrin*. J Clin Invest, 2001. **108**(11): p. 1621-9.

56. Shih, N.Y., et al., *Congenital nephrotic syndrome in mice lacking CD2-associated protein*. Science, 1999. **286**(5438): p. 312-5.
57. Chuang, P.Y. and J.C. He, *Signaling in regulation of podocyte phenotypes*. Nephron Physiol, 2009. **111**(2): p. p9-15.
58. Kreidberg, J.A., et al., *Alpha 3 beta 1 integrin has a crucial role in kidney and lung organogenesis*. Development, 1996. **122**(11): p. 3537-47.
59. Kanasaki, K., et al., *Integrin beta1-mediated matrix assembly and signaling are critical for the normal development and function of the kidney glomerulus*. Dev Biol, 2008. **313**(2): p. 584-93.
60. Pozzi, A., et al., *Beta1 integrin expression by podocytes is required to maintain glomerular structural integrity*. Dev Biol, 2008. **316**(2): p. 288-301.
61. Vogtlander, N.P., et al., *Ligation of alpha-dystroglycan on podocytes induces intracellular signaling: a new mechanism for podocyte effacement?* PLoS One, 2009. **4**(6): p. e5979.
62. Dai, C., et al., *Essential role of integrin-linked kinase in podocyte biology: Bridging the integrin and slit diaphragm signaling*. J Am Soc Nephrol, 2006. **17**(8): p. 2164-75.
63. El-Aouni, C., et al., *Podocyte-specific deletion of integrin-linked kinase results in severe glomerular basement membrane alterations and progressive glomerulosclerosis*. J Am Soc Nephrol, 2006. **17**(5): p. 1334-44.
64. Doyonnas, R., et al., *Anuria, omphalocele, and perinatal lethality in mice lacking the CD34-related protein podocalyxin*. J Exp Med, 2001. **194**(1): p. 13-27.
65. Schmieder, S., et al., *Podocalyxin activates RhoA and induces actin reorganization through NHERF1 and Ezrin in MDCK cells*. J Am Soc Nephrol, 2004. **15**(9): p. 2289-98.
66. Takeda, T., *Podocyte cytoskeleton is connected to the integral membrane protein podocalyxin through Na<sup>+</sup>/H<sup>+</sup>-exchanger regulatory factor 2 and ezrin*. Clin Exp Nephrol, 2003. **7**(4): p. 260-9.
67. Orlando, R.A., et al., *The glomerular epithelial cell anti-adhesin podocalyxin associates with the actin cytoskeleton through interactions with ezrin*. J Am Soc Nephrol, 2001. **12**(8): p. 1589-98.
68. Morrison, A.A., et al., *New insights into the function of the Wilms tumor suppressor gene WT1 in podocytes*. Am J Physiol Renal Physiol, 2008. **295**(1): p. F12-F17.
69. Wagner, K.D., N. Wagner, and A. Schedl, *The complex life of WT1*. J Cell Sci, 2003. **116**(Pt 9): p. 1653-8.
70. Palmer, R.E., et al., *WT1 regulates the expression of the major glomerular podocyte membrane protein Podocalyxin*. Curr Biol, 2001. **11**(22): p. 1805-9.
71. Wagner, N., et al., *The major podocyte protein nephrin is transcriptionally activated by the Wilms' tumor suppressor WT1*. J Am Soc Nephrol, 2004. **15**(12): p. 3044-51.
72. Guo, G., et al., *WT1 activates a glomerular-specific enhancer identified from the human nephrin gene*. J Am Soc Nephrol, 2004. **15**(11): p. 2851-6.
73. Guo, J.K., et al., *WT1 is a key regulator of podocyte function: reduced expression levels cause crescentic glomerulonephritis and mesangial sclerosis*. Hum Mol Genet, 2002. **11**(6): p. 651-9.
74. Mrowka, C. and A. Schedl, *Wilms' tumor suppressor gene WT1: from structure to renal pathophysiologic features*. J Am Soc Nephrol, 2000. **11 Suppl 16**: p. S106-15.
75. Grubb, G.R., et al., *Expression of WT1 protein in fetal kidneys and Wilms tumors*. Lab Invest, 1994. **71**(4): p. 472-9.

76. Macconi, D., et al., *Pathophysiologic implications of reduced podocyte number in a rat model of progressive glomerular injury*. Am J Pathol, 2006. **168**(1): p. 42-54.
77. Sharma, P.M., et al., *RNA editing in the Wilms' tumor susceptibility gene, WT1*. Genes Dev, 1994. **8**(6): p. 720-31.
78. Hewitt, S.M. and G.F. Saunders, *Differentially spliced exon 5 of the Wilms' tumor gene WT1 modifies gene function*. Anticancer Res, 1996. **16**(2): p. 621-6.
79. Natoli, T.A., et al., *A mammal-specific exon of WT1 is not required for development or fertility*. Mol Cell Biol, 2002. **22**(12): p. 4433-8.
80. Larsson, S.H., et al., *Subnuclear localization of WT1 in splicing or transcription factor domains is regulated by alternative splicing*. Cell, 1995. **81**(3): p. 391-401.
81. Laity, J.H., H.J. Dyson, and P.E. Wright, *Molecular basis for modulation of biological function by alternate splicing of the Wilms' tumor suppressor protein*. Proc Natl Acad Sci U S A, 2000. **97**(22): p. 11932-5.
82. Menke, A., et al., *The Wilms' tumor suppressor WT1: approaches to gene function*. Kidney Int, 1998. **53**(6): p. 1512-8.
83. Hosono, S., et al., *E-cadherin is a WT1 target gene*. J Biol Chem, 2000. **275**(15): p. 10943-53.
84. Lee, S.B., et al., *The Wilms tumor suppressor WT1 encodes a transcriptional activator of amphiregulin*. Cell, 1999. **98**(5): p. 663-73.
85. Kim, M.S., et al., *A novel Wilms tumor 1 (WT1) target gene negatively regulates the WNT signaling pathway*. J Biol Chem, 2010. **285**(19): p. 14585-93.
86. Jefferson, J.A., S.J. Shankland, and R.H. Pichler, *Proteinuria in diabetic kidney disease: a mechanistic viewpoint*. Kidney Int, 2008. **74**(1): p. 22-36.
87. Shi, Y. and J. Massague, *Mechanisms of TGF-beta signaling from cell membrane to the nucleus*. Cell, 2003. **113**(6): p. 685-700.
88. Khalil, N., *TGF-beta: from latent to active*. Microbes Infect, 1999. **1**(15): p. 1255-63.
89. Brunner, A.M., et al., *Site-directed mutagenesis of cysteine residues in the pro region of the transforming growth factor beta 1 precursor. Expression and characterization of mutant proteins*. J Biol Chem, 1989. **264**(23): p. 13660-4.
90. Miyazono, K., et al., *A role of the latent TGF-beta 1-binding protein in the assembly and secretion of TGF-beta 1*. EMBO J, 1991. **10**(5): p. 1091-101.
91. Lopez, A.R., et al., *Dominant negative mutants of transforming growth factor-beta 1 inhibit the secretion of different transforming growth factor-beta isoforms*. Mol Cell Biol, 1992. **12**(4): p. 1674-9.
92. Saharinen, J., J. Taipale, and J. Keski-Oja, *Association of the small latent transforming growth factor-beta with an eight cysteine repeat of its binding protein LTBP-1*. EMBO J, 1996. **15**(2): p. 245-53.
93. Rifkin, D.B., *Latent transforming growth factor-beta (TGF-beta) binding proteins: orchestrators of TGF-beta availability*. J Biol Chem, 2005. **280**(9): p. 7409-12.
94. Annes, J.P., J.S. Munger, and D.B. Rifkin, *Making sense of latent TGFbeta activation*. J Cell Sci, 2003. **116**(Pt 2): p. 217-24.
95. Lyons, R.M., J. Keski-Oja, and H.L. Moses, *Proteolytic activation of latent transforming growth factor-beta from fibroblast-conditioned medium*. J Cell Biol, 1988. **106**(5): p. 1659-65.



96. Yu, Q. and I. Stamenkovic, *Cell surface-localized matrix metalloproteinase-9 proteolytically activates TGF-beta and promotes tumor invasion and angiogenesis*. Genes Dev, 2000. **14**(2): p. 163-76.
97. Sato, Y. and D.B. Rifkin, *Inhibition of endothelial cell movement by pericytes and smooth muscle cells: activation of a latent transforming growth factor-beta 1-like molecule by plasmin during co-culture*. J Cell Biol, 1989. **109**(1): p. 309-15.
98. Crawford, S.E., et al., *Thrombospondin-1 is a major activator of TGF-beta1 in vivo*. Cell, 1998. **93**(7): p. 1159-70.
99. Munger, J.S., et al., *The integrin alpha v beta 6 binds and activates latent TGF beta 1: a mechanism for regulating pulmonary inflammation and fibrosis*. Cell, 1999. **96**(3): p. 319-28.
100. Mu, D., et al., *The integrin alpha(v)beta8 mediates epithelial homeostasis through MT1-MMP-dependent activation of TGF-beta1*. J Cell Biol, 2002. **157**(3): p. 493-507.
101. Barcellos-Hoff, M.H., et al., *Transforming growth factor-beta activation in irradiated murine mammary gland*. J Clin Invest, 1994. **93**(2): p. 892-9.
102. Dore, J.J., Jr., et al., *Heteromeric and homomeric transforming growth factor-beta receptors show distinct signaling and endocytic responses in epithelial cells*. J Biol Chem, 1998. **273**(48): p. 31770-7.
103. Cheifetz, S., J.L. Andres, and J. Massague, *The transforming growth factor-beta receptor type III is a membrane proteoglycan. Domain structure of the receptor*. J Biol Chem, 1988. **263**(32): p. 16984-91.
104. Rotzer, D., et al., *Type III TGF-beta receptor-independent signalling of TGF-beta2 via TbetaRII-B, an alternatively spliced TGF-beta type II receptor*. EMBO J, 2001. **20**(3): p. 480-90.
105. Sankar, S., et al., *Expression of transforming growth factor type III receptor in vascular endothelial cells increases their responsiveness to transforming growth factor beta 2*. J Biol Chem, 1995. **270**(22): p. 13567-72.
106. Gagliardini, E. and A. Benigni, *Therapeutic potential of TGF-beta inhibition in chronic renal failure*. Expert Opin Biol Ther, 2007. **7**(3): p. 293-304.
107. Blobe, G.C., W.P. Schiemann, and H.F. Lodish, *Role of transforming growth factor beta in human disease*. N Engl J Med, 2000. **342**(18): p. 1350-8.
108. Wang, W., et al., *Signaling mechanism of TGF-beta1 in prevention of renal inflammation: role of Smad7*. J Am Soc Nephrol, 2005. **16**(5): p. 1371-83.
109. Dennler, S., et al., *Direct binding of Smad3 and Smad4 to critical TGF beta-inducible elements in the promoter of human plasminogen activator inhibitor-type 1 gene*. EMBO J, 1998. **17**(11): p. 3091-100.
110. Shi, Y., et al., *Crystal structure of a Smad MH1 domain bound to DNA: insights on DNA binding in TGF-beta signaling*. Cell, 1998. **94**(5): p. 585-94.
111. Massague, J., *How cells read TGF-beta signals*. Nat Rev Mol Cell Biol, 2000. **1**(3): p. 169-78.
112. Schnaper, H.W. and J.B. Kopp, *Renal fibrosis*. Front Biosci, 2003. **8**: p. e68-86.
113. Shihab, F.S., *Do we have a pill for renal fibrosis?* Clin J Am Soc Nephrol, 2007. **2**(5): p. 876-8.
114. Yamamoto, T., et al., *Expression of transforming growth factor-beta isoforms in human glomerular diseases*. Kidney Int, 1996. **49**(2): p. 461-9.

115. Pfeiffer, A., et al., *Elevated plasma levels of transforming growth factor-beta 1 in NIDDM*. Diabetes Care, 1996. **19**(10): p. 1113-7.
116. Sato, H., et al., *Increased excretion of urinary transforming growth factor beta 1 in patients with diabetic nephropathy*. Am J Nephrol, 1998. **18**(6): p. 490-4.
117. Hong, S.W., et al., *Increased glomerular and tubular expression of transforming growth factor-beta1, its type II receptor, and activation of the Smad signaling pathway in the db/db mouse*. Am J Pathol, 2001. **158**(5): p. 1653-63.
118. Yamamoto, T., et al., *Expression of transforming growth factor beta is elevated in human and experimental diabetic nephropathy*. Proc Natl Acad Sci U S A, 1993. **90**(5): p. 1814-8.
119. Nakamura, T., et al., *Messenger RNA expression for growth factors in glomeruli from focal glomerular sclerosis*. Clin Immunol Immunopathol, 1993. **66**(1): p. 33-42.
120. Abbate, M., et al., *Proximal tubular cells promote fibrogenesis by TGF-beta1-mediated induction of peritubular myofibroblasts*. Kidney Int, 2002. **61**(6): p. 2066-77.
121. Roberts, A.B., et al., *Transforming growth factor-beta. Major role in regulation of extracellular matrix*. Ann N Y Acad Sci, 1990. **580**: p. 225-32.
122. Branton, M.H. and J.B. Kopp, *TGF-beta and fibrosis*. Microbes Infect, 1999. **1**(15): p. 1349-65.
123. Tomooka, S., et al., *Glomerular matrix accumulation is linked to inhibition of the plasmin protease system*. Kidney Int, 1992. **42**(6): p. 1462-9.
124. Zavadil, J. and E.P. Bottinger, *TGF-beta and epithelial-to-mesenchymal transitions*. Oncogene, 2005. **24**(37): p. 5764-74.
125. Li, Y., et al., *PINCH-1 promotes tubular epithelial-to-mesenchymal transition by interacting with integrin-linked kinase*. J Am Soc Nephrol, 2007. **18**(9): p. 2534-43.
126. Li, Y., et al., *Tubular epithelial cell dedifferentiation is driven by the helix-loop-helix transcriptional inhibitor Id1*. J Am Soc Nephrol, 2007. **18**(2): p. 449-60.
127. Phanish, M.K., et al., *The differential role of Smad2 and Smad3 in the regulation of pro-fibrotic TGFbeta1 responses in human proximal-tubule epithelial cells*. Biochem J, 2006. **393**(Pt 2): p. 601-7.
128. Carver, E.A., et al., *The mouse snail gene encodes a key regulator of the epithelial-mesenchymal transition*. Mol Cell Biol, 2001. **21**(23): p. 8184-8.
129. Schiffer, M., et al., *Apoptosis in podocytes induced by TGF-beta and Smad7*. J Clin Invest, 2001. **108**(6): p. 807-16.
130. Border, W.A., et al., *Natural inhibitor of transforming growth factor-beta protects against scarring in experimental kidney disease*. Nature, 1992. **360**(6402): p. 361-4.
131. Miyajima, A., et al., *Antibody to transforming growth factor-beta ameliorates tubular apoptosis in unilateral ureteral obstruction*. Kidney Int, 2000. **58**(6): p. 2301-13.
132. Fukasawa, H., et al., *Treatment with anti-TGF-beta antibody ameliorates chronic progressive nephritis by inhibiting Smad/TGF-beta signaling*. Kidney Int, 2004. **65**(1): p. 63-74.
133. Islam, M., et al., *Effect of anti-transforming growth factor-beta antibodies in cyclosporine-induced renal dysfunction*. Kidney Int, 2001. **59**(2): p. 498-506.
134. Sharma, K., et al., *Neutralization of TGF-beta by anti-TGF-beta antibody attenuates kidney hypertrophy and the enhanced extracellular matrix gene expression in STZ-induced diabetic mice*. Diabetes, 1996. **45**(4): p. 522-30.

135. Grygielko, E.T., et al., *Inhibition of gene markers of fibrosis with a novel inhibitor of transforming growth factor-beta type I receptor kinase in puromycin-induced nephritis*. J Pharmacol Exp Ther, 2005. **313**(3): p. 943-51.
136. Hwang, M., et al., *TGF-beta1 siRNA suppresses the tubulointerstitial fibrosis in the kidney of ureteral obstruction*. Exp Mol Pathol, 2006. **81**(1): p. 48-54.
137. Lan, H.Y., et al., *Inhibition of renal fibrosis by gene transfer of inducible Smad7 using ultrasound-microbubble system in rat UUO model*. J Am Soc Nephrol, 2003. **14**(6): p. 1535-48.
138. Yang, J., C. Dai, and Y. Liu, *A novel mechanism by which hepatocyte growth factor blocks tubular epithelial to mesenchymal transition*. J Am Soc Nephrol, 2005. **16**(1): p. 68-78.
139. Legate, K.R., et al., *ILK, PINCH and parvin: the tIPP of integrin signalling*. Nat Rev Mol Cell Biol, 2006. **7**(1): p. 20-31.
140. Hynes, R.O., *Integrins: bidirectional, allosteric signaling machines*. Cell, 2002. **110**(6): p. 673-87.
141. Kagami, S. and S. Kondo, *Beta1-integrins and glomerular injury*. J Med Invest, 2004. **51**(1-2): p. 1-13.
142. Wu, C., *The PINCH-ILK-parvin complexes: assembly, functions and regulation*. Biochim Biophys Acta, 2004. **1692**(2-3): p. 55-62.
143. Wu, C. and S. Dedhar, *Integrin-linked kinase (ILK) and its interactors: a new paradigm for the coupling of extracellular matrix to actin cytoskeleton and signaling complexes*. J Cell Biol, 2001. **155**(4): p. 505-10.
144. Yang, Y., et al., *Formation and phosphorylation of the PINCH-1-integrin linked kinase-alpha-parvin complex are important for regulation of renal glomerular podocyte adhesion, architecture, and survival*. J Am Soc Nephrol, 2005. **16**(7): p. 1966-76.
145. Hannigan, G.E., et al., *Regulation of cell adhesion and anchorage-dependent growth by a new beta 1-integrin-linked protein kinase*. Nature, 1996. **379**(6560): p. 91-6.
146. Pasquet, J.M., M. Noury, and A.T. Nurden, *Evidence that the platelet integrin alphaIIb beta3 is regulated by the integrin-linked kinase, ILK, in a PI3-kinase dependent pathway*. Thromb Haemost, 2002. **88**(1): p. 115-22.
147. Dedhar, S., B. Williams, and G. Hannigan, *Integrin-linked kinase (ILK): a regulator of integrin and growth-factor signalling*. Trends Cell Biol, 1999. **9**(8): p. 319-23.
148. Delcommenne, M., et al., *Phosphoinositide-3-OH kinase-dependent regulation of glycogen synthase kinase 3 and protein kinase B/AKT by the integrin-linked kinase*. Proc Natl Acad Sci U S A, 1998. **95**(19): p. 11211-6.
149. Persad, S., et al., *Regulation of protein kinase B/Akt-serine 473 phosphorylation by integrin-linked kinase: critical roles for kinase activity and amino acids arginine 211 and serine 343*. J Biol Chem, 2001. **276**(29): p. 27462-9.
150. Filipenko, N.R., et al., *Integrin-linked kinase activity regulates Rac- and Cdc42-mediated actin cytoskeleton reorganization via alpha-PIX*. Oncogene, 2005. **24**(38): p. 5837-49.
151. Lynch, D.K., et al., *Integrin-linked kinase regulates phosphorylation of serine 473 of protein kinase B by an indirect mechanism*. Oncogene, 1999. **18**(56): p. 8024-32.
152. Troussard, A.A., et al., *Conditional knock-out of integrin-linked kinase demonstrates an essential role in protein kinase B/Akt activation*. J Biol Chem, 2003. **278**(25): p. 22374-8.
153. Mackinnon, A.C., et al., *C. elegans PAT-4/ILK functions as an adaptor protein within integrin adhesion complexes*. Curr Biol, 2002. **12**(10): p. 787-97.

154. Zervas, C.G., S.L. Gregory, and N.H. Brown, *Drosophila integrin-linked kinase is required at sites of integrin adhesion to link the cytoskeleton to the plasma membrane*. J Cell Biol, 2001. **152**(5): p. 1007-18.
155. Grashoff, C., et al., *Integrin-linked kinase regulates chondrocyte shape and proliferation*. EMBO Rep, 2003. **4**(4): p. 432-8.
156. Wickstrom, S.A., et al., *The ILK/PINCH/parvin complex: the kinase is dead, long live the pseudokinase!* EMBO J, 2010. **29**(2): p. 281-91.
157. Zhang, Y., et al., *Assembly of the PINCH-ILK-CH-ILKBP complex precedes and is essential for localization of each component to cell-matrix adhesion sites*. J Cell Sci, 2002. **115**(Pt 24): p. 4777-86.
158. Fukuda, T., et al., *PINCH-1 is an obligate partner of integrin-linked kinase (ILK) functioning in cell shape modulation, motility, and survival*. J Biol Chem, 2003. **278**(51): p. 51324-33.
159. Jung, K.Y., et al., *TGF-beta1 regulates the PINCH-1-integrin-linked kinase-alpha-parvin complex in glomerular cells*. J Am Soc Nephrol, 2007. **18**(1): p. 66-73.
160. Tu, Y., et al., *The LIM-only protein PINCH directly interacts with integrin-linked kinase and is recruited to integrin-rich sites in spreading cells*. Mol Cell Biol, 1999. **19**(3): p. 2425-34.
161. Zhang, Y., et al., *Characterization of PINCH-2, a new focal adhesion protein that regulates the PINCH-1-ILK interaction, cell spreading, and migration*. J Biol Chem, 2002. **277**(41): p. 38328-38.
162. Chiswell, B.P., et al., *Structural basis of competition between PINCH1 and PINCH2 for binding to the ankyrin repeat domain of integrin-linked kinase*. J Struct Biol, 2010. **170**(1): p. 157-63.
163. Kadrmas, J.L. and M.C. Beckerle, *The LIM domain: from the cytoskeleton to the nucleus*. Nat Rev Mol Cell Biol, 2004. **5**(11): p. 920-31.
164. Michelsen, J.W., et al., *The LIM motif defines a specific zinc-binding protein domain*. Proc Natl Acad Sci U S A, 1993. **90**(10): p. 4404-8.
165. Tu, Y., F. Li, and C. Wu, *Nck-2, a novel Src homology2/3-containing adaptor protein that interacts with the LIM-only protein PINCH and components of growth factor receptor kinase-signaling pathways*. Mol Biol Cell, 1998. **9**(12): p. 3367-82.
166. Buday, L., L. Wunderlich, and P. Tamas, *The Nck family of adapter proteins: regulators of actin cytoskeleton*. Cell Signal, 2002. **14**(9): p. 723-31.
167. Campana, W.M., R.R. Myers, and A. Rearden, *Identification of PINCH in Schwann cells and DRG neurons: shuttling and signaling after nerve injury*. Glia, 2003. **41**(3): p. 213-23.
168. Xu, Z., et al., *Molecular dissection of PINCH-1 reveals a mechanism of coupling and uncoupling of cell shape modulation and survival*. J Biol Chem, 2005. **280**(30): p. 27631-7.
169. Liang, X., et al., *PINCH1 plays an essential role in early murine embryonic development but is dispensable in ventricular cardiomyocytes*. Mol Cell Biol, 2005. **25**(8): p. 3056-62.
170. Hobert, O., et al., *A conserved LIM protein that affects muscular adherens junction integrity and mechanosensory function in Caenorhabditis elegans*. J Cell Biol, 1999. **144**(1): p. 45-57.

171. Clark, K.A., M. McGrail, and M.C. Beckerle, *Analysis of PINCH function in Drosophila demonstrates its requirement in integrin-dependent cellular processes*. Development, 2003. **130**(12): p. 2611-21.
172. Sakai, T., et al., *Integrin-linked kinase (ILK) is required for polarizing the epiblast, cell adhesion, and controlling actin accumulation*. Genes Dev, 2003. **17**(7): p. 926-40.
173. Zhu, Z., et al., *PINCH expression and its significance in esophageal squamous cell carcinoma*. Dis Markers, 2008. **25**(2): p. 75-80.
174. Zhang, J.T., et al., *Up-regulation of PINCH in the stroma of oral squamous cell carcinoma predicts nodal metastasis*. Oncol Rep, 2005. **14**(6): p. 1519-22.
175. Wang, M.W., et al., *Expression of PINCH protein in gliomas and its clinicopathological significance*. Oncology, 2007. **72**(5-6): p. 343-6.
176. Liang, X., et al., *Pinch1 is required for normal development of cranial and cardiac neural crest-derived structures*. Circ Res, 2007. **100**(4): p. 527-35.
177. Chen, K., et al., *PINCH-1 regulates the ERK-Bim pathway and contributes to apoptosis resistance in cancer cells*. J Biol Chem, 2008. **283**(5): p. 2508-17.
178. Shi, X., et al., *Roles of PINCH-2 in regulation of glomerular cell shape change and fibronectin matrix deposition*. Am J Physiol Renal Physiol, 2008. **295**(1): p. F253-63.
179. Clevers, H., *Wnt/beta-catenin signaling in development and disease*. Cell, 2006. **127**(3): p. 469-80.
180. Coudreuse, D. and H.C. Korswagen, *The making of Wnt: new insights into Wnt maturation, sorting and secretion*. Development, 2007. **134**(1): p. 3-12.
181. Barker, N., *The canonical Wnt/beta-catenin signalling pathway*. Methods Mol Biol, 2008. **468**: p. 5-15.
182. Katoh, M., *WNT/PCP signaling pathway and human cancer (review)*. Oncol Rep, 2005. **14**(6): p. 1583-8.
183. Kohn, A.D. and R.T. Moon, *Wnt and calcium signaling: beta-catenin-independent pathways*. Cell Calcium, 2005. **38**(3-4): p. 439-46.
184. *Entrez Gene: catenin (cadherin-associated protein)*.
185. Reya, T. and H. Clevers, *Wnt signalling in stem cells and cancer*. Nature, 2005. **434**(7035): p. 843-50.
186. Morin, P.J., et al., *Activation of beta-catenin-Tcf signaling in colon cancer by mutations in beta-catenin or APC*. Science, 1997. **275**(5307): p. 1787-90.
187. Kawano, Y. and R. Kypta, *Secreted antagonists of the Wnt signalling pathway*. J Cell Sci, 2003. **116**(Pt 13): p. 2627-34.
188. Glinka, A., et al., *Dickkopf-1 is a member of a new family of secreted proteins and functions in head induction*. Nature, 1998. **391**(6665): p. 357-62.
189. Niehrs, C., *Function and biological roles of the Dickkopf family of Wnt modulators*. Oncogene, 2006. **25**(57): p. 7469-81.
190. Mao, B., et al., *Kremen proteins are Dickkopf receptors that regulate Wnt/beta-catenin signalling*. Nature, 2002. **417**(6889): p. 664-7.
191. Wu, W., et al., *Mutual antagonism between dickkopf1 and dickkopf2 regulates Wnt/beta-catenin signalling*. Curr Biol, 2000. **10**(24): p. 1611-4.
192. Brott, B.K. and S.Y. Sokol, *Regulation of Wnt/LRP signaling by distinct domains of Dickkopf proteins*. Mol Cell Biol, 2002. **22**(17): p. 6100-10.
193. He, W., et al., *Wnt/beta-catenin signaling promotes renal interstitial fibrosis*. J Am Soc Nephrol, 2009. **20**(4): p. 765-76.

194. Niida, A., et al., *DKK1, a negative regulator of Wnt signaling, is a target of the beta-catenin/TCF pathway*. *Oncogene*, 2004. **23**(52): p. 8520-6.
195. Stark, K., et al., *Epithelial transformation of metanephric mesenchyme in the developing kidney regulated by Wnt-4*. *Nature*, 1994. **372**(6507): p. 679-83.
196. Carroll, T.J., et al., *Wnt9b plays a central role in the regulation of mesenchymal to epithelial transitions underlying organogenesis of the mammalian urogenital system*. *Dev Cell*, 2005. **9**(2): p. 283-92.
197. Park, J.S., M.T. Valerius, and A.P. McMahon, *Wnt/beta-catenin signaling regulates nephron induction during mouse kidney development*. *Development*, 2007. **134**(13): p. 2533-9.
198. Hwang, I., E.Y. Seo, and H. Ha, *Wnt/beta-catenin signaling: a novel target for therapeutic intervention of fibrotic kidney disease*. *Arch Pharm Res*, 2009. **32**(12): p. 1653-62.
199. Petersen, C.E., S. Amaral, and E. Frosch, *Lithium-induced nephrotic syndrome in a prepubertal boy*. *J Child Adolesc Psychopharmacol*, 2008. **18**(2): p. 210-3.
200. Presne, C., et al., *Lithium-induced nephropathy: Rate of progression and prognostic factors*. *Kidney Int*, 2003. **64**(2): p. 585-92.
201. Dai, C., et al., *Wnt/beta-catenin signaling promotes podocyte dysfunction and albuminuria*. *J Am Soc Nephrol*, 2009. **20**(9): p. 1997-2008.
202. Matsui, I., et al., *Snail, a transcriptional regulator, represses nephrin expression in glomerular epithelial cells of nephrotic rats*. *Lab Invest*, 2007. **87**(3): p. 273-83.
203. Saleem, M.A., et al., *A conditionally immortalized human podocyte cell line demonstrating nephrin and podocin expression*. *J Am Soc Nephrol*, 2002. **13**(3): p. 630-8.
204. Dai, C., et al., *Wnt/ $\beta$ -catenin signaling promotes podocyte dysfunction and albuminuria*. *J Am Soc Nephrol*, 2009. **20**: p. 1997-2008.
205. Dai, C., et al., *Intravenous administration of hepatocyte growth factor gene ameliorates diabetic nephropathy in mice*. *J Am Soc Nephrol*, 2004. **15**(10): p. 2637-2647.
206. Dai, C., J. Yang, and Y. Liu, *Single injection of naked plasmid encoding hepatocyte growth factor prevents cell death and ameliorates acute renal failure in mice*. *J Am Soc Nephrol*, 2002. **13**(2): p. 411-422.
207. Liu, Y., et al., *Primary structure of rat HGF receptor and induced expression in glomerular mesangial cells*. *Am J Physiol*, 1996. **271**(3 Pt 2): p. F679-F688.
208. Brunner, A.M., et al., *Site-directed mutagenesis of cysteine residues in the pro region of the transforming growth factor  $\beta$ 1 precursor: expression and characterization of mutant proteins*. *J. Biol. Chem.*, 1989. **264**: p. 13660-13664.
209. Li, Y., et al., *Inhibition of integrin-linked kinase reduces renal interstitial fibrosis*. *J Am Soc Nephrol*, 2009. **20**: p. 1907-1918.
210. Li, Y., et al., *Epithelial-to-mesenchymal transition is a potential pathway leading to podocyte dysfunction and proteinuria*. *Am. J. Pathol.*, 2008. **172**: p. 299-308.
211. Dai, C., et al., *Essential role of integrin-linked kinase in podocyte biology: bridging the integrin and slit diaphragm signaling*. *J Am Soc Nephrol*, 2006. **17**(8): p. 2164-2175.
212. Bottinger, E.P., *TGF-beta in renal injury and disease*. *Semin Nephrol*, 2007. **27**(3): p. 309-320.
213. Li, Y., et al., *PINCH-1 promotes tubular epithelial-to-mesenchymal transition by interacting with integrin-linked kinase*. *J Am Soc Nephrol*, 2007. **18**(9): p. 2534-2543.

214. Lange, A., et al., *Classical nuclear localization signals: definition, function, and interaction with importin alpha*. J Biol Chem, 2007. **282**(8): p. 5101-5.
215. Nielsen, J.S. and K.M. McNagny, *The role of podocalyxin in health and disease*. J Am Soc Nephrol, 2009. **20**(8): p. 1669-76.
216. Legate, K.R., et al., *ILK, PINCH and parvin: the tIPP of integrin signalling*. Nat. Rev. Mol. Cell Biol, 2006. **7**: p. 20-31.
217. Wu, C., *PINCH, N(ick) and the ILK: network wiring at cell-matrix adhesions*. Trends Cell Biol, 2005. **15**(9): p. 460-466.
218. Verma, R., et al., *Nephrin ectodomain engagement results in Src kinase activation, nephrin phosphorylation, Nck recruitment, and actin polymerization*. J Clin Invest, 2006. **116**(5): p. 1346-1359.
219. Jones, N., et al., *Nck adaptor proteins link nephrin to the actin cytoskeleton of kidney podocytes*. Nature, 2006. **440**(7085): p. 818-823.
220. Srichai, M.B., et al., *A WT1 co-regulator controls podocyte phenotype by shuttling between adhesion structures and nucleus*. J Biol Chem, 2004. **279**(14): p. 14398-408.
221. Rico, M., et al., *WT1-interacting protein and ZO-1 translocate into podocyte nuclei after puromycin aminonucleoside treatment*. Am J Physiol Renal Physiol, 2005. **289**(2): p. F431-F441.
222. Takeda, T., et al., *Loss of glomerular foot processes is associated with uncoupling of podocalyxin from the actin cytoskeleton*. J Clin Invest, 2001. **108**(2): p. 289-301.
223. Tan, X., Y. Li, and Y. Liu, *Paricalcitol attenuates renal interstitial fibrosis in obstructive nephropathy*. J Am Soc Nephrol, 2006. **17**(12): p. 3382-93.
224. Dai, C., et al., *Intravenous administration of hepatocyte growth factor gene ameliorates diabetic nephropathy in mice*. J Am Soc Nephrol, 2004. **15**(10): p. 2637-47.
225. Dai, C., J. Yang, and Y. Liu, *Single injection of naked plasmid encoding hepatocyte growth factor prevents cell death and ameliorates acute renal failure in mice*. J Am Soc Nephrol, 2002. **13**(2): p. 411-22.
226. Bottinger, E.P. and M. Bitzer, *TGF-beta signaling in renal disease*. J Am Soc Nephrol, 2002. **13**(10): p. 2600-10.
227. Attisano, L. and E. Labbe, *TGFbeta and Wnt pathway cross-talk*. Cancer Metastasis Rev, 2004. **23**(1-2): p. 53-61.
228. Nishita, M., et al., *Interaction between Wnt and TGF-beta signalling pathways during formation of Spemann's organizer*. Nature, 2000. **403**(6771): p. 781-5.
229. Fodde, R. and T. Brabletz, *Wnt/beta-catenin signaling in cancer stemness and malignant behavior*. Curr Opin Cell Biol, 2007. **19**(2): p. 150-8.
230. Schmidt-Ott, K.M. and J. Barasch, *WNT/beta-catenin signaling in nephron progenitors and their epithelial progeny*. Kidney Int, 2008. **74**(8): p. 1004-8.
231. Terada, Y., et al., *Expression and function of the developmental gene Wnt-4 during experimental acute renal failure in rats*. J Am Soc Nephrol, 2003. **14**(5): p. 1223-33.
232. Lin, C.L., et al., *Wnt/beta-catenin signaling modulates survival of high glucose-stressed mesangial cells*. J Am Soc Nephrol, 2006. **17**(10): p. 2812-20.
233. Liu, Y., *Epithelial to mesenchymal transition in renal fibrogenesis: pathologic significance, molecular mechanism, and therapeutic intervention*. J Am Soc Nephrol, 2004. **15**(1): p. 1-12.
234. Huber, M.A., N. Kraut, and H. Beug, *Molecular requirements for epithelial-mesenchymal transition during tumor progression*. Curr Opin Cell Biol, 2005. **17**(5): p. 548-58.

235. ten Berge, D., et al., *Wnt signaling mediates self-organization and axis formation in embryoid bodies*. Cell Stem Cell, 2008. **3**(5): p. 508-18.
236. Cano, A., et al., *The transcription factor snail controls epithelial-mesenchymal transitions by repressing E-cadherin expression*. Nat Cell Biol, 2000. **2**(2): p. 76-83.
237. Hovanes, K., et al., *Beta-catenin-sensitive isoforms of lymphoid enhancer factor-1 are selectively expressed in colon cancer*. Nat Genet, 2001. **28**(1): p. 53-7.
238. Rao, V.H., et al., *Increased expression of MMP-2, MMP-9 (type IV collagenases/gelatinases), and MT1-MMP in canine X-linked Alport syndrome (XLAS)*. Kidney Int, 2003. **63**(5): p. 1736-48.
239. Cabrera, S., et al., *Overexpression of MMP9 in macrophages attenuates pulmonary fibrosis induced by bleomycin*. Int J Biochem Cell Biol, 2007. **39**(12): p. 2324-38.
240. Mundel, P., et al., *Rearrangements of the cytoskeleton and cell contacts induce process formation during differentiation of conditionally immortalized mouse podocyte cell lines*. Exp Cell Res, 1997. **236**(1): p. 248-58.
241. Kopp, J.B., et al., *Transgenic mice with increased plasma levels of TGF-beta 1 develop progressive renal disease*. Lab Invest, 1996. **74**(6): p. 991-1003.
242. Rico, M., et al., *WT1-interacting protein and ZO-1 translocate into podocyte nuclei after puromycin aminonucleoside treatment*. Am J Physiol Renal Physiol, 2005. **289**(2): p. F431-41.
243. Surendran, K., S. Schiavi, and K.A. Hruska, *Wnt-dependent beta-catenin signaling is activated after unilateral ureteral obstruction, and recombinant secreted frizzled-related protein 4 alters the progression of renal fibrosis*. J Am Soc Nephrol, 2005. **16**(8): p. 2373-84.
244. He, W., et al., *Blockade of Wnt/{beta}-Catenin Signaling by Paricalcitol Ameliorates Proteinuria and Kidney Injury*. J Am Soc Nephrol, 2010.
245. Kim, J.H., et al., *Podocyte injury induces nuclear translocation of WTIP via microtubule-dependent transport*. J Biol Chem, 2010. **285**(13): p. 9995-10004.
246. Acconcia, F., et al., *Phosphorylation-dependent regulation of nuclear localization and functions of integrin-linked kinase*. Proc Natl Acad Sci U S A, 2007. **104**(16): p. 6782-7.